Effective field theory for fractional quantum Hall systems near $\nu = 5/2$

Po-Shen Hsin,[1,*] Ying-Hsuan Lin,[1,†] Natalie M. Paquette,[1,‡] and Juven Wang[2,3,§]

[1]*Walter Burke Institute for Theoretical Physics, California Institute of Technology, Pasadena, California 91125, USA*
[2]*Center of Mathematical Sciences and Applications, Harvard University, Cambridge, Massachusetts 02138, USA*
[3]*School of Natural Sciences, Institute for Advanced Study, Princeton, New Jersey 08540, USA*

(Received 8 June 2020; revised 16 October 2020; accepted 20 October 2020; published 16 November 2020)

We propose an effective field theory (EFT) of fractional quantum Hall systems near the filling fraction $\nu = 5/2$ that flows to pertinent IR candidate phases, including non-Abelian Pfaffian, anti-Pfaffian, and particle-hole Pfaffian states (Pf, APf, and PHPf). Our EFT has a $(2+1)$D $O(2)_{2,L}$ Chern-Simons gauge theory coupled to four Majorana fermions by a discrete charge-conjugation gauge field, with Gross-Neveu-Yukawa-Higgs terms. Including deformations via a Higgs condensate and fermion mass terms, we can map out a phase diagram with tunable parameters, reproducing the prediction of the recently proposed percolation picture and its gapless topological quantum phase transitions. Our EFT captures known features of both gapless and gapped sectors of time-reversal-breaking domain walls between Pf and APf phases. Moreover, we find that Pf | APf domain walls have higher tension than domain walls in the PHPf phase. Then the former, if formed, may transition to the energetically favored PHPf domain walls; this could, in turn, help further induce a bulk transition to PHPf.

DOI: 10.1103/PhysRevResearch.2.043242

I. INTRODUCTION

One of the first non-Abelian topologically ordered candidate states was observed experimentally in 1987 [1]. It is the filling fraction $\nu = 5/2$ fractional quantum Hall (fQH) state of an interacting electron gas in $2+1$ space-time dimensions [denoted as $(2+1)$D]. It has a fractional quantized Hall conductance $\sigma_{xy} = 5/2$ in units of e^2/h where e is the electron charge and h is the Planck constant. There have been many proposed candidate states to describe the underlying topological orders of this system: the major non-Abelian candidates include Moore-Read's Pfaffian state [2] (see also [3]), its particle-hole conjugate known as the anti-Pfaffian state [4,5], and a particle-hole symmetric state known as the particle-hole Pfaffian state [6]. The particle-hole Pfaffian state [6] was originally proposed to be a particle-hole symmetric version of a composite fermion theory for the half-filled Landau level system [7]. References [8,9] made earlier attempts to propose candidate wave functions for the particle-hole Pfaffian state.

In 2017, a remarkable experimental measurement by Banerjee *et al.* [10] suggested that the thermal Hall conductance of the $\nu = 5/2$ fQH state is $\kappa_{xy} = 5/2$ in units of $\pi^2 k_B^2 T/3h$, where k_B is the Boltzmann constant and T is the temperature.[1]

In this work, we propose a unified bulk effective field theory (EFT) that gives rise to various topological quantum field theories (TQFTs) and their edge modes pertinent to the $\nu = 5/2$ fQH system. We map the EFT parameters to experimental quantities to produce a phase diagram in terms of the filling fraction (or the magnetic field) vs the disorder strength. The phase diagram produced from our EFT turns out to be qualitatively similar to the previous theoretically proposed phase diagrams via the percolating phase transitions from the $(2+1)$D disordered systems with random puddles and domain walls of Pfaffian and anti-Pfaffian states [13–15]. In the following, we first recall pertinent proposals from the literature.

A. Overview of theoretical proposals and questions

While both the theoretical proposals of Pfaffian state [2] and anti-Pfaffian state [4,5] have a consistent fractional quantized Hall conductance $\sigma_{xy} = 5/2$, their thermal Hall

*phsin@caltech.edu
†yhlin@caltech.edu
‡nataliep@caltech.edu
§Corresponding author: jw@cmsa.fas.harvard.edu

[1]The edge modes of the quantum Hall system can be understood via the bulk-boundary correspondence of $(2+1)$D Chern-Simons theory. In fact, the thermal Hall conductance $\kappa_{xy} = (c_L - c_R)\frac{\pi^2 k_B^2}{3h}T$ is proportional to the chiral central charge $c_- \equiv c_L - c_R$, which is the difference between the left and right central charges c_L and c_R. It counts the degrees of freedom of chiral modes of the $(1+1)$D edge conformal field theory (CFT) living on the boundary of a bulk-gapped $(2+1)$D topological state [11]. For non-Abelian fQH states, the half-integer κ_{xy} is attributable to an odd number of $(1+1)$D chiral real Majorana-Weyl fermions on the boundary [12], in addition to $(1+1)$D chiral bosons or chiral complex fermions.

conductances $\kappa_{xy} = 7/2$ and $3/2$, respectively, seem to contradict with the result of [10]. By contrast, the particle-hole Pfaffian state proposed by Son [6] predicts[2] both $\sigma_{xy} = 5/2$ and $\kappa_{xy} = 5/2$, consistent with this recent experiment. On the other hand, vast numerical studies [18–27] on the $\nu = 5/2$ fQH system at low energy favor either the Pfaffian state or the anti-Pfaffian state. The dilemma between the experiment (favoring $\kappa_{xy} = 5/2$) and the numerical data (favoring $\kappa_{xy} = 7/2$ or $3/2$) raises an important issue: Can the seemingly contradictory experimental and numerical results be reconciled?

Reference [9] argued that the numerical simulations are simplified systems lacking both disorder (say, induced by impurities of experimental samples) and Landau-level mixing (LLM), which occur in real laboratory experiments. Reference [9] further suggested that the particle-hole Pfaffian may be stabilized by disorder, i.e., LLM and impurities that break particle-hole symmetry. However, Ref. [9] did not provide analytic details on how disorder can help realize this possibility in practice.

Building on this suggestion, Refs. [13–15] investigated the possibility of particle-hole Pfaffian (PHPf) topological order emerging from disordered puddle systems of Pfaffian (Pf) and anti-Pfaffian (APf) states[3] with percolating random domain walls.

We recall the following:

(1) Neither the Pf nor the APf state has particle-hole (PH) symmetry [28]. Both Pf and APf have their lower Landau levels fully occupied with spin-polarized electrons (which contribute $\sigma_{xy} = 2$). However, in the absence of LLM, if we assume that spin-polarized electrons in the highest, half-filled Landau level (so there is another contribution of $\sigma_{xy} = 1/2$ and $\nu = 5/2$ in total) interact only through two-body interactions, then exact PH symmetry *is* present in the *idealized* Hamiltonian.[4] With the PH symmetry at $\nu = 5/2$, the two PH symmetry-breaking states, Pf and APf, are related by a PH transformation. Thus, they have the same energy and become two degenerate states at $\nu = 5/2$. PH symmetry is broken away from $\nu = 5/2$, so either Pf or APf is favored on each side of $\nu > 5/2$ and $\nu < 5/2$. At $\nu = 5/2$, if PH symmetry is spontaneously broken, one of Pf and APf is realized.

(2) With LLM, PH symmetry is only approximate, so the critical ν may be shifted to $\nu_c = 5/2 + \delta\nu$. Second-order perturbation theory from LLM modifies the Hamiltonian and induces PH-symmetry-breaking three-body interaction terms, so both Pf or APf can be candidate ground states near ν_c. Whether Pf or APf is the candidate ground state for ν near ν_c partly depends on the sign of the three-body terms. For a small deviation away from ν_c, we gain quasiparticles for $\nu > \nu_c$ and quasiholes for $\nu < \nu_c$. If the quasiparticles of APf have a lower energy than those of Pf for $\nu > \nu_c$, then in turn quasiholes of Pf have a lower energy than those of APf for $\nu < \nu_c$, due to their PH conjugate properties at ν_c (and vice versa). As long as ν is within the $\nu_c \simeq 5/2$ fractional quantized Hall plateau, we assume Pf is favored for $\nu < \nu_c$ (and hence APf is favored for $\nu > \nu_c$) for simplicity [4].[5]

(3) Under the presence of spatial disorder (e.g., quenched disorder arising from the presence of impurities, or spatial variations in the chemical potential) and spatial density fluctuations on the sample, many puddles of Pf or APf of radii ℓ_0 would form, with puddle sizes bounded by $\ell_B < \ell_0 < L$ where $\ell_B = \sqrt{\hbar c/eB}$ is the magnetic length under a magnetic field B, and L is the sample size. The disorder-induced puddles [29] separate Pf and APf into patterns analogous to that of islands and seas in an archipelago (see the picture illustration in Figs. 1 and 3 in [15]). The boundaries of puddles then form $(1+1)$D domain walls (between Pf and APf regions) hosting four gapless chiral real Majorana-Weyl fermions (with chiral central charge $c_- = 4 \times \frac{1}{2} = 2$) and two copies of the so-called gappable nonchiral double-semion theory of compact complex bosons (with $c_- = 0$, and $c_L = c_R = 1$). It is proposed that the domain walls percolating in the bulk drive the bulk phase into the so-called *percolating phase*.[6] The question about the nature of the percolating phase becomes the

[2]The particle-hole Pfaffian is analogous to the T-Pfaffian or CT-Pfaffian that occur on the surface of $(3+1)$D topological superconductors (see [16,17]).

[3]For the sake of brevity, below we abbreviate Pfaffian state as Pf, anti-Pfaffian state as APf, and particle-hole Pfaffian as PHPf. See Appendix A of Ref. [15] for the systematic list of data of the pertinent $\nu = 5/2$ quantum Hall liquids in terms of $(2+1)$D bulk topological quantum field theories (TQFTs) and $(1+1)$D edge theories.

[4]In the literature, there are two conventions for naming the Landau levels. One convention is to call the lowest level the zeroth Landau level (which here is fully occupied, with spin-up and -down polarized electrons contributing $\sigma_{xy} = 2$), and call the next the first Landau level (which here is half-filled with polarized spin, contributing $\sigma_{xy} = 1/2$) [13,15]. Another convention instead calls the lowest Landau level the first Landau level, and the half-filled Landau level the second Landau level [14]. We use the first convention for this $\nu = 5/2$ system.

[5]There are two cases: (1) The quasiparticles of APf have a lower energy than those of Pf for $\nu > \nu_c$. Then quasiholes of Pf have a lower energy than quasiholes of APf for $\nu < \nu_c$. In this case, Pf is favored for $\nu < \nu_c$ and APf is favored for $\nu > \nu_c$. (2) The quasiparticles of Pf have a lower energy than quasiparticles of APf for $\nu > \nu_c$. Then, quasiholes of APf have a lower energy than quashioles of Pf for $\nu < \nu_c$. In this case, APf is favored for $\nu < \nu_c$ and Pf is favored for $\nu > \nu_c$. Numerical simulations have favored both possibilities (see the discussions in [14] and the references therein), so we cannot exclude (1) or (2). We will assume (1) without losing generality.

[6]Let us briefly define what we mean by disorder/order, percolation, and delocalized/localized.

(i) Order vs disorder. We use order to mean Landau-Ginzburg symmetry-breaking order, as well as Wen's long-range entangled topological order (beyond Landau). Disorder here is mainly used to mean quenched disorder caused by impurities or a spatially nonuniform chemical potential, inducing puddles of Pf or APf near ν_c.

(ii) Percolation. When we say that a phase percolates, we mean that the phase can extend through the whole bulk-boundary system [e.g., see Figs. 3(a) and 3(c) of [15]]. When we instead say the domain walls percolate, we mean that Pf | APf domain walls can extend through the whole bulk-boundary system [e.g., see Fig. 3(b) of [15]].

(iii) Localized vs delocalized. When we say the neutral Majorana modes are delocalized, we mean that the Majorana modes

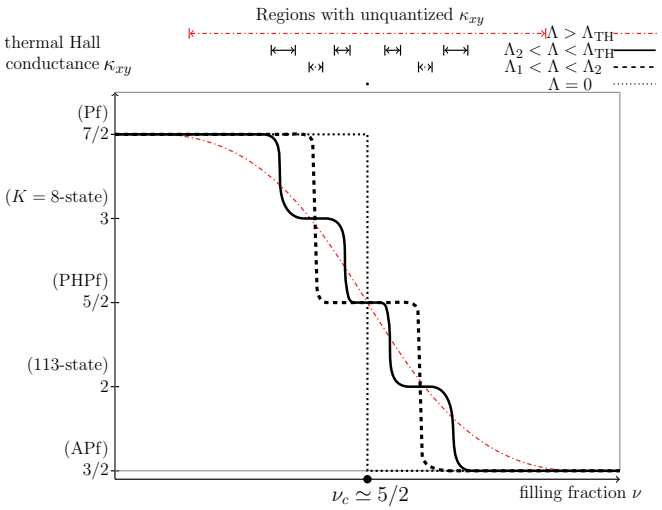

FIG. 1. Thermal Hall conductance κ_{xy} vs filling fraction ν for the scenario proposed in Ref. [15]; see also Fig. 3 for a phase diagram. At different disorder energy scales Λ, we plot several curves of (ν, κ_{xy}). At $\Lambda = 0$, the κ_{xy} (drawn as a dotted line) jumps at ν_c under a first-order phase transition. From $0 < \Lambda < \Lambda_1$, the jump can become smoother due to disorder. In the regime $\Lambda_1 < \Lambda < \Lambda_2$, drawn as a dashed line, an intermediate $\kappa_{xy} = 5/2$ plateau phase appears. Finally, when $\Lambda_2 < \Lambda < \Lambda_{TH}$, there are multiple plateau phases at $\kappa_{xy} = 3,\ 5/2$, and 2. Notice that when $\Lambda > 0$, all transitions between different quantized κ_{xy} can have *broadening*, where the jumps at transitions become smoother slopes. On the top panel, we show different line intervals which represent the extent of broadening over ranges of ν demarcated on the horizontal axis, for the values stated of Λ on the top right corner. When $\Lambda > \Lambda_{TH}$, the slope is smooth enough to become a thermal metal so there is no quantized κ_{xy} between $7/2$ and $3/2$. See the following remark (3).

question of understanding whether the domain wall degrees of freedom are *localized* in the bulk or *delocalized* through the whole bulk-boundary system (see the picture illustration in Fig. 3 in [15]).

References [13,14] modeled the $\nu = 5/2$ system in terms of a checkerboard network (of alternating Pf and APf in each checkered pattern) known as a Chalker-Coddington network model [30] (previously used in modeling the integer quantum Hall plateau transition). Reference [15] performed perturbative and nonperturbative analyses of the $(1+1)$D edge theory on the domain wall between Pf and APf states at different disorder energy scales, with particular focus on the emergent symmetries

B. Comparison of three related proposals on disordered percolating systems

We compare the results of Refs. [13–15], which we also summarize pictorially in Figs. 1 and 2.[7]

(1) Reference [13] proposed that a single first-order-like transition between Pf and APf occurs at ν_c and at zero disorder, due to an O(4) symmetry rotating four gapless chiral Majorana modes. The presence of these Majoranas induces a jump $\Delta\kappa_{xy} = \Delta c_- = 2$. In the presence of any nonzero disorder, which weakly perturbs the first-order critical point, Ref. [13] proposed four consecutive continuous phase transitions (e.g., second-order transitions). Each transition causes κ_{xy} to jump by $1/2$, due to a single neutral chiral Majorana mode: from Pf ($\kappa_{xy} = 7/2$) $\to$ $\kappa_{xy} = 3$ $\to$ $\kappa_{xy} = 5/2$ $\to$ $\kappa_{xy} = 2$ $\to$ APf($\kappa_{xy} = 3/2$). Reference [13] also expected the same universality class for disorder anisotropic models and uniform models. See the Fig. 1 phase diagram of [13]. We illustrate Ref. [13]'s thermal Hall prediction in scenario (I) in Fig. 2.

(2) Reference [14] suggested that for a finite range of $\nu \simeq \nu_c$, the Pf | APf domain walls percolate.[8] If the charge neutral Majorana edge modes can diffuse freely in the network of domain walls in the bulk-boundary system, Ref. [14] proposed a *thermal metal* phase with an unquantized thermal Hall κ_{xy} but a divergent κ_{xx} (and, as usual, a quantized Hall conductance $\sigma_{xy} = 5/2$, and $\sigma_{xx} = 0$ at zero temperature). If the neutral Majorana modes are localized, Ref. [14] proposed a quantized $\sigma_{xy} = 5/2$ phase with a quantized thermal Hall conductance $\kappa_{xy} = 5/2$. Reference [14] suggested that between the Pf and APf phases, there is a possible wide range of thermal metal behavior, even at low disorder. By tuning ν, in the absence of disorder, there is a first-order-like transition between Pf $\to$ APf. At low disorder, there is a sequence of transitions from Pf $\to$ thermal metal $\to$ APf. At larger disorder, there is a sequence of transitions from Pf ($\kappa_{xy} = 7/2$) $\to$ thermal metal $\to$ $\kappa_{xy} = 5/2$ $\to$ thermal metal $\to$ APf ($\kappa_{xy} = 3/2$). The intermediate thermal metal phase is a distinct key feature of the proposal in [14]. See the phase diagrams in Figs. 1 and 8 of [14]. We illustrate the thermal Hall prediction of Ref. [14] in scenario (II) in Fig. 2.

(3) Reference [15] performed perturbative and nonperturbative analyses on the $(1+1)$D edge theory, and studied

can diffuse freely on the network of domain walls. The delocalization happens at the percolation transition (approximately near a percolation critical point). When the neutral Majorana modes are delocalized, the thermal Hall κ_{xy} is unquantized, thus either causing a *percolation transition* or a *thermal metal phase*. When neutral Majorana modes are localized (on the domain walls), we have a quantized κ_{xy}.

"Percolation" is used to indicate when a *spatial subregion* (e.g., Pf, APf, or domain walls) spreads in the spatial sample, whereas "(de)localization" is used to indicate when *zero-energy modes or energetic modes* in the energy spectrum are delocalized/localized in the spatial sample.

[7] There is an alternative interpretation from [31–35] favoring the anti-Pfaffian state (see also the criticism [36] of Ref. [31]'s interpretation). Some of these works propose that partial or nonthermal equilibrium of anti-Pfaffian edge modes can explain the $\kappa_{xy} = 5/2$ measurement [10], even though the anti-Pfaffian bulk state has $\kappa_{xy} = 3/2$ at equilibrium. We shall not discuss this scenario [31,33–35] since we wish to obtain an effective bulk field theory motivated by the scenario of [15].

[8] In the language of Ref. [14], neither Pf nor APf percolates, but the Pf | APf domain walls percolate. However, in the language of Ref. [15], not only the Pf | APf domain walls percolate, but also both Pf and APf percolate, because some regions of Pf or APf extend through the whole bulk boundary.

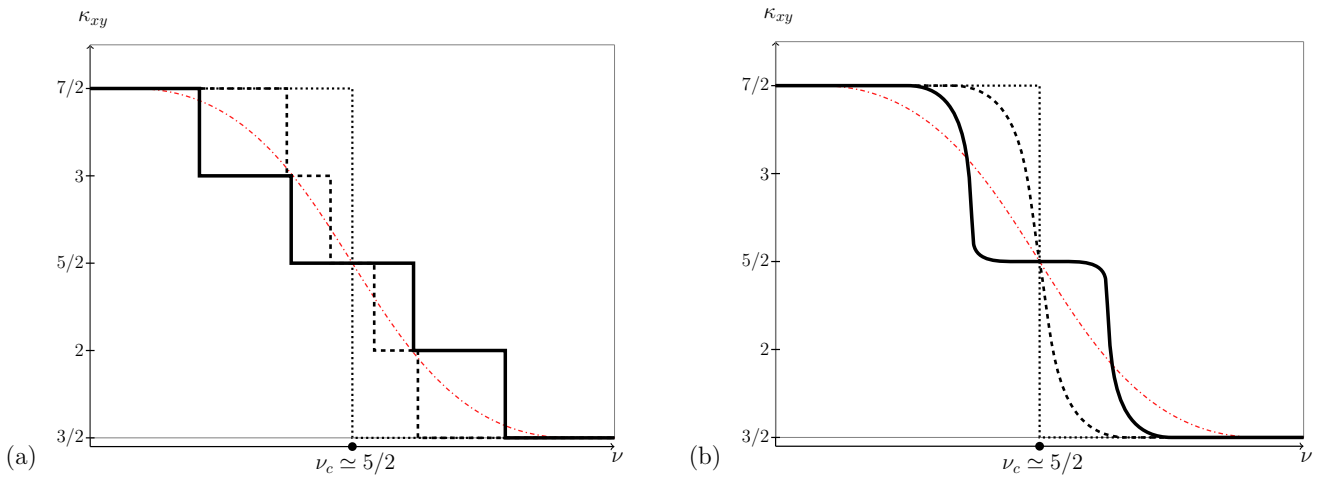

FIG. 2. Thermal Hall conductances: (a) scenario (I) from Ref. [13] (left) and (b) scenario (II) from Ref. [14] (right). We use the same legend for drawing curves at different scales Λ as in Fig. 1. At $\Lambda = 0$, κ_{xy} (drawn as a dotted line) jumps at ν_c under a first-order phase transition. For $\Lambda > 0$, scenarios (I) and (II) differ. Scenario (I)'s κ_{xy} has four jumps at the plateau for any $0 < \Lambda < \Lambda_{\rm TH}$, and κ_{xy} becomes smooth with nonquantized values for $\Lambda > \Lambda_{\rm TH}$.

emergent symmetries on the domain wall between Pf and APf states at different disorder energy scales $\Lambda = \overline{v}/\ell_0$ (which is related to the inverse of the puddle size ℓ_0 but proportional to the mean value of the edge-state velocity $\overline{v}$). Then, Ref. [15] proposed a more specific phase diagram of the $\nu = 5/2$ disordered system, schematically shown in Fig. 3. An example of thermal Hall prediction of Ref. [15] is illustrated in Fig. 1. By the perturbative renormalization group (RG) analysis on disorder and scattering, Ref. [15] finds different emergent symmetries at different disorder energy scales. By a Berezinskii-Kosterlitz-Thouless (BKT) type RG analysis, Ref. [15] finds for weak disorder

$$\Lambda < \Lambda_1 \simeq \overline{v}(\overline{v}^2/W_v^*)^{-1/d_v},$$

there is an emergent O(4) symmetry among the four gapless chiral Majorana modes.[9] This describes a transition

$$\text{Pf}\ (\kappa_{xy} = 7/2) \to \text{APf}\ (\kappa_{xy} = 3/2). \tag{1}$$

(For $\Lambda = 0$, this is a first-order transition. For $0 < \Lambda < \Lambda_1$, this can be a second-order transition or a first-order transition with weak disorder broadening the transition.) For

$$\Lambda_1 < \Lambda < \Lambda_2 \simeq e^2/\epsilon\ell_B,$$

where Λ_2 is set by the electron's Coulomb interaction and ϵ is a dielectric constant, we have two transitions

$$\text{Pf}\ (\kappa_{xy} = 7/2) \to\ \kappa_{xy} = 5/2\ \to \text{APf}\ (\kappa_{xy} = 3/2). \tag{2}$$

(Again, the two intermediate steps can be first-order transitions but with disorder broadening, or second-order transitions.) For the disorder scale

$$\Lambda_2 < \Lambda < \Lambda_{\rm TH},$$

we have four transitions

$$\begin{aligned}\text{Pf}(\kappa_{xy} = 7/2) \to\ \kappa_{xy} = 3\ \to\ \kappa_{xy} = 5/2\ \to\ \kappa_{xy}\\ = 2\ \to \text{APf}(\kappa_{xy} = 3/2),\end{aligned} \tag{3}$$

all of which can be (broadened) first-order transitions, or second order.

Finally, for $\Lambda > \Lambda_{\rm TH}$, when the disorder is very strong, the κ_{xy} becomes unquantized and we enter into the thermal metal (TH) regions (the light red area on the top of Fig. 3). The percolation transition to the thermal metal phase guarantees the divergence of the correlation length, which therefore guarantees that the transitions from all topological orders to the thermal metal (drawn as the red solid curves in Fig. 3) are second-order phase transitions.

Note that the aforementioned disorder-broadening regions have unquantized κ_{xy} and hence can behave similarly to a thermal metal as an intermediate phase. However, to be a precise thermal metal, one needs to check that κ_{xx} diverges at zero temperature.

We expect the first-order disorder-broadening spreads to a region of size that is exponentially suppressed by $e^{-f(\Lambda_1,\Lambda_2)/\Lambda^2}$ with some functional form f of Λ_1 and Λ_2 [14], which grows wider as the disorder increases (i.e., the light red area becomes wider in Fig. 3 along the phase boundaries) [29]. What might be the outcomes of this phase boundary broadening?

(a) One possibility is that the broadening region becomes a new intermediate phase, such as a thermal metal, with unquantized κ_{xy}, while the split phase boundaries (the dotted red lines in Fig. 3 along the phase boundaries) become *two* new second-order phase transitions.

(b) Another possibility is that the percolation transition of the domain walls can be induced within the broadening

[9]Here, $\overline{v}$ is the average edge-state velocity along the puddle, and W_v^* has the dimension of [length]$^{-d_v}$ where the length scale is the correlation length of the BKT-type transition. The energy scale Λ_1 is around ℓ_φ^{-1} set by the correlation length ℓ_φ of superconducting pairing fluctuation in the composite fermion picture of Pf and APf. We thank B. Haleprin pointing out that this Λ_1 is also related to the energy scale w^{-1} of the domain wall width w, which can be solved from a setup with Haldane pseudopotential.

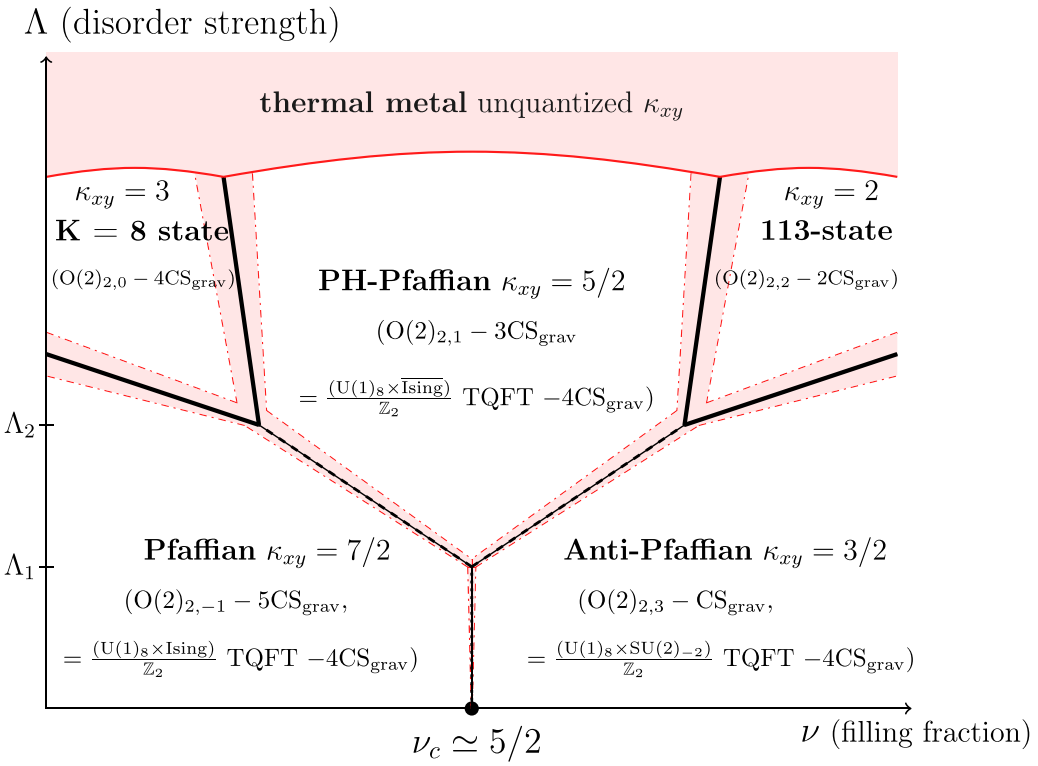

FIG. 3. A schematic phase diagram similar to the proposal in Ref. [15]. To see all these phases with varying κ_{xy} requires that the $\nu_c \simeq 5/2$ plateau spans a sufficient range around ν_c. Previous work [13–15] can obtain various quantized values of κ_{xy} but cannot directly derive the bulk topological orders via the percolation transition argument. In this work, we propose a bulk effective field theory (EFT) not only consistent with [13–15] but can reproduce all the implicated bulk topological orders. At zero disorder, $\Lambda = 0$, the transition at ν_c is *first order*. For $\Lambda > 0$, there are different possibilities for transitions, depending on the microscopic details of samples. One scenario in [15] suggests that there are *second-order* phase transitions (drawn in solid black lines) between topological orders for $\Lambda > 0$. Another scenario in [15] suggests that there can be *first-order* phase transitions between topological orders for $\Lambda > 0$, but that disorder broadens these first-order transitions to regions (light red shaded regions) with unquantized κ_{xy}. These broadened regions cannot merely be crossovers because the topological orders and global symmetries are distinct on the two sides. The boundaries of these broadened regions (drawn as dashed-dotted red curves) could also be *second-order* phase transitions. At larger $\Lambda \gg \Lambda_2$, a percolation transition from topological order to a thermal metal, also with unquantized κ_{xy}, is known to be a *second-order* phase transition (drawn as solid red curves). We propose a unified EFT in Eq. (4) in Sec. II and an upgraded version in Sec. II E to describe all phases in the phase diagram.

region. Since at the percolation transition critical point, the domain wall size and correlation length diverge (at least for an infinite-sized system), this induces a new *single* second-order transition within the broadening.[10]

Broadening regions cannot become crossovers between neighboring phases because the bulk phases have different topological orders and/or global symmetries.

In fact, remark (3), following the scenario from Ref. [15], can be regarded as a general scenario that recovers both of the two scenarios from remarks (1) and (2) in certain limits.

The key point for us is that Refs. [13–15] suggested that a $\kappa_{xy} = 5/2$ plateau may be induced when Pf | APf domain walls percolate. However, Refs. [13–15] have *not* directly demonstrated that the resulting bulk order is indeed PHPf. Although PHPf has $\kappa_{xy} = 5/2$, it remains an open question to show the bulk PHPf induces this $\kappa_{xy} = 5/2$. In this work, we propose a unified effective field theory that can be viewed as a *parent* or *mother* quantum field theory at some higher-energy scale,[11] which at low energies can give rise to all the relevant

[10] In fact, our EFT can provide a second-order phase transition at the disorder scale $0 < \Lambda < \Lambda_1$. In this case, the second-order phase transition within the range $0 < \Lambda < \Lambda_1$ can be understood as broadening of the first-order phase transition at $\Lambda = 0$ due to finite disorder. Within the broadening region, a new *single* second-order transition is induced; a similar statement holds for other second-order transitions of our EFT when $\Lambda > 0$; see Sec. II.

[11] The energy scale of our EFT is at an intermediate energy scale ($\sim \xi^{-1}$), somewhere above the IR low-energy topological field theory ($\sim L^{-1}$) but below the inverse magnetic length scale ${\ell_B}^{-1}$ of electrons or the high-energy lattice cutoff scale a_{lattice}^{-1} in the far UV. The length scales run from small to large as follows: lattice cutoff $a_{\text{lattice}} <$ magnetic length $\ell_B <$ phase-coherence length $\ell_\varphi \lesssim \xi <$ sample size L. The corresponding energy scales, the inverse of the length scales, run from large to small accordingly. The fluctuation length ξ is the length scale of the chemical potential fluctuation due to the impurity and doping in the system and it is roughly the length scale of disorder Λ^{-1}. The ℓ_0 is the puddle linear size which is the link size for the Chalker-Coddington network model [30]. The disorder energy

IR TQFT phases listed in Fig. 3, including $K = 8$, PHPf, and 113 state, etc.

C. Outline

In the previous subsections, we have summarized several proposed phase diagrams in the literature for the $\nu = 5/2$ fractional quantum Hall state. We will focus on reproducing the phase diagram of [15], illustrated in Fig. 3. Our $(2+1)$D EFT will also be able, in special limits, to reproduce phase diagrams arising from the other proposals [13,14], as will become clear in the subsequent sections. The EFT description also reproduces the $(1+1)$D domain wall world-volume theory predicted by [15], and it additionally fixes the type of phase transitions at the various phase boundaries (i.e., first order vs second order). We also begin a preliminary study of the energetics of our EFT by performing computation of the domain wall tension, valid in a semiclassical limit, in the relevant phases. The tension of the walls differs in the Pf | APf and PHPf phases of the theory due to the presence of the chiral Majorana fermions in the former regime.

We conclude this introduction by summarizing the plan for the rest of this paper. In Sec. II, we introduce our effective field theory, discuss its various IR phases, and describe in detail how it maps to the phase diagram in Fig. 3. In Sec. III, we describe the anyon spectra in the various IR phases of our EFT in terms of TQFTs and their quantum numbers, which will be matched to the many-body wave functions later (in Appendix F). In Sec. IV, we analyze the domain wall theory and excitations in some detail. In particular, we study the gapless sectors and evaluate the tension of the walls. In Sec. V, we conclude, make final remarks, and point out several future directions. Several appendices contain additional background and some technical details used in the body of the paper. In Appendix A, we review the relation between the gravitational Chern-Simons term and the thermal Hall response. In Appendix B, we describe Abelian and non-Abelian versions of $\mathbb{Z}_2$ gauge theory in $(2+1)$D. In Appendix C, we clarify some details about the fermion path integral and counterterms. In Appendix D, we discuss the procedure for gauging a one-form symmetry in a $(2+1)$D TQFT. In Appendix E, we systematically introduce $\mathrm{O}(2)_{2,L}$ Chern-Simons theories, their Hall conductance, and other relevant physical properties. In Appendix F, we review the wave-function descriptions of the IR TQFTs relevant for our study. In Appendix G, we provide some additional details regarding our one-loop computation of the domain wall tension.

II. EFFECTIVE FIELD THEORY NEAR THE CRITICAL FILLING FRACTION IN $(2+1)$D

We now present our effective field theory (EFT).

$\Lambda = \overline{v}/\ell_0$ is tunable and set by the inverse of the tunable puddle size ℓ_0 [15]. When the length ℓ_0 is large compared to the *domain wall thickness* w, the domain walls tend to expand and the energetics of the system warrant a more careful analysis [14] to determine if the system prefers Pf or APf percolation, instead of domain wall percolation. See more on energy and length scales in Sec. II B 2. We discuss the tension of the domain walls in Sec. IV.

A. Gauge sector, global symmetry, and 't Hooft anomaly

The $(2+1)$D EFT consists of three sectors:

(i) [O(2)] gauge field with Chern-Simons (CS) term $\mathrm{O}(2)_{2,1}$ (in the notation of [37]).[12]

(ii) Two Dirac fermions Ψ^j with flavor index $j \in \{1,2\}$ in the determinant sign representation of the [O(2)] gauge group. Namely, fermions are odd (-1) under the $\det([\mathrm{O}(2)]) = \pm 1$.

(iii) A real noncompact scalar $\phi \in \mathbb{R}$ field coupled to the Dirac fermions by a Yukawa term. The ϕ also has a Higgs potential.

To make the connection with fQH, the Chern-Simons gauge field is coupled to a background $\mathrm{U}(1)_{\mathrm{EM}}$ gauge field. We begin by considering a particular mass term for the Dirac fermions and an *even* exponent scalar potential so that the EFT preserves particle-hole symmetry and captures the phase transition at the critical filling fraction ν_c. More general extra deformations, including particle-hole symmetry-breaking potential (an *odd* exponent scalar potential) for ϕ and Majorana mass terms for four Majorana fermions, where each complex Dirac $\Psi^j = \eta_{j1} + i\eta_{j2}$ is written as two real Majorana η_{j1} and η_{j2}, with $j \in \{1,2\}$, will be considered in subsequent sections to produce the entire phase diagram of Fig. 3.

Explicitly, the theory is a $(2+1)$D gauged Gross-Neveu-Yukawa-Higgs theory coupled to a non-Abelian Chern-Simons theory

$$\mathrm{O}(2)_{2,1}\ \mathrm{CS} + \sum_{j=1,2} \overline{\Psi}^j (i\not{D}_{\mathcal{C}} - g\phi)\Psi^j - m(\overline{\Psi}^1\Psi^1 - \overline{\Psi}^2\Psi^2)$$
$$+ \frac{1}{2}(\partial\phi)^2 + \frac{\mu^2}{2}\phi^2 - \frac{\lambda}{4}\phi^4 - 3\mathrm{CS}_{\mathrm{grav}}, \tag{4}$$

where $\mathcal{C}$ indicates that the fermions are odd under the charge conjugation $\mathcal{C}: \Psi_j \to -\Psi_j$ where $[\mathbb{Z}_2^{\mathcal{C}}] \subset [\mathrm{O}(2)] = [\mathrm{SO}(2) \rtimes \mathbb{Z}_2^{\mathcal{C}}]$ becomes part of the gauge group.[13] Since the entire [O(2)] is gauged, the fermions couple to the $\mathrm{O}(2)_{2,1}$ Chern-Simons gauge theory by this $\mathbb{Z}_2^{\mathcal{C}}$ gauging (see Appendix E). Each of the complex Dirac fermions (Ψ^1 or Ψ^2), regarded as two real Majorana fermions, respectively ($\Psi^j = \eta_{j1} + i\eta_{j2}$), enjoys an O(2) global symmetry. There is a faithful $\frac{\mathrm{O}(2)\times\mathrm{O}(2)}{\mathbb{Z}_2}$ global symmetry rotating the two Dirac fermions independently that we will explain later below.

The theory can be obtained by starting from the decoupled semion theory $\mathrm{U}(1)_2 = \mathrm{SO}(2)_2$ CS and the Gross-Neveu-

[12] Since the discussions here involving several orthogonal groups $\mathrm{O}(N)$ for global or gauge groups, to avoid confusion, we may sometimes use the bracket [O(2)] to specify the gauge group or gauge sectors arising from $\mathrm{O}(2)_{2,L}$ CS gauge theory, in contrast with the global symmetries groups [e.g., O(2) and O(4)] that have no brackets. In general, for a group G_g which is dynamically gauged, we may denote it as $[G_g]$.

[13] Originally, there was a fermion parity symmetry $\mathbb{Z}_2^F$ where $(-1)^F: \Psi_j \to -\Psi_j$ in the Dirac fermion theory. But, this $\mathbb{Z}_2^F$ is identified with the charge conjugation $[\mathbb{Z}_2^{\mathcal{C}}]$ in the gauge group $[\mathrm{O}(2)] = [\mathrm{SO}(2) \rtimes \mathbb{Z}_2^{\mathcal{C}}]$, and thus $[\mathbb{Z}_2^F]$ is gauged since $[\mathbb{Z}_2^{\mathcal{C}}]$ is gauged in [O(2)]. Beware that here the gauged $[\mathbb{Z}_2^{\mathcal{C}}]$ and $[\mathbb{Z}_2^F]$ are different from the familiar charge-conjugation C symmetry $\mathbb{Z}_2^C$ of the Dirac fermion, where $C: \Psi_j \to \Psi_j^\dagger$, which remains ungauged. Readers should be careful to distinguish the $\mathcal{C}$ and C transformations.

Yukawa theory and then gauging the diagonal $\mathbb{Z}_2$ symmetry that acts on $SO(2)_2$ as the charge-conjugation symmetry $[\mathbb{Z}_2^C]$ and acts on the Gross-Neveu-Yukawa sector as the fermion parity $[\mathbb{Z}_2^F]$. This changes the gauge group from [SO(2)] to [O(2)]. We add a fermionic counterterm for the $\mathbb{Z}_2$ gauge field, which gives the $\mathbb{Z}_2$ level in $O(2)_{2,1}$, and makes the resulting theory still depend on the spin structure. The spin structure dependence *only* comes from this discrete gauged $\mathbb{Z}_2$ Chern-Simons level.

Despite the appearance of the Chern-Simons term, the theory in fact has a *particle-hole PH symmetry*, also called the *time-reversal CT symmetry*[14] (possibly with a 't Hooft anomaly discussed later): $\Psi^i \to \epsilon^{ij}\gamma^0\Psi^j$ and $\phi \to -\phi$, so that ϕ transforms as a real-valued pseudoscalar. To see this, we express the theory in (4) as

$$\frac{O(2)_{2,1}\ \text{CS}+[(\mathbb{Z}_2)_0\ \text{coupled to Gross-Neveu-Yukawa}]}{\mathbb{Z}_2}, \quad (5)$$

where the quotient denotes gauging the $\mathbb{Z}_2$ one-form symmetry generated by the composite line given by the product of the O(2) Wilson line in the nontrivial one-dimensional representation and the $\mathbb{Z}_2$ electric line.[15] We briefly review the notion of gauging one-form symmetries in Appendix D. The $O(2)_{2,1}$ Chern-Simons theory is time-reversal invariant by level and rank duality [37,38]. Each of the two theories in the numerator has time-reversal zero-form symmetry and $\mathbb{Z}_2$ one-form symmetry, where the zero-form and one-form symmetries do not have a mixed anomaly [since gauging the one-form symmetry reduces the two theories to $SO(2)_2$ and the Gross-Neveu-Yukawa theory, respectively, both of which are time-reversal invariant]. Therefore, the quotient theory is also time-reversal invariant.

As discussed in Appendix E 1, the theory can couple to a background $U(1)_{EM}$ electromagnetic gauge field A to have a fractional quantum Hall conductivity $\sigma_{xy} = 5/2$ under the $U(1)_{EM}$ electromagnetic charge's transverse conductivity measurement. The $U(1)_{EM}$ electromagnetic gauge field only couples to the Chern-Simons gauge field, and hence all the phases we discuss have the same Hall conductivity σ_{xy}.[16]

We will consider phases with $\mu^2 > 0$, which implies that the real (pseudo)scalar field ϕ condenses with a vacuum expectation value (vev):

$$\langle\phi\rangle = \pm v, \quad v \sim \mu/\sqrt{\lambda} > 0. \quad (6)$$

This spontaneously breaks the time-reversal CT symmetry, and there can be two symmetry-breaking vacua exchanged by the (broken) symmetry transformation in the $(2+1)$D bulk. The spontaneously broken time-reversal symmetry CT leads to a $(1+1)$D domain wall that interpolates between the two vacua. We will investigate the domain walls in Sec. IV.

Let us elaborate more on the global symmetries and gauge group in Eq. (4):

(A) Continuous global symmetries. If we turn off the mass deformation $m = 0$, then the theory has an enlarged $O(4)/\mathbb{Z}_2 \equiv PO(4)$ symmetry, where the four Majorana components from the two Dirac fermions transform in a vector representation of O(4). Let us explain why we mod out by a $\mathbb{Z}_2$ subgroup of the näive rotational O(4) global symmetry. The $\mathbb{Z}_2$ center of O(4) [in fact the same as $\mathbb{Z}_2^F \subset SO(4) \subset O(4)$, where $\mathbb{Z}_2^F$ sends $\Psi_j \to -\Psi_j$] is identified with the charge-conjugation element $[\mathbb{Z}_2^C]$ of the [O(2)] gauge group. If we turn on $m \neq 0$, there is a faithful $\frac{[O(2)\times O(2)]}{\mathbb{Z}_2}$ global symmetry in Eq. (4). We mod out by a $\mathbb{Z}_2$ subgroup of the näive $O(2) \times O(2)$ symmetry because the diagonal $\mathbb{Z}_2$ center of $O(2) \times O(2)$ [in fact the same as $\mathbb{Z}_2^F \subset SO(2) \times SO(2) \subset O(2) \times O(2)$, where $\mathbb{Z}_2^F$ sends $\Psi_j \to -\Psi_j$] is identified with the charge-conjugation element of $[\mathbb{Z}_2^C]$ of [O(2)] gauge group. By contrast, if we allow the four Majorana fermions to all have different masses, then there is no continuous global symmetry (because the fermion parity $\mathbb{Z}_2^F$ that flips the sign of the fermions is identified with a gauge rotation $[\mathbb{Z}_2^C]$). The different mass deformations considered in the subsequent sections can be organized by the breaking pattern of PO(4). The continuous global symmetry PO(4) that transforms the fermions has the standard mixed anomaly with the time-reversal CT symmetry given by the $(3+1)$D θ term for a PO(4) background gauge field with $\theta = (\pi, \pi)$.[17]

(B) Discrete global symmetries:

(1) $\mathbb{Z}_2^f$ fermion parity symmetry. This $\mathbb{Z}_2^f$ should not be confused with the already gauged $[\mathbb{Z}_2^F]$ (acting by $\Psi_j \to -\Psi_j$ only in the Dirac fermion sectors). The $[\mathbb{Z}_2^F]$ and $[\mathbb{Z}_2^C]$ charge conjugations are identified and both dynamically gauged due to $\not{D}_C$. (Neither Ψ_1 nor Ψ_2 are gauge-invariant local fermionic operators.) In fact, the $\mathbb{Z}_2^f$ acts *not* on Gross-Neveu-Yukawa sector, but *only* on the $O(2)_{2,1}$ CS and $-3\text{CS}_{\text{grav}}$. Note that Eq. (4) is an intrinsically fermionic theory (defined on spin manifolds) because both $O(2)_{2,1}$ CS and $-3\text{CS}_{\text{grav}}$ are spin Chern-Simons actions whose UV completion, say on a lattice, requires some gauge-invariant local fermionic operators.

[14]The time-reversal symmetry in our field theory language is an antiunitary symmetry sometimes known as the CT symmetry with its square $(CT)^2 = (-1)^f$ giving the fermion parity $\mathbb{Z}_2^f$ of the whole theory. The time-reversal CT indeed corresponds to the antiunitary particle-hole (PH) conjugation transformation in the condensed matter literature of $\nu = 5/2$ quantum Hall systems. We will see in Appendix E that among the $O(2)_{2,L}$ gauge theories with $L \in \mathbb{Z}_8$ classes, only $L = 1$ and 5 produce time-reversal-invariant theories. The $O(2)_{2,1}$ gauge theory will be later used for the particle-hole Pfaffian (PH-Pfaffian).

[15]Gauging this one-form symmetry identifies the $\mathbb{Z}_2$ gauge field in $(\mathbb{Z}_2)_0$ with the first Stiefel-Whitney class w_1 of the O(2) gauge field. Namely, the $\mathbb{Z}_2$ gauge field in $(\mathbb{Z}_2)_0$ is $w_1(E)$, with E the O(2) gauge bundle. The one-form symmetry involved is different from the center one-form symmetry of O(2). Note the $\mathbb{Z}_2$ electric line in the $\mathbb{Z}_2$ gauge theory with matter is topological, while the magnetic line is not topological.

[16]As discussed in Appendix E 1, the Hall conductivity only depends on the first Chern-Simons level in $O(2)_{2,L}$, while integrating out massive fermions in the sign representation only changes the second level L [37].

[17]The gauge Lie algebra of PO(4) is $\mathfrak{su}(2) \times \mathfrak{su}(2)$, hence the two θ angles.

(2) $\mathbb{Z}_4^{CT}$ symmetry. This is the particle-hole (PH) symmetry, also known as the CT symmetry. This is an antiunitary symmetry. Its normal subgroup is the $\mathbb{Z}_2^f$ fermion parity since $(CT)^2 = (-1)^f$. As mentioned, $\Psi^i(t,x) \to \epsilon^{ij}\gamma^0\Psi^j(-t,x)$ and $\phi(t,x) \to -\phi(-t,x)$.[18] We will further explain how the CT acts on the CS theories in TQFT sectors in Sec. III. The 't Hooft anomaly of the CT symmetry can be derived by adding a large time-reversal preserving mass m to the fermions and studying the anomaly in the infrared PH-Pfaffian theory $\mathrm{O}(2)_{2,1}$; our theory can have the $\nu \in \mathbb{Z}_{16}$ anomaly of CT symmetry with $\nu = 0$ for PH-Pfaffian$_+$ and $\nu = 8$ for PH-Pfaffian$_-$ [39–44].[19]

(3) $\mathbb{Z}_4$ one-form global symmetry [45] from the O(2) Chern-Simons theory. The $\mathbb{Z}_2$ subgroup is generated by the O(2) Wilson line in the determinant sign representation. The $\mathbb{Z}_4$ one-form symmetry has a 't Hooft anomaly, characterized by the spin-$\frac{1}{4}$ statistics of the generating line [46]. The 't Hooft anomaly of the one-form symmetry is related to the fractional part of the Hall conductivity (see Appendix E 1). We will not focus on this global symmetry in this work.

(4) $\mathbb{Z}_2$ magnetic 0-form symmetry of the O(2) gauge field [37]. We will not discuss this symmetry in this work.

(C) Gauge sector:[20]

$$\begin{aligned}
&\mathrm{O}(2)_{2,1}\ \mathrm{CS}\\
&\cong \frac{\mathrm{U}(1)_8 \times T_{L=1}}{\mathbb{Z}_2}\ \mathrm{CS}\\
&\cong \frac{\mathrm{U}(1)_8 \times [\overline{\mathrm{Ising}} \times (\text{spin-Ising})]}{\mathbb{Z}_2}\ \mathrm{CS}\\
&\cong \frac{\mathrm{U}(1)_8 \times \left(\frac{\mathrm{SU}(2)_{-2}\times \mathrm{U}(1)_4}{\mathbb{Z}_2} \times [\mathrm{SO}(3)_1 \times \mathrm{U}(1)_{-1}]\right)}{\mathbb{Z}_2}\ \mathrm{CS}. \quad (7)
\end{aligned}$$

The second line rewrites Ising and spin-Ising TQFTs as CS theories.[21] For background information on this sector, see Appendix E around Eq. (E2).

In the following subsections, we discuss several deformations of our theory (4). (1) In Sec. II C, we consider a CT-preserving mass deformation, but the CT symmetry turns out to be spontaneously broken. The deformation explicitly breaks $\mathrm{PO}(4) = \mathrm{O}(4)/\mathbb{Z}_2$ down to $[\mathrm{O}(2) \times \mathrm{O}(2)]/\mathbb{Z}_2$. (2) In Sec. II D, we add an odd polynomial potential in ϕ to our action, which explicitly breaks CT symmetry, but preserves the $[\mathrm{O}(2) \times \mathrm{O}(2)]/\mathbb{Z}_2$ symmetry [or PO(4) if $m = 0$]. (3) In Sec. II E, we add additional Majorana mass terms that break the entire PO(4) symmetry, but preserve the CT symmetry.

B. Physical arguments supporting the EFT

Here we provide some arguments and intuition to support our EFT from simple physical considerations, following the setup in Ref. [15] (see Fig. 4).

1. From gapless or gapped Fermi surfaces to four gapless Majorana nodes

The first question to ask about our EFT equation (4) is as follows: Why do we introduce two Dirac fermions (or four Majorana fermions)? This can be understood from solving the Bogoliubov–de Gennes (BdG) equation [15], which allows us to analyze the gap function $\Delta(\vec{k}, \vec{r})$ around the domain wall between the Pf and APf regions. We remind ourselves that the Pf and APf (and other related topological orders) can be obtained by the superconductivity (SC) pairing of composite fermions (CF) in the Halperin-Lee-Read (HLR) theory [7] or the superconductivity pairing of composite Dirac fermions (CDF) in Son's theory:

	CF (HLR)	CDF (Son)
Pf :	p wave,	d wave.
$K = 8$ state :	s wave,	p wave.
PHPf :	p^* wave,	s wave.
113 state :	d^* wave,	p^* wave.
APf :	f^* wave,	d^* wave.

(8)

The HLR and Son theories describe *gapless* theories with infinitely many gapless modes along a continuous Fermi surface [more precisely, a 1D Fermi circle for a $(2+1)$D theory]. However, we can gap the Fermi surface and go to a *gapped* theory by introducing the superconductivity pairing to CF or CDF as Eq. (8) above. Here we present the pairing gap function $\Delta(\vec{k}) \propto (k_x + ik_y)^{L_z}$ to obtain the five topological orders in the phase diagram Fig. 3, where s, p, d, f wave pairing has the z-directional angular momentum $L_z = 0, 1, 2, 3$, respectively, while the complex conjugate p^*, d^*, f^* wave pairing has the opposite sign of the angular momentum.

We can find that in the CF (HLR's) picture, the pairing function is $\Delta(\vec{k}, \vec{r}) = \Delta_{\mathrm{Pf}}(\mathbf{r})e^{i\theta_k} - \Delta_{\mathrm{APf}}(\mathbf{r})e^{-i3\theta_k} \propto |\Delta|e^{-i\theta_k}\sin(2\theta_k)$; while in the CDF (Son's) picture, the pairing function is $\Delta(\vec{k}, \vec{r}) = \Delta_{\mathrm{Pf}}(\mathbf{r})e^{i2\theta_k} - \Delta_{\mathrm{APf}}(\mathbf{r})e^{-i2\theta_k} \propto$

[18] There are also other discrete charge C and parity P symmetries for our EFT as a Lorentz-invariant QFT, which should be familiar to the readers. There are also other time-reversal symmetries given by composing this antiunitary symmetry with additional $\mathbb{Z}_2$ subgroup unitary symmetries.

[19] There are two versions of PH-Pfaffian$_\pm$ depending on how $(CT)^2$ assigns to the odd $q = 1, 3, 5, 7$ anyons of $\mathrm{U}(1)_8$ (see [39,41,42] and Sec. III). The two choices are related by shifting the background gauge field for the $\mathbb{Z}_2$ subgroup one-form symmetry (generated by a fermion line) by w_1^2 (see also [44]). Readers should beware that we use ν as topological classification index while ν as filling fraction.

[20] Readers may be curious about how the semidirect product gauge structure of $[\mathrm{O}(2)] = [\mathrm{SO}(2) \rtimes \mathbb{Z}_2^C]$ in $\mathrm{O}(2)_{2,L}$ can be related to the direct product gauge structure of $[\mathrm{U}(1)]$ and $[\mathbb{Z}_2]$ in $\frac{\mathrm{U}(1)_8 \times T_L}{\mathbb{Z}_2}$ CS with T_L as some $L \in \mathbb{Z}_8$ class of $[\mathbb{Z}_2]$ gauge theory. The answer is that there is a duality between the two gauge theories at the level 2 of $\mathrm{O}(2)_{2,L}$ (see [37] and Appendix E).

[21] The Ising TQFT can be expressed as a non-Abelian CS theory with a gauge group $\mathrm{U}(2)_{2,-4} \cong [\mathrm{SU}(2)_2 \times \mathrm{U}(1)_{-4}]/\mathbb{Z}_2$ from [47]. By $\mathrm{SO}(3)_1$, we denoted the spin-CS theory with the level normalized such that the states on a 2-torus T^2 are subset of $\mathrm{SU}(2)_2$ states corresponding to odd SU(2) representations (**1** and **3**). The spin-Ising TQFT is given by the $[\mathrm{SO}(3)_1 \times \mathrm{U}(1)_{-1}]$ CS.

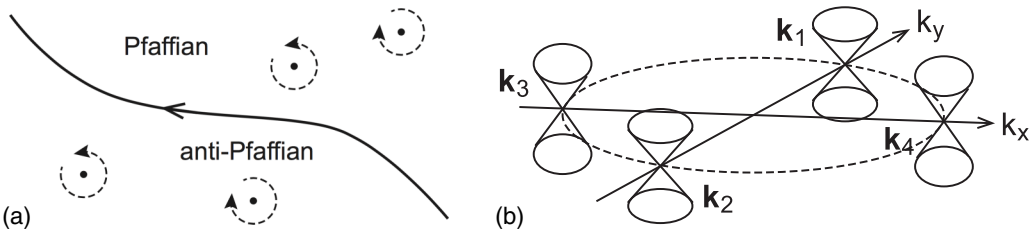

FIG. 4. Follow the setup in Ref. [15]. (a) By solving the BdG equation in the mean-field, single-particle, semiclassical quantum mechanical manner [15], we can analyze the gap function $\Delta(\vec{k}, \vec{r})$ around the domain wall between the Pf and APf regions. There are also $\pm\pi$ vortices shown in dashed circles. (b) Four Dirac nodes solved from the BdG equation on Pf | APf domain wall in a momentum $\vec{k}$ space. Due to BdG Nambu space double counting, we only have physical degrees of freedom of two Dirac nodes or four Majorana nodes. The four Majorana nodes are precisely the fermion nodes that we need in our EFT that we study in the real space.

$|\Delta| \sin(2\theta_k)$.[22] In either case, the $\sin(2\theta_k)$ gives four gapless nodes around the otherwise fully gapped Fermi surface at $\theta_k = 0, \pi/2, \pi, 3\pi/2$, when we are spatially near the Pf | APf domain wall. Thus, Ref. [15] finds four Dirac nodes solved from the BdG equation on Pf | APf domain wall in a momentum $\vec{k}$ space. Due to BdG Nambu space double counting degrees of freedom at $\vec{k}$ and $-\vec{k}$, we only have physical degrees of freedom of two Dirac nodes or equivalently four Majorana nodes. The four Majorana nodes explain precisely the origin of the fermions that we need in our EFT equation (4) that we study in the real space. Furthermore, it will become clear in the later subsections how the additional gauge theory sectors and deformations can help to span the full phase diagram Fig. 4. This physical picture helps to motivate our EFT.

Our EFT, including the deformations, can describe both the gapped TQFT phases and gapless topological quantum phase transitions predicted in the phase diagram Fig. 3, similarly to the percolating phases and transitions in Ref. [15]. For condensed-matter purposes, we remark that the $(2+1)$D gapless phases in our Lorentz-invariant EFT have four interacting Majorana fermions [$(2+1)$D Majorana cones in a momentum $\vec{k}$ space, in the noninteracting band theory limit in Fig. 4(b)] but without a Fermi surface; the Fermi surface is gapped and left with only isolated gapless nodes. In other words, we emphasize that the $(2+1)$D gapless phase transitions in our EFT are similar to that of a *semimetallic* phase transition with isolated gapless nodes, instead of a *metallic* phase transition with a gapless continuous Fermi surface.

2. *More on energy and length scales, and emergent symmetries*

Before we dive into the detailed phase diagrams of our EFT in the next subsections, we first summarize what we expect from the story in Ref. [15], about the energy and length scales (see also footnote 11), and emergent symmetries of the system.

We take the limit of no Landau-level mixing (LLM), so the energy gap between Landau levels from the cyclotron frequency $\omega_c = B/m \gg \Lambda_2 = e^2/\epsilon\ell_B \sim \sqrt{B}$ is assumed to be much larger than the Coulomb energy scale, which we set to be Λ_2, the disorder energy scale in Fig. 3. The $\ell_B = \sqrt{\hbar c/eB}$ is the magnetic length scale. There is yet another length scale set by the domain wall width w, which is microscopically related to the phase-coherence length ℓ_φ of superconducting pairing fluctuations in the composite fermion picture of Eq. (8).

Reference [15] analyzes the relation between energy and length scales and emergent symmetries of the $(1+1)$D domain wall, showing the following:

(i) The disorder energy $\Lambda \sim 1/\ell$ (the vertical axis of Fig. 3) is related to the domain length scale ℓ which controls the Pf and APf puddle sizes.

(ii) The energy scale Λ_2 is defined by the inverse of magnetic length scale $\ell_B = \sqrt{\hbar c/eB}$. The Λ_2 is around the Fermi energy of the composite fermion.

(iii) The energy scale Λ_1 is defined by the inverse of the correlation length ℓ_φ of superconducting phase pairing fluctuations in the composite fermion picture of Pf and APf, which is also related to the inverse of the domain wall width w.

(iv) When the disorder energy scale $\Lambda < \Lambda_1$, we have weaker disorder and hence larger Pf and APf puddle sizes, so the domain length scale ℓ is large. For large ℓ, the $(1+1)$D four Majorana edge modes running on the domain wall can be mixed together via scattering along the domain wall, which induces an emergent O(4) symmetry and a uniform velocity.[23]

(iv) When the disorder energy Λ scale sits at $\Lambda_2 > \Lambda > \Lambda_1$, then Λ is below the Coulomb energy $e^2/\epsilon\ell_B$ and the Fermi energy $\overline{v}k_F$ set by Λ_2. The Λ is also below some factor of the magnitude of SC gap size $|\Delta|$. This implies that, from Fig. 4(b), the two physical Dirac nodes solved from BdG have internal symmetries O(2) × O(2), where each O(2) rotates the two Majorana nodes of a given Dirac node.

(v) When the disorder energy scale $\Lambda > \Lambda_2$, we have stronger disorder $\Lambda \sim 1/\ell$, hence smaller Pf and APf puddle

[22] In general, $\vec{k} = -i\frac{\partial}{\partial \vec{r}}$ is a differential operator in a disordered system since $[\vec{k} = -i\frac{\partial}{\partial \vec{r}}, H(\vec{k}, \vec{r})] \neq 0$ and $\vec{k}$ is not a good quantum number globally. See the detailed analysis in [15].

[23] Reference [15] also uses a BKT-type perturbative analysis to show that, regardless of spatial fluctuations (from impurity) or temporal fluctuations (from the SC pairing phase), the velocity fluctuation correlation function $\langle \delta v_I(x) \delta v_I(x') \rangle = W_v \delta(x - x')$ has an irrelevant perturbation driven by the phase fluctuation. This means the the $\langle \delta v_I(x) \delta v_I(x') \rangle$ flows to zero. Therefore, with weak disorder $\Lambda < \Lambda_1$, either at zero temperature or some small finite temperature (the experiment is performed around $10 \sim 30$ mK [10]), we have an emergent O(4) symmetry.

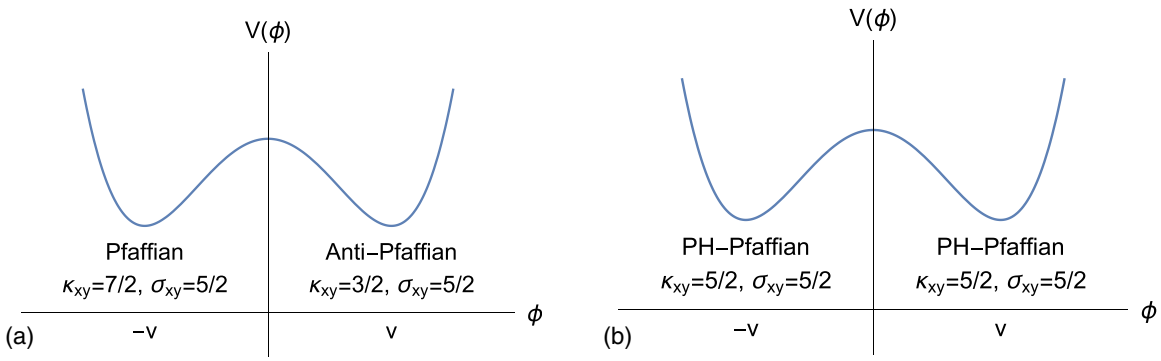

FIG. 5. The theories comprising the vacua of the system (4) depend on the deformation m. (a) No disorder $m \sim 0$. (b) Strong disorder $|m| > gv$.

sizes, so the domain length scale ℓ is smaller. For smaller ℓ, it is difficult to mix the $(1+1)$D four Majorana edge modes running on the domain wall, so we expect only the fermion parity symmetry when $\Lambda > \Lambda_2$. The $O(2) \times O(2)$ symmetry will be broken when $\Lambda > \Lambda_2$ because the disorder is strong enough to exceed the gap size $|\Delta|$ or even the Fermi energy $\overline{v}k_F$, so the Dirac nodes in Fig. 4(b) fluctuate and their dispersion and energy spectra can overlap with each other. Because of this, we can no longer make sense of the two internal rotational symmetries.

To summarize all the length scales, we have

$$\begin{aligned} \text{lattice cutoff } a_{\text{lattice}} &< \text{magnetic length } \ell_B \\ &< \text{domain wall width } w \\ &\simeq \text{phase-coherence length } \ell_\varphi \\ &\lesssim \text{our EFT typical length scale } \xi \\ &< \text{sample size } L. \end{aligned} \tag{9}$$

The energy scales are given by the inverse of length scales:

$$a_{\text{lattice}}^{-1} > \Lambda_2 = \ell_B^{-1} > \Lambda_1 = \ell_\varphi^{-1} \simeq w^{-1} \gtrsim \xi^{-1} > L^{-1}. \tag{10}$$

C. Particle-hole (time-reversal CT) preserving deformation

Let us turn on the deformation m in Eq. (4).

$0 \leqslant m < gv$. When m increases from zero to gv, the theory has the following phases in the two vacua:

(1) At the vacuum $\langle\phi\rangle = -v$, Ψ^1 has mass $m - gv$, while Ψ^2 has mass $-m - gv$. For m below gv, at low energies we can integrate out both negative mass Dirac fermions, and the theory becomes the gapped TQFT:

$$\text{Pfaffian}: \quad O(2)_{2,-1}\ \text{CS} - 5\text{CS}_{\text{grav}}. \tag{11}$$

The $O(2)_{2,L}$ Chern-Simons gauge theory (see Appendix E) contains a $U(1)_8$ Chern-Simons theory that contributes a net chiral central charge $c_- = c_L - c_R = 1$, while the matter sectors do not contribute any net chiral central charge. The theory has Hall conductivity σ_{xy} and thermal Hall conductivity κ_{xy} matching those of the Pfaffian state:[24]

$$\sigma_{xy} = 5/2, \quad \kappa_{xy} = 1 + 5/2 = 7/2.$$

(2) At the vacuum $\langle\phi\rangle = +v$, Ψ^1 has mass $m + gv$, while Ψ^2 has mass $-m + gv$. For m below gv, then at low energies we can integrate out the two positive mass Dirac fermions, and the theory becomes the gapped TQFT

$$\text{anti-Pfaffian}: \quad O(2)_{2,3}\ \text{CS} - \text{CS}_{\text{grav}}. \tag{12}$$

The theory has Hall conductivity σ_{xy} and thermal Hall conductivity κ_{xy}:

$$\sigma_{xy} = 5/2, \quad \kappa_{xy} = 1 + 1/2 = 3/2.$$

The TQFT becomes, under level and rank duality [37,38], $O(2)_{2,3} \leftrightarrow O(2)_{-2,1}$ up to 4CS_{grav}, and thus it is the time-reversal image of the Pfaffian theory.

The two different regimes capturing our time-reversal-symmetric deformations are depicted in Fig. 5.

$m = gv$. When $m = gv = g|\langle\phi\rangle|$, one of the Dirac fermions becomes massless, and the theories are[25]

$$\begin{aligned} \langle\phi\rangle = -v: &\quad O(2)_{2,0}\ \text{CS} + \Psi^1 \text{ in } \mathbf{1}_{\text{odd}} - 4\text{CS}_{\text{grav}}, \\ \langle\phi\rangle = +v: &\quad O(2)_{2,2}\ \text{CS} + \Psi^2 \text{ in } \mathbf{1}_{\text{odd}} - 2\text{CS}_{\text{grav}}. \end{aligned} \tag{13}$$

$m > gv$. When $m > gv$, the two Dirac fermions acquire masses of *opposite* signs, and the two vacua become the *same* gapped TQFT:

$$\text{PH-Pfaffian}: \quad O(2)_{2,1}\ \text{CS} - 3\text{CS}_{\text{grav}}. \tag{14}$$

The theory has the Hall conductivity σ_{xy} and thermal Hall conductivity κ_{xy}:

$$\sigma_{xy} = 5/2, \quad \kappa_{xy} = 1 + 3/2 = 5/2.$$

With m treated as a proxy for disorder strength (the precise relation is discussed in Sec. II F), the gapped phases in the above discussion are precisely those that appear in the scenario of [14,15]: for small disorder strength, the microscopic theory is at a first-order-like phase transition with coexisting Pfaffian and anti-Pfaffian phases, while increasing the disorder strength produces the PH-Pfaffian phase. From the above discussion, it is thus natural to identify the parameter m (or its magnitude $|m|$) in the effective phenomenological theory with the disorder strength in the microscopic material.

[24] The spin gravitational Chern-Simons term has chiral edge modes contributing to the thermal Hall conductivity κ_{xy} by a chiral central charge $c_- = -1/2$; see Appendix A.

[25] For $m = gv$, when $\langle\phi\rangle = -v$, the fermion Ψ^1 becomes massless; when $\langle\phi\rangle = +v$, Ψ^2 becomes massless.

We remark that the first-order phase transition with distinct gapped vacua persists for a range of the parameter $m \in [0, gv)$, which is consistent with the phase diagram proposed in [14,15]. We may identify Λ_1 in [14,15] with gv, with v controlled by the scalar mass μ in the effective theory. When gv is small, the phase diagram approaches that described in [13,14].

D. Particle-hole (time-reversal CT) breaking deformation

In this section, we investigate the effect of adding a time-reversal breaking deformation that preserves the $\frac{O(2)\times O(2)}{\mathbb{Z}_2}$ symmetry ($\frac{O(4)}{\mathbb{Z}_2}$ when $m = 0$). In the experiment, this corresponds to applying an additional time-reversal breaking magnetic field that changes the filling fraction ν slightly. In this discussion, we set the Yukawa coupling to $g = 1$ for simplicity.

Since ϕ is a time-reversal-odd pseudoscalar field, we consider the simple time-reversal breaking deformation given by an odd polynomial of ϕ. The most relevant deformation will be $\delta V(\phi) \propto -m_{\rm odd}\,\phi$. This modifies the scalar potential and lifts the degenerate vacua.

In the lowest-order approximation, we can take the effect to be such that the original vacua shift to the locations $\langle\phi\rangle = v + m_{\rm odd} + \mathcal{O}(m_{\rm odd}^2)$ and $-v + m_{\rm odd} + \mathcal{O}(m_{\rm odd}^2)$. Depending on the sign of $m_{\rm odd}$, one of the above is the true vacuum: for $m_{\rm odd} > 0$ it is the former and for $m_{\rm odd} < 0$ it is the latter. In other words, the true vacuum has a vev

$$\begin{aligned}\langle\phi\rangle &= v\,\mathrm{sgn}(m_{\rm odd}) + m_{\rm odd} + \mathcal{O}\big(m_{\rm odd}^2\big)\\ &= (v + |m_{\rm odd}|)\,\mathrm{sgn}(m_{\rm odd}) + \mathcal{O}\big(m_{\rm odd}^2\big).\end{aligned}$$

The two Dirac fermions then have masses given by (with $g = 1$)

$$\begin{aligned}m_1 &= m + \langle\phi\rangle = m + m_{\rm odd} + v\,\mathrm{sgn}(m_{\rm odd}) + \mathcal{O}\big(m_{\rm odd}^2\big),\\ m_2 &= -m + \langle\phi\rangle = -m + m_{\rm odd} + v\,\mathrm{sgn}(m_{\rm odd}) + \mathcal{O}\big(m_{\rm odd}^2\big).\end{aligned} \tag{15}$$

There are critical lines when any of the fermions become massless.[26]

The phase diagram whose coordinates are our two parameters $(m, m_{\rm odd})$ for a fixed v is given in Fig. 6. Given by the mass deformation formula (15), the left critical line in Fig. 6 has $m_2 \simeq 0$, while the right critical line in Fig. 6 has $m_1 \simeq 0$. It is in qualitative agreement with the schematic phase diagram discussed in [14,15], and suggests that the corresponding Pf|PHPF and APf|PHPf phase boundaries are given by second-order phase transitions.

E. $K = 8$ and 113 states from $\frac{O(2)\times O(2)}{\mathbb{Z}_2}$ breaking masses

In our earlier discussion, we mainly focused on mass deformations preserving the $\frac{O(2)\times O(2)}{\mathbb{Z}_2}$ symmetry that transforms the two Dirac fermions. If we allow Majorana masses that break the $\frac{O(2)\times O(2)}{\mathbb{Z}_2}$ symmetry, the effective theory can also describe the $K = 8$ state and the 113 state (the two states are related to one another by the particle-hole CT symmetry). Denote the four Majorana fermions by η_{ia} where $i = 1, 2$ labels the Dirac fermions and $a = 1, 2$ labels the Majorana components. Consider the Majorana mass deformation[27]

$$\begin{aligned}&-M(m)\big(\eta_{11}^2 - \eta_{12}^2 - \eta_{21}^2 + \eta_{22}^2\big),\\ &M(m) = \epsilon(m - m^*)\Theta(m - m^*),\end{aligned} \tag{16}$$

where ϵ is a small number, Θ is the step function: $\Theta(x) = 0$ for $x \leqslant 0$ and $\Theta(x) = 1$ for $x > 0$. Then, the deformation is only nonzero when $m > m^*$, where we take $m^* > gv$. The deformation preserves the time-reversal CT symmetry. The four Majorana fermions have

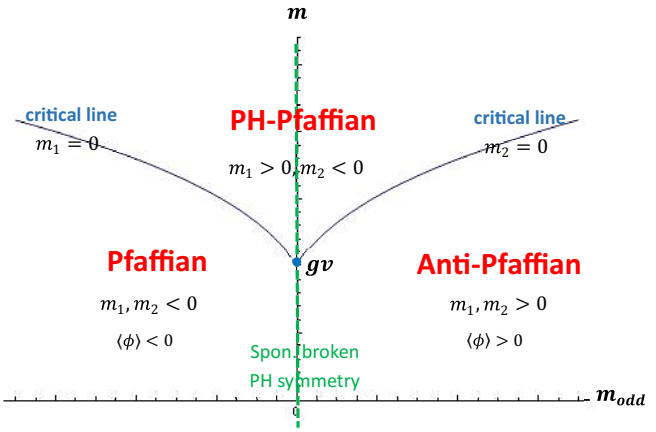

FIG. 6. Phase diagram of the theory (4) deformed by the PH-symmetry breaking scalar potential $\delta V(\phi) = -m_{\rm odd}\,\phi$. Phase boundaries are plotted *analytically* by *Mathematica*. Here, the parameter m is from the Dirac mass term in (4). The m_1 and m_2 are the induced masses in the IR for the ground states: $m_1 = m + g\langle\phi\rangle$, $m_2 = -m + g\langle\phi\rangle$. The blue lines are critical lines where one of the Dirac fermions becomes massless, joined by blue dots where both fermions are massless at a critical $m = gv = g|\langle\phi\rangle|$. The green line in the middle represents a first-order phase transition with spontaneously broken time-reversal symmetry (i.e., antiunitary particle-hole symmetry) that gives rise to domain wall excitations that interpolate between the Pfaffian and anti-Pfaffian phases. The phase diagram is in qualitative agreement with the schematic phase diagram discussed in [14,15] with the time-reversal breaking deformation $m_{\rm odd}$ identified with the external magnetic field in the experiment and the time-reversal preserving deformation $|m|$ identified with the microscopic disorder strength. In experiment, it is so far undetermined whether Pfaffian or anti-Pfaffian is favored at $\nu < \nu_c \simeq 5/2$ (or $\nu > \nu_c \simeq 5/2$); we can easily flip our phase diagram by defining the sign of $m_{\rm odd}$ to match the tuning parameter for the filling fraction ν.

[26]The situation is similar to Eq. (13). One might worry that the critical line can receive a quantum correction; however, since the scalar field has a mass of the order $m_\phi \propto \mu$ around the vacuum, in the vicinity of the critical line with distance less than m_ϕ there is a light fermion.

[27]We take $(\gamma^0)_{\alpha\beta} = (i\sigma^y)_{\alpha\beta} = \epsilon_{\alpha\beta}$ with the spinor indices α, β. Note that the Dirac mass term $\overline{\Psi}^j\Psi^j = \Psi^{j\dagger}\gamma^0\Psi^j$. In the Majorana basis, we write $\Psi^j = \eta_{j1} + i\,\eta_{j2}$, and $\overline{\Psi}^j\Psi^j = \epsilon_{\alpha\beta}(\eta_{j1,\alpha}\eta_{j1,\beta} + \eta_{j2,\alpha}\eta_{j2,\beta}) \equiv (\eta_{j1}^2 + \eta_{j2}^2)$. We define the Majorana mass term as $\epsilon_{\alpha\beta}\eta_\alpha\eta_\beta \equiv \eta^2$.

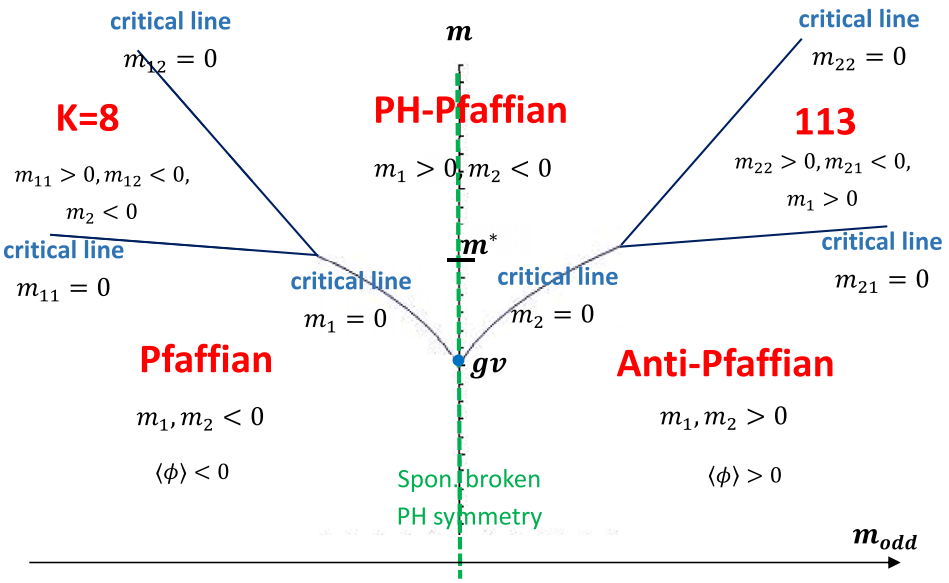

FIG. 7. Phase diagram of the theory (4) deformed by the PH-symmetry breaking term $\delta V(\phi) = -m_{\text{odd}}\phi$ and the Majorana mass $M(m)$. Here, the parameter m is from the Dirac mass term in (4). We abbreviate $m_{11}, m_{12} < 0$ as $m_1 < 0$, etc. Phase boundaries can be plotted *analytically* by *Mathematica*.

masses

$$\begin{aligned} m_{11} &= m + g\langle\phi\rangle + M(m), \\ m_{12} &= m + g\langle\phi\rangle - M(m), \\ m_{21} &= -m + g\langle\phi\rangle - M(m), \\ m_{22} &= -m + g\langle\phi\rangle + M(m), \end{aligned} \tag{17}$$

where the vev $\langle\phi\rangle = v\,\text{sgn}(m_{\text{odd}}) + m_{\text{odd}} + \mathcal{O}(m_{\text{odd}}^2)$ depends on the CT symmetry-breaking deformation m_{odd}.

What becomes of the phase diagram under the deformation? For $m \leqslant m^*$ it is the same as before, while for $m > m^*$ there are new gapped phases:

(i) $m_{21}, m_{22} < 0$ and $m_{12} < 0, m_{11} > 0$. The theory flows to

$$K = 8 \text{ state:} \quad \text{O}(2)_{2,0}\,\text{CS} - 4\text{CS}_{\text{grav}}, \tag{18}$$

as a $\text{U}(1)_8$ CS theory or, equivalently, the Abelian $K = 8K$ matrix CS theory. If we write the $\text{U}(1)_8$ CS one-form gauge field as b, and the $\text{U}(1)_{\text{EM}}$ gauge field as A, then the action is $\int \frac{8}{4\pi} b\,db + \frac{2b}{2\pi} dA - 4\text{CS}_{\text{grav}}$, up to a trivial spin-TQFT to represent a fermionic gapped sector (see Appendix A of [15]). It has quantum Hall conductivity and thermal Hall conductivity

$$\sigma_{xy} = 5/2, \quad \kappa_{xy} = 1 + 2 = 3.$$

(ii) $m_{11}, m_{12} > 0$ and $m_{21} < 0, m_{22} > 0$. The theory flows to

$$113 \text{ state} : \text{O}(2)_{2,2}\,\text{CS} - 2\text{CS}_{\text{grav}} \leftrightarrow \text{U}(1)_{-8}\,\text{CS} - 6\text{CS}_{\text{grav}}, \tag{19}$$

where we used the duality $\text{O}(2)_{2,2} \leftrightarrow \text{O}(2)_{-2,0} - 4\text{CS}_{\text{grav}}$ [37] and $\text{O}(2)_{2,0} \leftrightarrow \text{U}(1)_8$. This phase is called the 113 state since it can be described by the 3D Abelian Chern-Simons theory action, with one-form gauge field b, as

$$\frac{K_{IJ}}{4\pi} \int b_I db_J - 4\text{CS}_{\text{grav}}, \text{ with a } K \text{ matrix } \begin{pmatrix} 1 & 3 \\ 3 & 1 \end{pmatrix}.$$

It has quantum Hall conductivity and thermal Hall conductivity

$$\sigma_{xy} = 5/2, \quad \kappa_{xy} = -1 + 1 + 2 = 2.$$

It is related to the previous phase by the antiunitary particle-hole symmetry (up to an anomaly).

In addition, there are critical lines separating the gapped phases where some of the fermions become massless. The phase diagram is in Fig. 7. In the rest of the discussion we will focus on the case without the deformation $M(m)$.

F. Random coupling and the thermal metal phase

In the theory (4), we can further choose the parameter m to be a random coupling with Gaussian distribution

$$\overline{m} = m_0, \quad \overline{m^2} = \delta^2. \tag{20}$$

The theory depends on the average m_0 and the fluctuation δ. In [48], it is found that for strong fluctuations $\delta \to \infty$, the system of free Dirac fermions becomes a thermal metal. We will set the magnitude of fluctuation to be

$$\delta = h(m_0) \tag{21}$$

for some non-negative, monotonically increasing function h that grows faster than a linear function [for instance, $h(m_0) = m_0^2$]. Then, m_0 controls the disorder strength of the system. At large enough m_0, i.e., strong disorder, the fluctuation becomes sufficiently strong and the model (4) with random coupling m enters a thermal metal phase. Since in our model the electromagnetic background field only couples to the O(2) gauge field and does not couple to the fermions, the Hall conductivity does not depend on the mass of the fermions and remains

TABLE I. Pfaffian data from $\frac{\mathrm{U}(1)_8\times\mathrm{Ising}}{\mathbb{Z}_2}$ CS. We provide $(\exp(i2\pi s), Q/e)$ for 12 anyons. The σ_{-1} anyon has $e^{i\frac{\pi}{8}}$ statistics.

Pfaffian	$\mathrm{U}(1)_8$ CS							
$T_{L=-1}$	0	1	2	3	4	5	6	7
1	$(+1,0)$		$(+i,\frac{1}{2})$		$(+1,1)$		$(+i,\frac{3}{2})$	
σ_{-1}		$(e^{i\frac{\pi}{4}},\frac{1}{4})$		$(-e^{i\frac{\pi}{4}},\frac{3}{4})$		$(-e^{i\frac{\pi}{4}},\frac{5}{4})$		$(e^{i\frac{\pi}{4}},\frac{7}{4})$
f	$(-1,0)$		$(-i,\frac{1}{2})$		$(-1,1)$		$(-i,\frac{3}{2})$	

the same value $\sigma_{xy}=\frac{5}{2}$. This is consistent with the proposal in [14,15].

Near the critical lines of the phase diagram, the physical mass of one of the fermions becomes close to zero. If the disorder strength is nonzero for zero mass, $h(0)>0$, the disorder will cause the region sufficiently near the critical lines to have thermal metal behavior, which accommodates the behavior described in [14] and illustrated in Fig. 3.

III. ANYONIC EXCITATIONS AND QUANTUM OBSERVABLES FROM THE EFT

Let us spell out the key properties of the TFT phases and their anyonic excitations.[28] We assume standard knowledge from the Chern-Simons (CS) description of fQHE. We will delineate the following: (a) fractionalized anyon statistics, i.e., the spin or exchange statistics $\exp(i2\pi s)$ of anyons with spin s; (b) fractionalized $\mathrm{U}(1)_{\mathrm{EM}}$ electromagnetic charge Q/e (e is the electron charge); (c) their PH-symmetry (time-reversal CT) transformation properties.

They are summarized in Tables I, II, III, IV, and V, for the Pfaffian, anti-Pfaffian, PH-Pfaffian, $K=8$, and 113 states, respectively, in the notation

$$(\exp(i2\pi s), Q/e). \tag{22}$$

For the PH-Pfaffian, since it enjoys PH symmetry (time-reversal CT), we also specify the $(CT)^2$ quantum number for the appropriate anyons, and write

$$(\exp(i2\pi s), Q/e)_{(CT)^2}. \tag{23}$$

We will first examine the non-Abelian states, i.e., the Pfaffian in Eq. (11), anti-Pfaffian in Eq. (12), and PH-Pfaffian in Eq. (14). They can be written as the following Chern-Simons theories (see Appendix A of Ref. [15], and Appendix E):

$$\text{Pfaffian:}\quad \frac{\mathrm{U}(1)_8\times\mathrm{Ising}}{\mathbb{Z}_2}-4\mathrm{CS}_{\mathrm{grav}},\qquad c_-=1+1/2+4/2=7/2, \tag{24}$$

$$\text{PH-Pfaffian:}\quad \frac{\mathrm{U}(1)_8\times\overline{\mathrm{Ising}}}{\mathbb{Z}_2}-4\mathrm{CS}_{\mathrm{grav}},\qquad c_-=1-1/2+4/2=5/2, \tag{25}$$

$$\text{Anti-Pfaffian:}\quad \frac{\mathrm{U}(1)_8\times\mathrm{SU}(2)_{-2}}{\mathbb{Z}_2}-4\mathrm{CS}_{\mathrm{grav}},\qquad c_-=1-3/2+4/2=3/2, \tag{26}$$

with their chiral central charges $c_-=\kappa_{xy}$. These TQFTs are obtained from gauging a diagonal one-form $\mathbb{Z}_2$ symmetry in the [$\mathrm{U}(1)_8$ CS theories] and the ($\nu\in\mathbb{Z}_8$-class spin-TQFTs)[29] in $(2+1)$D. More generally, these TQFTs are $\frac{\mathrm{U}(1)_8\times T_L}{\mathbb{Z}_2}$ for $L=-1,+1,+3$, and one gauges a diagonal $\mathbb{Z}_2$ one-form symmetry generated by the composite line given by the tensor product of the charge-4 Wilson line of $\mathrm{U}(1)_8$ and a nontransparent fermion line in T_L. See Appendix E for details on the T_L theories. When gauging a diagonal $\mathbb{Z}_{2,[1]}$ symmetry, we identify their *charged objects* [the line with odd U(1) charge in $\mathrm{U}(1)_8$ and the σ line in T_L] and their *symmetry generators* or *charge operators* [the operator with U(1) charge 4 in $\mathrm{U}(1)_8$ and the f line in T_L]. This reduces the 24 anyons in the quasiexcitation spectrum of $\mathrm{U}(1)_8\times T_L$ theory to the 12 anyons in the $\frac{\mathrm{U}(1)_8\times T_L}{\mathbb{Z}_2}$ theory.

(1) *Spin statistics*. The spin of an anyon is given by

$$\exp(i2\pi s)=\exp\left[i2\pi\left(s_{\mathrm{nab}}+\frac{q^2}{2K}\right)\right], \tag{27}$$

[28]The world line of an anyon in quantum Hall liquids corresponds to a line operator in the low-energy effective TQFT.

[29]Here, the $(2+1)$D $\nu\in\mathbb{Z}_8$ class spin TQFTs are obtained from gauging the $\mathbb{Z}_2$ internal "Ising" symmetry of the $(2+1)$D fermionic $\mathbb{Z}_2\times\mathbb{Z}_2^f$ SPTs, with fermion parity symmetry $\mathbb{Z}_2^f$ [47,49]. From this class of TQFTs, we will use the Ising, $\overline{\mathrm{Ising}}$, and $\mathrm{SU}(2)_{-2}$ cases.

TABLE II. Anti-Pfaffian data from the $\frac{\mathrm{U}(1)_8\times\mathrm{SU}(2)_{-2}}{\mathbb{Z}_2}$ CS. We provide $(\exp(i2\pi s), Q/e)$ for 12 anyons. The σ_3 anyon has $e^{-i\frac{3\pi}{8}}$ statistics.

Anti-Pfaffian	$\mathrm{U}(1)_8$ CS							
$T_{L=3}$	0	1	2	3	4	5	6	7
1	$(+1,0)$		$(+i,\frac{1}{2})$		$(+1,1)$		$(+i,\frac{3}{2})$	
σ_3		$(e^{-i\frac{\pi}{4}},\frac{1}{4})$		$(-e^{-i\frac{\pi}{4}},\frac{3}{4})$		$(-e^{-i\frac{\pi}{4}},\frac{5}{4})$		$(e^{-i\frac{\pi}{4}},\frac{7}{4})$
f	$(-1,0)$		$(-i,\frac{1}{2})$		$(-1,1)$		$(-i,\frac{3}{2})$	

TABLE III. PH-Pfaffian data from $\frac{\mathrm{U}(1)_8\times\overline{\mathrm{Ising}}}{\mathbb{Z}_2}$ CS. We provide $(\exp(i2\pi\mathrm{s}), Q/e)$ or $(\exp(i2\pi s), Q/e)_{(CT)^2}$ for 12 anyons. The σ_1 anyon has $e^{-i\frac{\pi}{8}}$ statistics. In comparison, Ref. [17] represents related TQFT data in terms of $\frac{\mathrm{U}(1)_{-8}\times\mathrm{Ising}}{\mathbb{Z}_2}$ CS. Moreover, there are two versions PH-Pfaffian$_\pm$ depending on how $(CT)^2$ assigns to the odd $q = 1, 3, 5, 7$ of $\mathrm{U}(1)_8$.

PH-Pfaffian$_\pm$	$\mathrm{U}(1)_8$ CS							
$T_{L=1}$	0	1	2	3	4	5	6	7
1	$(+1,0)_1$		$(+i,\frac{1}{2})$		$(+1,1)_{-1}$		$(+i,\frac{3}{2})$	
σ_1		$(1,\frac{1}{4})_{\pm1}$		$(-1,\frac{3}{4})_{\mp1}$		$(-1,\frac{5}{4})_{\mp1}$		$(1,\frac{7}{4})_{\pm1}$
f	$(-1,0)_1$		$(-i,\frac{1}{2})$		$(-1,1)_{-1}$		$(-i,\frac{3}{2})$	

where K is the level of Abelian CS theory, and q is the integer labeling the Abelian anyon associated with the line operator $e^{iq\oint b}$ of one-form gauge field b.[30] Here, $\mathrm{s}_{\mathrm{nab}}$ means the spin from the non-Abelian sector of the TQFT. For the Ising, $\overline{\mathrm{Ising}}$, and $\mathrm{SU}(2)_{-2}$ TQFTs in Eqs. (24), (25), and (26), their $\mathrm{s}_{\mathrm{nab}}$ for the $(1,\sigma,f)$ anyons are given by the diagonal of the modular T matrix: $(1, e^{i\frac{\pi}{8}}, -1)$, $(1, e^{-i\frac{\pi}{8}}, -1)$, and $(1, e^{-i\frac{3\pi}{8}}, -1)$, respectively. See, e.g., [15] for the data.

(2) *Electromagnetic charge.* For the anyon's $\mathrm{U}(1)_{\mathrm{EM}}$ charge Q/e, we can look at the coupling q of the electric current to the $\mathrm{U}(1)_{\mathrm{EM}}$ gauge field A. The charge can be changed by an integer by tensoring the line with a classical Wilson line $\oint A$.[31] The $\mathrm{U}(1)_{\mathrm{EM}}$ charge Q and the Hall conductance σ_{xy} can be computed via (see Appendix E for details)

$$Q/e = K^{-1}q, \quad \sigma_{xy} = qK^{-1}q = q(Q/e). \tag{28}$$

Based on the experimental constraint of $\sigma_{xy} = \nu = 1/2$, we have to introduce the appropriate $\mathrm{U}(1)_{\mathrm{EM}}$ coupling $\int \frac{2b}{2\pi} dA = \int \frac{1}{2\pi}(2b)dA$ to the action for the $\frac{\mathrm{U}(1)_8\times T_L}{\mathbb{Z}_2}$ theory, where the $\mathrm{U}(1)_8$ CS theory action is $\int \frac{8}{4\pi} b\,db$. This is a coupling with charge $q = 2$. Indeed, this gives half-filled $\nu = \sigma_{xy} = qK^{-1}q = 2^2/8 = 1/2$. The anyon with U(1) charge 2 is identified with the non-Abelian σ anyon in the gauged $\frac{\mathrm{U}(1)_8\times T_L}{\mathbb{Z}_2}$ CS theory. This non-Abelian anyon has $\mathrm{U}(1)_{\mathrm{EM}}$ charge $Q/e = K^{-1}q = 2/8 = 1/4$. We can obtain all 12 anyons' $\mathrm{U}(1)_{\mathrm{EM}}$ charges by the same argument, with the results shown in Tables I, II, and III.

(3) *PH symmetry*. In the PH-Pfaffian theory, PH symmetry (or time reversal CT) is preserved, so to those anyons not permuted by the time-reversal symmetry, whose spin statistics $\exp(i2\pi\mathrm{s})$ are real valued,[32] we can assign $(CT)^2 = \pm1$ quantum numbers. For those anyons α_a whose spin statistics $\exp(i2\pi\mathrm{s})$ are complex valued, the spin statistics are mapped to their complex conjugates $\exp(-i2\pi\mathrm{s})$ under the CT transformation. In fact, there are two versions of PH-Pfaffian denoted as PH-Pfaffian$_\pm$ depending on how the $(CT)^2$ quantum number is assigned to the odd-q charge of $\mathrm{U}(1)_8$ anyons, which we elaborate in Table III.

On the other hand, the Pfaffian and anti-Pfaffian states do not have CT symmetry. Instead, they map into each other under the CT transformation as follows.

(i) When the $\mathrm{U}(1)_8$ charge q is even, the Abelian sector is paired with the Abelian trivial anyon 1 or the fermionic anyon f, so under the CT transformation

$$\text{Pf: } (q_{\mathrm{even}}, f^n) \overset{CT}{\Longleftrightarrow} \text{APf: } (q_{\mathrm{even}}, f^{n+\frac{q_{\mathrm{even}}}{2}}),$$

where $f^2 = (f)^{\mathrm{even}} = 1$ and $n = 0, 1$. Namely,

$$\text{Pf: } (q_{\mathrm{even}}, f^n) \overset{CT}{\Longleftrightarrow} \text{APf: } (q_{\mathrm{even}}, f^n), \text{ if} \frac{q_{\mathrm{even}}}{2} \in \text{even},$$

$$\text{Pf: } (q_{\mathrm{even}}, f^n) \overset{CT}{\Longleftrightarrow} \text{APf: } (q_{\mathrm{even}}, f^{n+1}), \text{ if} \frac{q_{\mathrm{even}}}{2} \in \text{odd}.$$

(ii) When the $\mathrm{U}(1)_8$ charge q is odd, the Abelian sector is paired with the non-Abelian σ anyon, so under CT,

$$\text{Pf: } (q_{\mathrm{odd}}, \sigma) \overset{CT}{\Longleftrightarrow} \text{APf: } (q_{\mathrm{odd}}, \sigma).$$

The 12 anyons, and their spin statistics $\exp(i2\pi\mathrm{s})$, $\mathrm{U}(1)_{\mathrm{EM}}$ charges, and CT properties are organized in Tables I, II, and III.[33] The list of anyons in the tables contains not only *quasiparticles* but also *quasiholes* of quantum Hall liquids, to be

[30] In the K-matrix CS theory, we replace $\frac{q^2}{2K} \mapsto \frac{q^{\mathrm{T}}K^{-1}q}{2}$ where q is a charge vector in the second expression.

[31] If we demand the spin/charge relation with spin^c connection A, then the isolated $\oint A$ is not well defined and the transparent fermion line in all theories is charged under $\mathrm{U}(1)_{\mathrm{EM}}$. Then, the charge is instead taken modulo 2 from tensoring with $2\oint A$.

[32] In other words, $\exp(i2\pi\mathrm{s}) = \pm1$ for such anyons, so they are self-bosonic or self-fermionic.

[33] Note that the sigma anyon σ_n notation in this work is actually the σ_{-n} in Ref. [15].

TABLE IV. Data for the $K = 8$ state. We provide $(\exp(i2\pi\mathrm{s}), Q/e)$ for 16 anyons.

$K = 8$ state	$\mathrm{U}(1)_8$ CS							
$T_{L=0}$	0	1	2	3	4	5	6	7
1	$(+1,0)$	$(e^{i\frac{\pi}{8}},\frac{1}{4})$	$(e^{i\frac{\pi}{2}},\frac{1}{2})$	$(-e^{i\frac{\pi}{8}},\frac{3}{4})$	$(+1,1)$	$(-e^{i\frac{\pi}{8}},\frac{5}{4})$	$(e^{i\frac{\pi}{2}},\frac{3}{2})$	$(e^{i\frac{\pi}{8}},\frac{7}{4})$
f	$(-1,0)$	$(-e^{i\frac{\pi}{8}},\frac{1}{4})$	$(-e^{i\frac{\pi}{2}},\frac{1}{2})$	$(e^{i\frac{\pi}{8}},\frac{3}{4})$	$(-1,1)$	$(e^{i\frac{\pi}{8}},\frac{5}{4})$	$(-e^{i\frac{\pi}{2}},\frac{3}{2})$	$(-e^{i\frac{\pi}{8}},\frac{7}{4})$

TABLE V. Data for the 113 state. We provide $(\exp(i2\pi s), Q/e)$ for 16 anyons.

113 state	$U(1)_{-8}$ CS							
$T_{L=2}$	0	1	2	3	4	5	6	7
1	$(+1,0)$	$(e^{-i\frac{\pi}{8}},\frac{7}{4})$	$(e^{-i\frac{\pi}{2}},\frac{3}{2})$	$(-e^{-i\frac{\pi}{8}},\frac{5}{4})$	$(+1,1)$	$(-e^{-i\frac{\pi}{8}},\frac{3}{4})$	$(e^{-i\frac{\pi}{2}},\frac{1}{2})$	$(e^{-i\frac{\pi}{8}},\frac{1}{4})$
f	$(-1,1)$	$(-e^{-i\frac{\pi}{8}},\frac{3}{4})$	$(-e^{-i\frac{\pi}{2}},\frac{1}{2})$	$(e^{-i\frac{\pi}{8}},\frac{1}{4})$	$(-1,0)$	$(e^{-i\frac{\pi}{8}},\frac{7}{4})$	$(-e^{-i\frac{\pi}{2}},\frac{3}{2})$	$(-e^{-i\frac{\pi}{8}},\frac{5}{4})$

explained in Appendix F.[34] Although there are 12 anyons, the number of ground states on a spatial 2-torus T^2 known as the ground-state degeneracy (GSD) is only 6 for the Pf, APf, and PHPf states. The corresponding six ground states depend on the spin structure of the spin manifold T^2.

Now, we examine the Abelian states. The $K=8$ state in Eq. (18) has the action $\int \frac{8}{4\pi} b\,db + \frac{2b}{2\pi} dA - 4\mathrm{CS}_{\mathrm{grav}}$ plus a trivial spin-TQFT with $\{1, f\}$ (generated by a trivial line and a fermionic line). Note that the fermion f does not couple to $U(1)_{\mathrm{EM}}$.

The 113 state in Eq. (19) has the action $\frac{K_{IJ}}{4\pi}\int b_I db_J + \frac{(q_I^{\mathrm{T}} b_I)}{2\pi} dA - 4\mathrm{CS}_{\mathrm{grav}}$, where q^{T} denotes the transpose of the q charge vector. There are two convenient expressions for this theory, related by a GL(2,$\mathbb{Z}$) transformation [15]:

$$K=\begin{pmatrix}1&3\\3&1\end{pmatrix}, q^{\mathrm{T}}=(1,1) \xleftrightarrow{\mathrm{GL}(2,\mathbb{Z})\ \text{transformation}} K=\begin{pmatrix}-8&0\\0&1\end{pmatrix}, q^{\mathrm{T}}=(2,1).$$

(We omit an electron charge normalization factor e.)

The quantum numbers for the Abelian states are shown in Tables IV and V. The spin statistics can be obtained from Eq. (27) by dropping the s_{nab} part. The $U(1)_{\mathrm{EM}}$ charge can be determined from Eq. (28) as before.

The $K=8$ and 113 states do not have CT symmetry. Instead, they map into each other under the CT transformation. Quantum numbers of their anyons are mapped as

$$K=8: \quad (\exp(i2\pi s), Q/e \mod 1)$$
$$\overset{CT}{\Longleftrightarrow} 113: \quad (\exp(-i2\pi s), Q/e \mod 1).$$

The mod 1 comes from the freedom to tensor the anyons with the classical Wilson line $\oint A$.

Although there are 16 anyons in each Abelian state, the GSD is only 8. The corresponding eight ground states depend on the spin structure of the spin manifold 2-torus T^2.[35]

IV. DOMAIN WALL THEORY AND TENSION

As reviewed in the Introduction, the proposal of [15] suggests a percolation transition involving puddles of Pf and APf phases separated by domain walls. To this end, we consider the model (4) on the slice of parameter space with time-reversal symmetry preserved, i.e., $m_{\mathrm{odd}}=0$. We would like to study some basic properties of the domain walls, from the EFT point of view, that result when time-reversal symmetry is spontaneously broken.

Let us ignore the discrete gauge field which couples to the fermions, for now, and write the Lagrangian as (in the mostly positive Lorentzian signature)

$$\mathcal{L}=\sum_{i=1,2}\overline{\Psi}^i(i\not{\partial}-g\phi)\Psi^i + m(\overline{\Psi}^1\Psi^1-\overline{\Psi}^2\Psi^2) + \frac{1}{2}(\partial_\mu\phi)(\partial^\mu\phi)-\frac{1}{4}\lambda(\phi^2-v^2)^2. \tag{29}$$

[34] As mentioned in footnote 28, the line operator is a world line of an anyon. Moreover, the two open ends of a line operator correspond to two anyons that can be fused to nothing (i.e., the open line can become a closed line after fusing two ends). Thus, the two open ends of a line operator correspond to a *quasiparticle* and its *quasihole* in the quantum Hall liquids of Appendix F. The entries in Tables I, II, and III therefore contain data for anyons and their "antiparticles." The fusion of a quasiparticle and its quasihole must include a trivial anyon 1 that carries zero global symmetry charges and trivial spin statistics $\exp(i2\pi s)=\pm 1$. [More accurately, the spin statistics of the fusion outcome of two anyons contain not only the spin statistics of each individual anyon (from their modular $\mathcal{T}$ matrix), but also their mutual statistics from their relative angular momentum (from their modular $\mathcal{S}$ matrix). Here, spin 1/2 is allowed for intrinsically fermionic systems.]

[35] Since all five theories are fermionic spin TQFTs, we can specify various spin structures on the T^2 to characterize the GSD. There are four choices corresponding to the periodic (P) or antiperiodic (A) boundary conditions along each of two 1-cycles of T^2: (P,P), (A,P), (P,A), and (A,A). The Hilbert space up to an isomorphism only depends on the fermionic parity $\mathbb{Z}_2^f$ (the $\mathbb{Z}_2$ value of the Arf invariant). The fermionic parity $\mathbb{Z}_2^f$ is odd for (P,P), and the $\mathbb{Z}_2^f$ is even for (A,P), (P,A), (A,A). We denote the corresponding spin 2-tori T^2 as T^2_{o} for odd and T^2_{e} for even. The ground states on T^2_{o} or on T^2_{e} can come from different states. The six ground states on T^2 in Tables I, II, and III, depending on T^2_{o} or T^2_{e}, are chosen differently among 12 line operators. The eight ground states on T^2 in Tables IV and V, depending on T^2_{o} or T^2_{e}, are chosen differently among 16 line operators. In fact, rigorously speaking, only the (P,P) sector stays the same sector under the modular SL(2,$\mathbb{Z}$)'s $\mathcal{S}$ and $\mathcal{T}$ transformations, while (A,P), (P,A), and (A,A) permute to each other under the modular $\mathcal{S}$ and $\mathcal{T}$. The boundary conditions P and AP are also known as Ramond and Neveu-Schwarz sectors, respectively, in string theory. See more discussions about the spin structure dependence in [49–51].

The vacua are doubly degenerate, with the vevs given by $\pm v$ where $v \equiv \mu/\sqrt{\lambda}$. Throughout this section, we assume without loss of generality that $m,\ g \geqslant 0$.

The classical solution for a static domain wall is, as usual,

$$\phi_0(z) = \frac{\mu}{\sqrt{\lambda}} \tanh \frac{\mu(z - z_0)}{\sqrt{2}} \tag{30}$$

with z_0 the center-of-mass coordinate.[36] We assume that the effective perturbative expansion parameter in the scalar sector λ/μ is small to validate the semiclassical analysis that we perform presently. The classical action evaluated on the domain wall saddle is

$$S_\phi[\phi_0] = \frac{2\sqrt{2}}{3}\frac{\mu^3}{\lambda}\int d^2x\,, \tag{31}$$

where d^2x is over the parallel directions to the domain wall, and the transverse z direction has already been integrated over. Divided by the area world-volume area $\int d^2x$, this famously gives the classical domain wall tension [52,53]

$$\sigma_{\rm cl} = \frac{2\sqrt{2}}{3}\frac{\mu^3}{\lambda}. \tag{32}$$

For nonzero fermion mass, the two vacua are gapped. At energies smaller than the $(2+1)$D bulk gap, we have well-defined $(1+1)$D domain wall theories. To derive the domain wall theories, we first analyze the fermionic zero modes (which survive the low-energy limit) in Sec. IV A, and then proceed to quantize the zero modes to obtain the domain wall theories in Sec. IV B. We then study another aspect of the domain walls (their tension), and we do so at one-loop order.

A. Fermionic zero modes in the domain wall background

In the semiclassical approximation, the transverse profile of fermion modes solves the Dirac equation in the domain wall background:

$$\left(\epsilon_r\gamma^0 + i\gamma^1\frac{\partial}{\partial z} \pm m - g\phi_0(z)\right)\Psi_0^j(z) = 0. \tag{33}$$

We have, for the moment, suppressed dependence on the spatial direction parallel to the domain wall. We use the Majorana basis for Γ matrices $\gamma^0 = -i\sigma^y,\ \gamma^1 = \sigma^z,\ \gamma^2 = \sigma^x$, and write the two-component spinors explicitly as $\Psi^j(z) = (u_r^j(z), v_r^j(z))^{\rm T},\ j = 1, 2$ (so the top component is of definite chirality and the bottom component has the opposite chirality). With these conventions, the above equation becomes

$$\left(-\frac{\partial}{\partial z} \pm m - g\phi_0(z)\right)v_r^j = \epsilon_r u_r^j(z),$$
$$\left(\frac{\partial}{\partial z} \pm m - g\phi_0(z)\right)u_r^j = -\epsilon_r v_r^j(z).$$

We are interested in the zero modes, which survive the low-energy limit. For $\epsilon_0 = 0$, we can solve these equations in the classical domain wall background:

$$u_0^1(z) = \psi_{0,+}^1 e^{-m(z-z_0)}\cosh\left((z-z_0)\frac{\mu}{\sqrt{2}}\right)^{\frac{\sqrt{2}g}{\sqrt{\lambda}}}, \tag{34}$$

$$v_0^1(z) = \psi_{0,-}^1 e^{m(z-z_0)}\cosh\left((z-z_0)\frac{\mu}{\sqrt{2}}\right)^{\frac{-\sqrt{2}g}{\sqrt{\lambda}}}, \tag{35}$$

and

$$u_0^2(z) = \psi_{0,+}^2 e^{m(z-z_0)}\cosh\left((z-z_0)\frac{\mu}{\sqrt{2}}\right)^{\frac{\sqrt{2}g}{\sqrt{\lambda}}}, \tag{36}$$

$$v_0^2(z) = \psi_{0,-}^2 e^{-m(z-z_0)}\cosh\left((z-z_0)\frac{\mu}{\sqrt{2}}\right)^{\frac{-\sqrt{2}g}{\sqrt{\lambda}}}. \tag{37}$$

Let us discuss the properties of the zero modes in the Pfaffian and anti-Pfaffian regime $m < gv$ and the PH-Pfaffian regime $m > gv$. These properties will be the key in our subsequent determination of the respective domain wall theories in Sec. IV B.

When $m < gv$, since the solution for $u_0^j(z),\ j = 1, 2$, is not normalizable, we set both $\psi_{0,+}^j = 0$ and are therefore left with two complex parameters $\psi_{0,-}^j$, which constitute our expected four real fermionic zero modes of a single chirality (thus, they correspond to four chiral Majorana fermions). In the extreme limit of $m \ll gv$, the zero modes satisfy $\overline{\Psi}\Psi \sim \Psi^\dagger\sigma_2\Psi = 0$, and hence do not back react on the scalar via the equations of motion.

When $m > gv$, the fermions delocalize and are essentially described by plane-wave solutions. For each Dirac fermion, the normalizable edge modes of opposite chiralities survive on different sides of a half-space:

Fermion	$z \geqslant z_0$	$z \leqslant z_0$
Ψ^1 (mass $m > 0$)	ψ_-^1	ψ_+^1
Ψ^2 (mass $-m < 0$)	ψ_+^2	ψ_-^2

The semiclassical limit $\mu/\lambda \gg 1$ is also a "hard-wall" limit, in which the soliton solution tends toward a steep step function at $z = z_0$ with an insurmountable height barrier. Then, we can indeed consider the normalizable edge modes on two half-spaces that can only interact via possible couplings on the interface. Among the relevant interactions, a $(1+1)$D Majorana mass term for each fermion species, induced from the bulk mass term, can survive precisely on the wall, and gaps out the fermionic degrees of freedom at low energies. This is rather analogous to wall-localized supersymmetric couplings that appear in [54].

B. Domain wall world-volume theory in (1 + 1)D

There is a natural proposal for the domain wall world-volume theory following from simple anomaly considerations. It is the O(2) Wess-Zumino-Witten (WZW) model coupled to two massless complex Dirac fermions by a common $\mathbb{Z}_2$ orbifold that acts as the charge conjugation in O(2). The chiral anomaly accounts for the relative shift of the Chern-Simons level in the two bulk vacua. Since the U(1) part of the

[36] One also has an antidomain wall of the opposite overall sign; we will focus on the properties of the domain wall.

gauge field is confined in $(1+1)$D, the theory naturally flows to $\mathbb{Z}_2$ coupled to two complex fermions. The domain wall theory has $\mathrm{O}(4)/\mathbb{Z}_2$ symmetry which rotates the four massless real fermions. This is consistent with the proposal in [15].

Let us now derive the domain wall world-volume theory from first principles to verify this intuition. For the moment, we will ignore the presence of the discrete gauge field, and reinstate its effect at the end. The vacua, which spontaneously break the time-reversal invariance, occur at $\langle\phi\rangle = \pm v$. The fermions in each of these vacua have tree-level masses $\pm m + g\langle\phi\rangle = \pm m \pm gv$.

To get the $(1+1)$D domain wall theories, we wish to quantize the zero modes in the two regimes of interest $m < gv$ and $m > gv$. We first describe a sector of the world-volume theory without fermions, and then describe the interesting fermionic sector alluded to above. In the following, all quantities are the renormalized versions, as we imagine having already integrated out the bulk massive modes.

Goldstone mode. Since the domain wall breaks translational invariance, there is an effective action for the bosonic Goldstone center-of-mass mode. It arises from promoting the modulus[37] $z_0 \in \mathbb{R}$ adiabatically to functions of the world-volume directions $m \in (t, x)$. Integrating over z and dropping a standard additive constant (hence our use of $\sim$ below) gives

$$\mathcal{L}^G[z_0] = \frac{1}{2}\int dz((\partial_z\phi_0)^2 + (\partial_m z_0(x,t)\partial_z\phi_0)^2) \sim \frac{\sigma_{\mathrm{cl}}}{2}(\partial_m z_0(x,t))^2, \tag{38}$$

where the bosonic tension is

$$\sigma_{\mathrm{cl}} = \frac{2\sqrt{2}}{3}\frac{\mu^3}{\lambda}, \tag{39}$$

in agreement with the tension (32) derived from evaluating the classical (effective) action on the domain wall solution. We neglect irrelevant higher-derivative terms in the fluctuation $z_0(x,t)$.

Wess-Zumino-Witten (WZW) models. Since the Chern-Simons sector of the bulk theory does not interact with the degrees of freedom on the wall except via the $\mathbb{Z}_2$ gauging of the fermions, the domain wall is transparent to the continuous gauge degrees of freedom. As is well known, the $(1+1)$D theory that furnishes a trivial interface for a Chern-Simons gauge field is the corresponding WZW theory.

This bulk Chern-Simons term on the two sides of the wall contributes a diagonal CFT on the wall due to the opposite orientations with respect to the bulk. The theory on the wall can be constructed as follows. First, we start with the bulk theory $\mathrm{SO}(2)_2 = \mathrm{U}(1)_2$ on both sides of the wall, so that the theory on the wall is naturally a compact boson at the self-dual radius. Then, we deposit additional L units of $\mathbb{Z}_2$ symmetry-protected topological (SPT) phases in the bulk, which induce additional fermions on the wall. The amount L of $\mathbb{Z}_2$ SPT phases appropriate for each phase was discussed in Sec. II C, which we summarize here for the convenience of the reader:

Phase	L
PH-Pfaffian	1
Pfaffian	-1
Anti-Pfaffian	$3 \equiv -5 \mod 8$

Finally, we gauge the diagonal $\mathbb{Z}_2$ symmetry of the entire configuration that acts as charge conjugation on the SO(2) gauge field. This introduces a single $\mathbb{Z}_2$ gauge field throughout the bulk and on the wall. In other words, at the interface we identify the $\mathbb{Z}_2$ gauge field on the left side of the wall with the gauge field on the right. We may employ the relation among Chern-Simons theories

$$\mathrm{SO}(2)_2 \xrightarrow{\text{gauging } \mathbb{Z}_2} \mathrm{O}(2)_{2,L} = \frac{\mathrm{U}(1)_8 \times T_L}{\mathbb{Z}_2}, \tag{40}$$

where the theories T_L, L mod 8 are described in Appendix E.

In the PH-Pfaffian regime, we have $L = 1$, and the contribution from the bulk on one side is given by gauging a diagonal $\mathbb{Z}_2$ symmetry in the product of a left-moving compact boson φ at the self-dual radius and a right-moving Majorana fermion ζ^R. The contribution from the other side of the wall is the same with left exchanged with right. Of course, the chiral anomaly of this sector from both sides of the wall is trivial.

In the Pfaffian and anti-Pfaffian regimes, an interface interpolating between the Pfaffian and anti-Pfaffian WZW theories differs from this basic one ($L = 1$) by precisely four additional Majorana fermions of the same chirality. On the Pfaffian side of the wall we have a left-moving compact boson and a left-moving Majorana fermion, while on the anti-Pfaffian side we have a right-moving compact boson and five right-moving fermions as appropriate for the theories with $L = -1$ ($3 \equiv -5$), respectively. Both sides are again gauged by a single $\mathbb{Z}_2$ gauge field. We denote the discrete $\mathbb{Z}_2$ gauge field below as a, which implements a projection on the spectrum, on the Ψ^j as well as φ, ζ.

Therefore, the domain wall theory before the contribution of the SPT-induced fermions is

$$S^G[z_0] + S^{\mathrm{WZW}}[a, \zeta, \varphi] \tag{41}$$

in the obvious notation, where the superscript WZW denotes the appropriate WZW model for a given phase. The theory for the fermions that the SPT phases deposit on the wall will now be derived using our previous analysis of bulk fermionic zero modes in Sec. IV A.

Fermionic sector. Let us study the Pfaffian and anti-Pfaffian regime $m < gv$ in the extreme limit of $m = 0$. We take the normalizable zero modes $\psi_{0,-}$ and promote them to world-volume fields. We substitute the corresponding solutions in terms of two complex Weyl fermions (34) and (36) into the Lagrangian (29) to obtain

$$\mathcal{L}^{\mathrm{Pf/APf}}[a, \Psi] \sim \widetilde{\sigma}\sum_{i=1,2}\overline{\psi}^i_{0,-}(x,t)(i\not{D}_a)\psi^i_{0,-}(x,t), \tag{42}$$

[37] Here, the term modulus refers to a massless scalar field with trivial potential (at least, at the order to which we are working in the derivative expansion; we discuss this more below). It has the geometric interpretation of being the center-of-mass coordinate of the domain wall.

where all derivatives only run over the world-volume coordinates $k = x, t$, and we have used the superscript to indicate that this is the domain wall theory that interpolates between the Pfaffian and anti-Pfaffian vacua. The coefficient of the kinetic term $\widetilde{\sigma}$ is[38] given by the integral

$$\widetilde{\sigma} = \int_{-\infty}^{\infty} dz\, \cosh[\mu(z-z_0)/\sqrt{2}]^{-\frac{2\sqrt{2}g}{\sqrt{\lambda}}} = \frac{\sqrt{2\pi}}{\mu}\frac{\Gamma\left(\frac{\sqrt{2}g}{\sqrt{\lambda}}\right)}{\Gamma\left(\frac{1}{2}+\frac{\sqrt{2}g}{\sqrt{\lambda}}\right)}, \tag{43}$$

which in the limit of small Yukawa coupling becomes

$$\widetilde{\sigma} \sim \frac{\sqrt{\lambda}}{\mu g}. \tag{44}$$

The gauge field couples to the fermions on the wall exactly as it did in the bulk. Note that the WZW sector is almost decoupled from the fermions except for the $\mathbb{Z}_2$ gauging.

In the PH-Pfaffian regime $m > gv$, let us set $g = 0$ for simplicity, and use the plane-wave solutions on opposite sides of the walls. Doing the respective integrals for the surviving zero modes over the two half-spaces ($z \leqslant z_0$, $z \geqslant z_0$) then gives

$$\mathcal{L}^{\mathrm{PHPf}}[a,\Psi] = \frac{m}{\mu}\left[\psi^1_{0,+}(x,t)\psi^1_{0,-}(x,t) - \psi^2_{0,+}(x,t)\psi^2_{0,-}(x,t)\right] + \frac{1}{2m}\sum_{i=1,2}\overline{\psi}^i_0(x,t)(i\not{D}_a)\psi^i_0(x,t)\,, \tag{45}$$

where now the superscript indicates that the domain wall theory is for the PH-Pfaffian phase.[39] The mass term gaps out the fermions at low energies, hence, only the Goldstone and WZW sectors of the domain wall theory survive on the wall.

The analysis of the zero modes in the two extreme regimes also suggests a natural candidate domain wall theory (in the universality class of the theory) that describes the wall's phase transition: a $(1+1)$D $\mathbb{Z}_2$-gauged Gross-Neveu-Yukawa theory [suppressing the dependence of the fields on the world-volume coordinates (x,t)][40]

$$\mathcal{L}^{\mathrm{wall}} = -\frac{1}{2}(\partial\varphi)^2 + g_2^2\varphi^2 - \frac{g_4}{4}\varphi^4 - g_3\phi(\overline{\psi}^1\psi^1 - \overline{\psi^2}\psi^2) + \sum_j \overline{\psi}^j(i\not{D}_a)\psi^j. \tag{46}$$

[38] Although we call this coefficient $\widetilde{\sigma}$, due to its formal similarity with σ as computed in Eq. (38), we stress that it is not to be confused with the tension. The fermionic contribution to the tension will be computed in later subsections.

[39] The appearance of $1/\mu$ is not only expected by dimensional analysis. Recall from Sec. IV A that the plane-wave solutions on opposite sides of the wall overlap in the vicinity of the wall, where a mass coupling is possible. On the domain wall, the mass term is therefore proportional to the width of the wall, which is $1/\mu$.

[40] Analogous studies and proposals of domain wall world-volume theories were made in the context of domain walls in four-dimensional QCD at $\theta = \pi$ [55] or four-dimensional SU(2) Yang-Mills gauge theory at $\theta = \pi$ [56].

Here, the condensation of the scalar σ as we tune the scalar mass term implements the phase transition between the two regimes. If we canonically normalize the fermions in $\mathcal{L}^{\mathrm{PHPf}}$, then the coefficient of the mass term becomes $\frac{m^2}{\mu}$, so that we set $\frac{m^2}{\mu} \sim \frac{g_3 g_2}{\sqrt{g_4}}$, which naively suggests $g_4 \sim \mu^2$, $g_3 \sim g_2 \sim m$. We defer a more detailed analysis for future work.

C. One-loop effective action and tension

Let us return to our $(2+1)$D bulk theory and study the (Euclidean) effective action and the domain wall tension from integrating out fermions at one loop.[41] We ignore the $\mathbb{Z}_2$ gauging and revisit its effect toward the end.

Consider expanding the theory in transverse fluctuations around a saddle $\phi = \phi_0 + \chi$, where ϕ_0 could be either the vacuum saddle $\phi_0 = \pm v$ or the domain wall saddle (30). The matter part of the action then takes the form

$$S_{\mathrm{bulk}} = \frac{2\sqrt{2}}{3}\frac{\mu^3}{\lambda} + S_{\mathrm{fluct}} + S_{\mathrm{ct}}, \tag{47}$$

where [suppressing the $(2+1)$D space-time dependence of the fields]

$$\begin{aligned} S_{\mathrm{fluct}} = \int d^3x\, \frac{1}{2}\Bigg\{\chi\left(-\frac{\partial^2}{\partial z^2} - \mu^2 + 3\lambda\phi_0^2\right)\chi \\ + \lambda\left(\phi_0\chi^3 + \frac{1}{4}\chi^4\right)\Bigg\} + \sum_{i=1,2}\overline{\Psi}^i i\not{D}_C\Psi^i \\ + + m(\overline{\Psi}^1\Psi^1 - \overline{\Psi}^2\Psi^2) \\ + \int dz\left\{-g\sum_{i=1,2}(\phi_0+\chi)\overline{\Psi}^i\Psi^i\right\} \end{aligned} \tag{48}$$

is the action for the fluctuations. We will study the counterterms S_{ct} below.

1. Effective action at $\phi_0 = v$

At one-loop order around the vacuum saddle $\phi_0 = v$, there are terms in the fluctuation action that contribute to $\langle\chi\rangle$ via tadpole diagrams:

$$-g\chi\overline{\Psi}^i\Psi^i + \lambda v\chi^3. \tag{49}$$

We need to include counterterms to cancel the tadpole so that the location of the vacuum remains fixed $\langle\phi\rangle = v$. Explicitly,

$$\begin{aligned} S_{\mathrm{ct}} &= -\frac{1}{2}\delta_b\mu^2\int d^3x\,\phi^2 - \frac{1}{2}\delta_f\mu^2\int d^3x\,\phi^2\,, \\ \delta_b\mu^2 &= \lambda v\int^{\Lambda}\frac{d^3k}{(2\pi)^3}\frac{1}{k^2+\mu^2}\,, \\ \delta_f\mu^2 &= 2g\int^{\Lambda}\frac{d^3k}{(2\pi)^3}\left[\frac{g+m/v}{k^2+(gv+m)^2} + \frac{g-m/v}{k^2+(gv-m)^2}\right], \end{aligned} \tag{50}$$

[41] Y. Lin thanks C.-M. Chang and D. Simmons-Duffin for useful discussions.

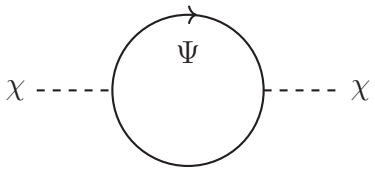

FIG. 8. Fermionic one-loop renormalization of the fluctuating scalar mass.

where δ_b and δ_f denote counterterms that arise from consideration of bosonic χ and fermionic Ψ^i loops, respectively, and Λ is a UV cutoff.

The mass of the fluctuating χ field is given by $\sqrt{2}\mu$ at tree level, but gets corrected at one loop, with the Feynman diagram given in Fig. 8. Since we want to focus on the effect of the fermions, let us ignore the bosonic loop corrections for now. The one-loop effective action from integrating out two Dirac fermions with masses $\pm m$ and coupled to the scalar with Yukawa coupling g is

$$\delta_f \mathcal{L}_{\text{eff}} = \ln \frac{\det \mathbb{D}^{\phi=v+\chi}_{m,g}}{\det \mathbb{D}^{\phi=v}_{m,g}} \frac{\det \mathbb{D}^{\phi=v+\chi}_{-m,g}}{\det \mathbb{D}^{\phi=v}_{-m,g}} - \frac{1}{2}\delta_f \mu^2 [(v+\chi)^2 - v^2], \tag{51}$$

where $\mathbb{D}^{\phi}_{m,g}$ is the effective Dirac operator

$$\mathbb{D}^{\phi}_{m,g} \equiv \begin{pmatrix} -\partial_1 + m + gv + g\chi & -i\partial_0 - \partial_2 \\ i\partial_0 - \partial_2 & \partial_1 + m + gv + g\chi \end{pmatrix}. \tag{52}$$

When $m \neq gv$, the leading terms in the derivative expansion amount to treating χ as a constant:

$$\delta_f \mathcal{L}_{\text{eff}} = \int \frac{d^3k}{(2\pi)^3} \left\{ \ln \frac{k^2 + (m+gv+g\chi)^2}{k^2 + (m+gv)^2} \frac{k^2 + (m-gv-g\chi)^2}{k^2 + (m-gv)^2} - g[(v+\chi)^2 - v^2] \left[\frac{g + m/v}{k^2 + (m+gv)^2} + \frac{g - m/v}{k^2 + (m-gv)^2} \right] \right\}$$
$$= \begin{cases} -\frac{g^2v^2 - m^2}{2\pi |gv|}(g\chi)^2 - \frac{1}{3\pi}(g\chi)^3, & m < gv \\ -\frac{1}{6\pi}(g\chi)^3, & m = gv \\ 0, & m > gv. \end{cases} \tag{53}$$

We see that the mass of χ is renormalized as

$$2\mu^2 = 2\mu_{\text{cl}}^2 + \frac{g^2v^2 - m^2}{\pi |gv|} g^2 \theta(g^2v^2 - m^2), \quad v = \frac{\mu}{\sqrt{\lambda}}. \tag{54}$$

In what regime can we trust this result? Let us estimate this by computing some higher-derivative terms in the one-loop effective action. For a single Dirac fermion with mass $\overline{m}$, the first few higher-derivative corrections quadratic in χ are

$$\delta_f S^{(2)}_{\text{eff}} = -\frac{g^2}{2} \chi \left(\frac{1}{12\pi |m - gv|} \partial^2 + \frac{1}{240\pi |m - gv|^3} \partial^4 + \mathcal{O}(\partial^6) \right) \chi + \mathcal{O}(\chi^3), \tag{55}$$

with some computational details given in Appendix G 1.[42] Estimating the ∂^2 for bosonic fluctuations by the mass $\sqrt{2}\mu$, we find that the higher-derivative corrections are suppressed by factors of $|m - gv|/\mu$. Thus, our result is a reasonable approximation in the regime

$$\frac{|m - gv|}{\mu} \gtrsim \mathcal{O}(1). \tag{56}$$

We will come back to this at the end of Sec. IV C 2.

[42]To apply the results of Appendix G 1, make the replacement $m \to m - gv$.

2. Domain wall tension

To evaluate the one-loop corrections to the tension, we will closely follow the method of [57] (see also [58]). First, we formulate the theory in a Euclidean box with half-length L in the z direction and area $V_{||}$ in the world-volume directions, so that the energy density is given in terms of the effective action Γ as

$$\sigma = \lim_{L, V_{||} \to \infty} \frac{\Gamma(\phi_0)}{V_{||}}, \tag{57}$$

under a scheme such that the expectation values of the vacua $\pm v$ are unrenormalized, and the effective action is normalized to vanish when evaluated on the vacua $\pm v$.

Formally, the full one-loop correction to this quantity receives contributions from the classical term σ_{cl} [taking the form of (32) with μ renormalized], the quantum correction σ_{qu}, and the counterterms σ_{ct}:

$$\sigma = \sigma_{\text{cl}} + \sigma_{\text{qu}} + \sigma_{\text{ct}} \tag{58}$$
$$= \int dz [\mathcal{L}(\phi_0) - \mathcal{L}(v)] + \lim_{L, V_{||} \to \infty} \left(\frac{1}{2V_{||}} \ln \det \frac{\Delta}{\Delta^{(0)}} \right). \tag{59}$$

The operators Δ, $\Delta^{(0)}$ are the inverse propagators of a fluctuating field in the soliton background and in the vacuum (trivial background), respectively. The central idea of [57] is that the fluctuations are independent of the world-volume coordinates and may therefore be partially diagonalized by a Fourier transform in those directions. Then, the ratio of functional determinants can be related to a ratio of solutions

of ordinary differential equations, which is then (numerically) integrated over the transverse coordinates.[43]

First, we express the one-loop tension in terms of the renormalized parameters of the theory. As is standard [57,59,65], the renormalized scalar mass μ can be related to the bare mass μ_{bare} by a one-loop computation in the perturbative sector of the fluctuation theory, i.e., in one of the two degenerate ground states. We follow [57] and use the $\overline{\text{MS}}$ scheme to fix the counterterms, and require that, as discussed above, the tadpole diagrams are canceled by the counterterms. This coincides with the condition to fix the renormalized mass by requiring $\langle\phi\rangle = \pm\sqrt{6\mu^2/\lambda}$.[44]

The full one-loop tension can be broken up into a sum of the classical tension and the bosonic and fermionic one-loop contributions of the form[45]

$$\sigma = \frac{2\sqrt{2}}{3}\frac{\mu^3}{\lambda} + \left[\frac{\delta_b\sigma_{\text{qu}}}{\mu^2}\right]\mu^2 + \left[\frac{\delta_f\sigma_{\text{qu}}}{\mu^2}\right]\mu^2, \tag{60}$$

where μ is the *renormalized* scalar mass, $[\delta_b\sigma_{\text{qu}}/\mu^2]$ is a dimensionless constant, and $[\delta_f\sigma_{\text{qu}}/\mu^2]$ is a dimensionless quantity with the following functional dependence on a dimensionless fermion mass w and a dimensionless Yukawa coupling γ:

$$\left[\frac{\delta_f\sigma_{\text{qu}}}{\mu^2}\right](w,\gamma), \quad w \equiv \frac{m}{\mu}\frac{\sqrt{\lambda}}{g}, \quad \gamma \equiv \frac{g}{\sqrt{2\lambda}}. \tag{61}$$

The normalization of w is chosen such that at $w = 1$, the effective mass $m - gv$ of one of the Dirac fermions vanishes. The normalization of γ is chosen so that $\gamma = 1$, $\nu = 0$ corresponds to the $\mathcal{N} = 1$ supersymmetric point in the case of a theory with a single Majorana fermion.

The classical piece of the domain wall tension in (60) with one-loop renormalized scalar mass is

$$\sigma_{\text{cl}} = \frac{2\sqrt{2}}{3\lambda}\left[\mu_0^2 + \frac{g^2v^2 - m^2}{2\pi|gv|}g^2\theta(g^2v^2 - m^2)\right]^{3/2}, \tag{62}$$

where the domain wall tension is renormalized at one loop by the bosonic χ fluctuations alone. In relative terms, this correction is

$$\frac{\delta_f\sigma_{\text{cl}}}{\sigma_{\text{cl}}} \sim \frac{g^3v}{\mu^2} \sim \frac{g^3}{\mu\sqrt{\lambda}} \sim \frac{\lambda}{\mu}\gamma^3, \tag{63}$$

which is small in the semiclassical approximation with $\gamma \sim \mathcal{O}(1)$. There is a first-order transition in the domain wall tension at the critical point $m = gv$, but we expect it to be smoothed out by higher-order corrections.

We can now determine $[\delta_b\sigma_{\text{qu}}/\mu^2]$, $[\delta_f\sigma_{\text{qu}}/\mu^2]$ using the technology of [57]. Since χ only self-interacts at one loop, and since the relevant computation was performed in [57], we can simply borrow their result, which was computed in dim-reg in terms of the analytically continued dimension n, and take $n \to 3$. The result is

$$\left[\frac{\delta_b\sigma_{\text{qu}}}{\mu^2}\right] = \frac{3\mu^2}{16\pi}[\ln(3) - 4] \sim -0.17. \tag{64}$$

It remains to determine the integral encapsulating the quantum fermionic contributions to the tension, following [57]. As always, we would like to keep λ/μ small. In addition, we also want the Yukawa coupling to be small to suppress large backreaction by the fermions, but we can keep the ratio g^2/λ finite. Of course, when $g = 0$, $\delta_f\sigma_{\text{qu}} = 0$.[46]

Including the counterterm (50), the formula for the *quantum* one-loop tension from integrating out the fermions is

$$\delta_f\sigma_{\text{qu}} = -\ln\frac{\det\mathbb{D}_{m,g}^{\phi=\phi_0}}{\det\mathbb{D}_{m,g}^{\phi=v}}\frac{\det\mathbb{D}_{-m,g}^{\phi=\phi_0}}{\det\mathbb{D}_{-m,g}^{\phi=v}} + F\int^{\Lambda}\frac{d^3k}{(2\pi)^3}\left[\frac{g(g+m/v)}{k^2+(gv+m)^2} + \frac{g(g-m/v)}{k^2+(gv-m)^2}\right], \tag{65}$$

where

$$\mathbb{D}_{m,g}^{\phi=\phi_0} \equiv \begin{pmatrix} -\partial_z + m + g\phi_0(z) & -i\partial_0 - \partial_2 \\ i\partial_0 - \partial_2 & \partial_z + m + g\phi_0(z) \end{pmatrix} \tag{66}$$

and

$$F = \int dz\left[\phi_0(z)^2 - \frac{\mu^2}{\lambda}\right] = -2\sqrt{2}\,\frac{\mu}{\lambda}. \tag{67}$$

This formal expression (65) can be evaluated explicitly as outlined in Appendix G 2. The results are shown in Fig. 9, expressed in terms of the dimensionless variables ν and γ defined in (61). Some notable features are as follows:

(i) The *quantum* one-loop correction to the tension $\delta_f\sigma_{\text{qu}}$ is of the same order as the correction from one-loop mass renormalization, namely, $\delta_f\sigma_{\text{qu}} \sim \delta_f\sigma_{\text{cl}} \sim \mathcal{O}(\mu^2\gamma^3)$.

(ii) Both are monotonically decreasing with respect to the fermion mass m.

(iii) The effect diminishes rapidly once the mass m increases past the critical point $m = gv$. Note that there is no mass renormalization at all for $m > gv$.

The qualitative dependence of the domain wall tension on the fermion mass m is shown in Fig. 10.

The validity of the lowest-order approximation in the derivative expansion was analyzed earlier, and the estimate (56) translated to dimensionless quantities becomes

$$|w - 1| \gtrsim \frac{\mathcal{O}(1)}{\gamma}. \tag{68}$$

[43]This bypasses numerous technical complications appearing in more traditional methods, and in particular provides a convenient way to deal with the regularization of sums of zero-point energies in different topological sectors. See, however, [52,59–61] for results in (1 + 1)D using analytic solutions of the fluctuation spectra and [62–64] for other approaches based on making successive Born approximations for scattering phase shifts.

[44]The quartic coupling is only renormalized by a finite amount.

[45]The coefficient $[\delta_b\sigma_{\text{qu}}/\mu^2]$ is also, in general, a function of the dimensionless scalar coupling λ/μ. We take λ/μ to be small throughout our analysis for the semiclassical approximation, and just consider the leading-order λ-independent contribution.

[46]An analogous computation performed in a supersymmetric theory with a single Majorana fermion and $g = \sqrt{2\lambda}$ in [58] gives $\delta_b\sigma_{\text{qu}}^{\text{SUSY}} + \delta_f\sigma_{\text{qu}}^{\text{SUSY}} = -\mu^2/4\pi$. We reproduce this result.

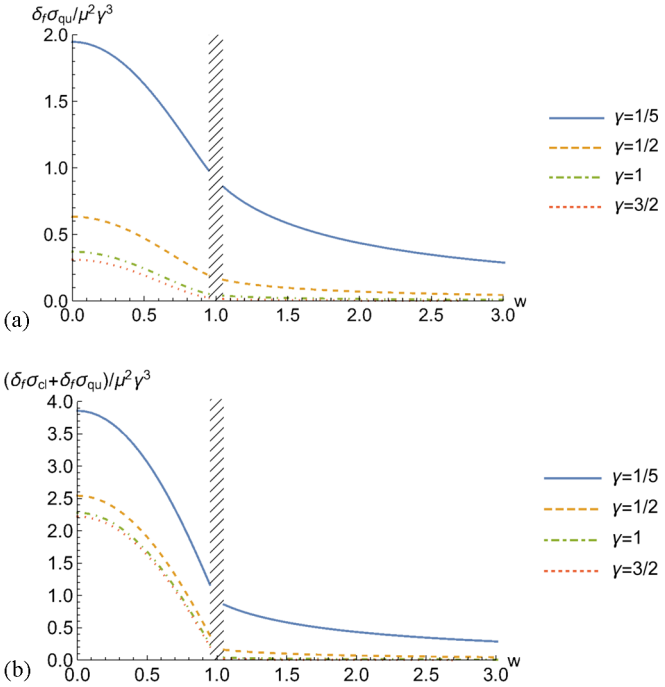

FIG. 9. (a) The fermionic *quantum* one-loop correction $\delta_f\sigma_{qu}$ to the domain wall tension. (b) The mass renormalization and *quantum* one-loop correction combined. The dimensionless fermion mass w and Yukawa coupling γ are defined in (61), and notice that we have divided out by $\mu^2\gamma^3$. The region near $w = 1$ ($m = gv$) is blocked out because the fermions become light and higher-derivative corrections become important.

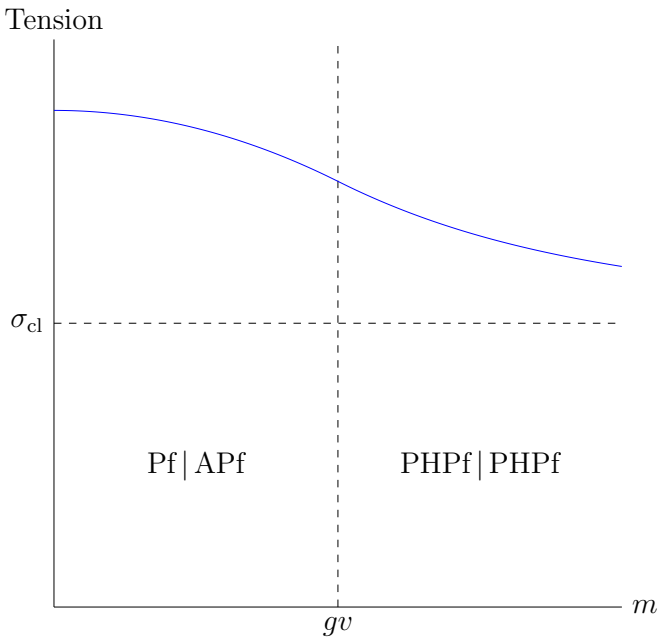

FIG. 10. Qualitative dependence of the domain wall tension on the fermion mass m, which is a proxy for the disorder strength Λ. The critical line $m = gv$ separates the Pf/APf and PHPf regimes, and σ_{cl} denotes the semiclassical tension in the absence of fermions.

As long as γ is $\mathcal{O}(1)$, the one-loop tension to leading order in the derivative expansion is a valid approximation when m is sufficiently large. Furthermore, if the Yukawa coupling g is large enough relative to λ, then we can also trust our results in some neighborhood of small m.[47] Finally, we have assumed that the couplings λ and g are small relative to the masses w and m, therefore, the higher-loop corrections and corrections involving more powers of χ are suppressed.

3. *Effect of gauging*

Let us discuss the effect of the $\mathbb{Z}_2$ gauge field on the one-loop tension. Recall that the $\mathbb{Z}_2$ gauge field acts as $\Psi^j \to -\Psi^j$ and leaves the scalar untouched. In the path integral, having a discrete gauge field amounts to summing over its holonomies. For a domain wall interpolating between two vacua, the Euclidean space-time is $\mathbb{R}^3$ with no boundary or nontrivial cycle, so it is unclear whether the gauging has any effect on the tension at all, even nonperturbatively. On a space-time with nontrivial cycles, it is logically possible that the sum over holonomies introduces new saddles that dominate over the original saddle (trivial holonomy), but such effects go beyond perturbation theory.

In fact, for the sake of argument, let us imagine that the $\mathbb{Z}_2$ is a subgroup of a continuous U(1) gauge symmetry acting on the fermions as $\Psi^j \to e^{i\alpha}\Psi^j$, with associated gauge connection A. In the one-loop effective action from integrating out the fermions, to lowest order in the derivative expansion there in principle is a coupling of the form $(\partial^\mu\chi)A_\mu$. However, we find that the coefficient of this term is zero by an explicit computation in Appendix G 1. Thus, the U(1) gauging has no effect at the order of our approximation.

V. CONCLUSION AND FUTURE DIRECTIONS

In this work, we have presented an effective field theory that captures the qualitative features of the phase diagram proposed in [15] to describe the $\nu = 5/2$ fractional quantum Hall system. We also studied some simple properties of domain walls present at the time-reversal-symmetric locus (or, in condensed-matter terminology, the particle-hole-symmetric locus), including their effective world-volume theory and their tension, computed to one-loop order in a semiclassical approximation. The tension computed with the EFT is *lower* in the PH-Pfaffian phase than in the Pfaffian/anti-Pfaffian phase, suggesting that the former phase may in fact be energetically favored over the latter in the presence of domain walls. This may explain the percolation transition, and serve as a resolution of the dilemma between the experiment [10] (favoring PH-Pfaffian) and bulk energetics studies [18–27] (favoring Pfaffian/anti-Pfaffian). We leave a more exhaustive and complete study of bulk and domain wall energetics to future work.

We make some additional remarks related to the bulk and domain wall systems.

[47]This may seem paradoxical at first since the fermions clearly have no effect when $g = 0$. However, we are interested in the dependence of the tension on the fermion mass m. When g is small, this dependence is small, but the higher-order corrections relative to the approximate dependence is large.

(1) Pf | APf *domain wall vs* PHPf |PHPf *domain wall*. The Pf | APf domain wall is well defined when particle-hole (PH) symmetry is broken, with two different vacua on two sides of bulk. But, what do we mean by PHPf | PHPf domain wall since PHPf presumably has a PH-symmetry preserving bulk?[48] An answer is that in our EFT, the two vacua of the Higgs potential shown in Fig. 5 indeed both break the PH symmetry:

(a) The left side of Fig. 5 gives vacua of the PH-symmetry breaking phases Pf and APf.

(b) The right side of Fig. 5 gives two vacua both in the PHPf phase, but the two PHPf vacua are exchanged by PH symmetry. We could have alternatively considered the Higgs potential with the sign of the ϕ^2 term flipped when we are in the PHPf phase: if so, we would have a single PH-symmetry preserving vacuum. But to impose that the ϕ^2 term flips sign[49] around the energy scale $m = gv$ would require a less natural fine tuning on our EFT. However, the fine tuning could potentially be avoided in the following way. Consider the region near $m = gv$, where the ϕ^2 term sign does not flip "by hand," but rather the sign flip is induced by the following mechanism. The PH-symmetry breaking Pf | APf domain wall can transition to the PH-symmetry breaking PHPf | PHPf domain wall, but the $(1+1)$D PHPf | PHPf domain wall percolation may then induce a $(2+1)$D bulk transition to the PHPf phase, which would restore the PH symmetry dynamically. We propose that this mechanism indeed occurs, while our proposal requires future study.

(2) We contrast *the order of quantum phase transitions* from two perspectives: (i) the domain wall percolating picture [15] versus (ii) our EFT.

(a) At zero disorder $\Lambda = 0$, both (i) and (ii) have a first-order discontinuous phase transition due to PH (or CT) breaking and the discontinuity jump at domain wall.

(b) At nonzero but small disorder at $\Lambda < \Lambda_1$ along the vertical axis $\nu = \nu_c$, the case (ii) gives a first-order transition, while the case (i) can have a second-order transition, or a first-order transition effected by disorder broadening the phase boundary (which can result in a new second-order transition within the broadening region).

(c) Away from the axis $\nu \simeq \nu_c$ but within topological orders in the phase diagram Fig. 3, we have second-order or continuous transitions derived in our EFT for the case (ii) due to the continuous deformation of mass sign flipping. In the case (i), the percolation phase transition can be indeed a second-order transition, at least in the free-fermion limit, chiral fermions running on the percolation domain walls where the length scale of puddle *diverges* at the transition.

(d) The upper phase boundary $\Lambda > \Lambda_2$ from the topological orders to the thermal metal is also a second-order or continuous transition, for both cases (i) and (ii). Physically, this transition is similar to an insulator-metal transition driven by strong disorder known as *Anderson localization-delocalization transition*, which is a second-order continuous transition.

(3) Our EFT should encode the *universality class of gapless topological quantum phase transitions*. In our case, we have a second-order continuous phase transition controlled by a free CFT given by $(2+1)$D Dirac or Majorana fermions whose masses flip sign. Naively, the O(2) gauge sector does not directly affect the dynamics and universality class. It will be important to explore further the nature of the phase transitions.

(4) We may contrast the emergent global symmetries on the $(1+1)$D domain wall [from lower to higher disorder: $\mathrm{O}(4) \to \mathrm{O}(2)\times\mathrm{O}(2) \to \mathbb{Z}_2^F$ [15]] with the $(2+1)$D bulk global symmetries of our $(2+1)$D EFT (from lower to higher disorder: $\frac{\mathrm{O}(4)}{\mathbb{Z}_2} \to \frac{\mathrm{O}(2)\times\mathrm{O}(2)}{\mathbb{Z}_2} \to \mathbb{Z}_2^F$). The two global symmetry patterns are almost equivalent, but differ by finite group sectors. It turns out that we can also formulate an alternative EFT (by modifying the deformation parameters of the original QFT) to exactly match the bulk and domain wall global symmetry patterns. This will be left for further exploration.

(5) Our EFT can choose either two versions PH-Pfaffian$_\pm$, depending on how $(CT)^2$ assigns to the anyons (they are the same topological order, but different symmetry-enriched topological orders). PH-Pfaffian$_{+/-}$ have different anomaly, with an anomaly index $\nu = 0$ or $8 \in \mathbb{Z}_{16}$, of CT symmetry. If the $\nu = 5/2$ system in the laboratory has PH-Pfaffian$_{+/-}$ order, then we have less/more IR constraints from the $\nu = 0$ or 8 anomaly. Moreover, other than this pure CT anomaly, there is also a CT-PO(4) mixed anomaly. The 't Hooft anomaly implies that the associated global symmetry (such as CT) is not strictly local and onsite, but it is an *emergent global symmetry* at low energy and long distances.

We conclude with an incomplete list of additional questions and future directions raised by this study. Of course, most interesting is whether the proposal of [15] indeed provides the correct microscopic description of the $\nu = 5/2$ state. If so, we hope our EFT provides a useful conceptual framework for studying aspects of this system.

(6) Our effective field theory is a standard relativistic QFT, though various nonrelativistic EFTs have been proposed to study quantum Hall systems (see, e.g., [6,7]). Is there a useful nonrelativistic bulk EFT description of this system?

It is worthwhile to note that our EFT is a (super)renormalizable QFT in $(2+1)$D, and it is UV complete by itself. Although our EFT does not require a further UV completion at higher energy, it may still be helpful to understand how this relativistic EFT can be obtained from RG flow from a nonrelativistic EFT, the electron wave functions, or a lattice model at the condensed-matter UV cutoff scale.

(7) We computed the tension of the domain walls in an approximation where $\lambda/\mu \ll 1$. Roughly speaking, λ and μ, respectively, govern the height and width of the domain walls, so that the limit corresponds to studying rigid and thick walls. It would be interesting to determine if the domain walls, assuming they are indeed realized in the $\nu = 5/2$ system, actually satisfy this limit so that our tension

[48] We thank D. T. Son for raising this question.

[49] For fine tuning, one can let $\frac{\mu^2}{2}\phi^2$ such that $\mu^2 > 0$ when $m < gv$, while $\mu^2 < 0$ when $m > gv$.

result can be used reliably to understand energetics of the system.

(8) It may be that the particle-hole symmetry is explicitly, weakly broken in the experimental setup. If so, the domain walls would be metastable. It would be instructive to compute the decay rate for these walls in our EFT when one turns on our small but nonvanishing m_{odd} deformation.

(9) It would be very instructive to compute the spin-structure-dependent ground-state degeneracy by performing an explicit path integral in our EFT. Such a quantity could potentially be measured in a real experimental setting if one fixes the boundary conditions of the laboratory sample, i.e., periodic or antiperiodic boundary conditions, similar to those on a spatial 2-torus.

ACKNOWLEDGMENTS

We thank B. Halperin for a conversation, and N. Seiberg and X.-G. Wen for comments on the manuscript. J.W. thanks B. Lian for a previous collaboration on [15] and especially acknowledges helpful comments from J. Wang, Y. You, and Y. Zheng. J.W. also thanks e-mail correspondences from D. Mross and C. Wang, and the feedback from the seminar attendees [66]. Y.L. and N.P. are each supported by a Sherman Fairchild Postdoctoral Fellowship. J.W. was supported by NSF Grant No. PHY-1606531 and Institute for Advanced Study. This work is also supported by NSF Grant No. DMS-1607871 "Analysis, Geometry and Mathematical Physics" and Center for Mathematical Sciences and Applications at Harvard University. This material is based upon work supported by the U. S. Department of Energy, Office of Science, Office of High Energy Physics, under Award No. DE-SC0011632, and by the Simons Foundation through the Simons Investigator Award.

APPENDIX A: GRAVITATIONAL CHERN-SIMONS TERM AND THERMAL HALL RESPONSE

Any 3-manifold has a spin connection ω. Explicitly, in terms of the frame metric $\eta_{ab} = g_{\mu\nu} e^{\mu}_{a} e^{\nu}_{b}$ and the coframe $\overline{e}^{a}_{\mu} e^{\mu}_{b} = \delta^{a}_{b}$

$$\omega^{i}_{j\mu} = \overline{e}^{i}_{\nu} \Gamma^{\nu}_{\lambda\mu} e^{\lambda}_{j} + \overline{e}^{i}_{\nu} \partial_{\mu} e^{\nu}_{j}, \tag{A1}$$

where Γ is the Christoffel symbol. The fermion spinor field of spin $1/2$ couples to the spin connection as $\nabla = \partial - \frac{1}{2}\omega$. Integrating out one massive Majorana fermion ψ gives the gravitational spin Chern-Simons term for positive mass m compared to negative mass:

$$\frac{Z_{\psi,m\gg 0}}{Z_{\psi,m\ll 0}} = \exp\left(i \int_{M_3} \text{CS}_{\text{grav}}\, d^3x \right). \tag{A2}$$

More explicitly,

$$\text{CS}_{\text{grav}}\, d^3x = \frac{1}{192\pi} \text{Tr}\left(\omega\, d\omega + \frac{2}{3}\omega^3 \right). \tag{A3}$$

The spin gravitational Chern-Simons term contributes to the thermal Hall conductivity by a chiral central charge $c_- = -1/2$.[50]

APPENDIX B: $\mathbb{Z}_2$ GAUGE THEORY IN (2 + 1)D

Fermionic SPT phases with an internal unitary $\mathbb{Z}_2$ symmetry are known to be classified by $\Omega^{\text{spin}}_3 = \mathbb{Z}_8$. Denote the background $\mathbb{Z}_2$ gauge field by $B \in H^1(M, \mathbb{Z}_2)$ for the spacetime M. Then, the partition function for the $\mathbb{Z}_2$ SPT phases can be described using the invertible fermionic TQFT $\text{SO}(L)_1$ with a special orthogonal $\text{SO}(L)$ gauge group as follows:

$$e^{i f_L(B)} = (Z_{\text{SO}(L)_1}[B])^* Z_{\text{SO}(L)_1}, \tag{B1}$$

where $Z_{\text{SO}(L)_1}[B]$ denotes the partition function of $\text{SO}(L)_1$ coupled to B by the magnetic symmetry $\pi \int w_2(\text{SO}(L)) \cup B$, while $(Z_{\text{SO}(L)_1}[B])^*$ is its complex conjugate. Since $\text{SO}(L)_1$ is an invertible spin TQFT, the right-hand side is a phase that depends on B, which gives the SPT phase $f_L(B)$ on the left-hand side. By the property $\text{SO}(L)_1 \times \text{SO}(L')_1 \leftrightarrow \text{SO}(L + L')_1$, the phase can be written as

$$f_L(B) = L\, f(B) \tag{B2}$$

for some $f(B)$.

For an even L, we can use the property $\text{SO}(2)_1 = \text{U}(1)_1$ to express $Lf(B) = (L/2)2f(B)$ as the $\text{U}(1) \times \text{U}(1)$ Chern-Simons term $-\frac{L/2}{4\pi} B\, dB + \frac{2}{2\pi} B\, du$ with u constrains B to be a $\mathbb{Z}_2$ gauge field. By the field redefinition $u \to u + B$, we find that for $L = 8$ the SPT phase is the same as $L = 0$. This reproduces the $\mathbb{Z}_8$ classification of the SPT phases

$$L \sim L + 8. \tag{B3}$$

Gauging the $\mathbb{Z}_2$ symmetry with a dynamical gauge field by summing over B gives rise to eight different $\mathbb{Z}_2$ gauge theories. For $L = 0$ it is the untwisted $\mathbb{Z}_2$ gauge theory (the $\mathbb{Z}_2$ toric code), while for $L = 4$ it is the Dijkgraaf-Witten twisted $\mathbb{Z}_2$ gauge theory (the so-called double-semion theory). See the list of eight different $\mathbb{Z}_2$ gauge theories (where $L \in$ even yields an Abelian TQFT and $L \in$ odd yields a non-Abelian TQFT) in Table 2 of [49].

APPENDIX C: FERMION PATH INTEGRAL AND COUNTERTERMS

Consider a (2 + 1)D Majorana fermion coupled to a $\mathbb{Z}_2$ gauge field $B \in H^1(M, \mathbb{Z}_2)$, and give it a large mass. The fermion path integral depends on the sign of the mass, given by

$$Z[B]_{m>0} = |Z| \exp\left(\frac{\pi i}{2} \eta(B) \right), \quad Z[B]_{m<0} = 1. \tag{C1}$$

The Atiyah-Patodi-Singer (APS) index theorem relates the exponential of the η invariant to the topological actions

$$\exp\left(\frac{\pi i}{2} \eta(B) \right) = \exp\left(i f(B) + i \int \text{CS}_{\text{grav}}\, d^3x \right), \tag{C2}$$

[50] This can be understood from the fact that the invertible TQFT $\text{U}(1)_{-1}$ has partition function $e^{2i \int \text{CS}_{\text{grav}}}$ [47], and thus 2CS_{grav} has $c = -1$, so CS_{grav} has $c = -1/2$.

where $f(B)$ is the basic fermionic $\mathbb{Z}_2$ SPT phase with a $\mathbb{Z}_2$ background B, and $\int_{\partial Y} \mathrm{CS}_{\mathrm{grav}}\, d^3x = \frac{1}{192\pi}\int_Y \mathrm{Tr}(R\wedge R)$ is the gravitational Chern-Simons term. There are eight fermionic SPT phases with $\mathbb{Z}_2$ symmetry $8f[B]\sim 0 \bmod 2\pi$, and they correspond to the eight pure $\mathbb{Z}_2$ gauge theories in $(2+1)$D (some of them need a spin structure). We will call them the eight levels of $(2+1)$D $\mathbb{Z}_2$ gauge theories; see Appendix B. In our convention, the $\mathrm{U}(1)_4\times\mathrm{U}(1)_{-1}$ theory corresponds to the sixth class.

The O(2) Chern-Simons gauge theory has two levels: $\mathrm{O}(2)_{K,L}$ with the level $K\in\mathbb{Z}$ associated with the instanton number in $4d$, while L represents eight $\mathbb{Z}_2$ gauge theories $Lf(w_1^{\mathrm{O}(2)})$, where $w_1^{\mathrm{O}(2)}$ is the $\mathbb{Z}_2$-valued first Stiefel-Whitney class of the O(2) bundle.

For massless Majorana fermions in the one-dimensional representation odd under $\mathbb{Z}_2$ charge conjugation, we will write the theory using the effective Chern-Simons levels

$$\mathrm{O}(2)_{K,L}\ \mathrm{CS} + N_f\psi \text{ in } \mathbf{1}_{\mathrm{odd}} + M\,\mathrm{CS}_{\mathrm{grav}}, \tag{C3}$$

where M, L are integers if N_f is even, and half-integers if N_f is odd. Integrating out a massive $(2+1)$D Majorana fermion shifts the effective Chern-Simons level to be

$$\begin{aligned} m>0:&\ \mathrm{O}(2)_{K,L+\frac{1}{2}}\ \mathrm{CS} + \left(M+\tfrac{1}{2}\right)\mathrm{CS}_{\mathrm{grav}},\\ m<0:&\ \mathrm{O}(2)_{K,L-\frac{1}{2}}\ \mathrm{CS} + \left(M-\tfrac{1}{2}\right)\mathrm{CS}_{\mathrm{grav}}. \end{aligned} \tag{C4}$$

The difference between the shifts for different signs is given by (C1) and (C2).

APPENDIX D: GAUGING ONE-FORM SYMMETRY IN (2 + 1)D TQFT

Here we review some rules for gauging a one-form symmetry in $(2+1)$D TQFT. For gauging a $\mathbb{Z}_2$ one-form symmetry generated by the symmetry generator charge line a of integer spin, the rules are as follows (see, e.g., [46,67–69]):

(i) Discard the lines that transform nontrivially under the one-form symmetry. These are the lines (of objects charged under the one-form symmetry) that braid nontrivially with a.

(ii) Identify every remaining line W with its fusion with a: $W\sim Wa$.

(iii) For the remaining lines that are fixed points under fusion with a, there are two copies of the line.

In the corresponding chiral algebra, the procedure is equivalent to extending the chiral algebra by a simple current that obeys, together with the identity, the $\mathbb{Z}_2$ fusion algebra.

For instance, $\mathrm{U}(1)_{8k}$ Chern-Simons theory has a $\mathbb{Z}_2$ subgroup one-form symmetry generated by the Wilson line of charge $4k$ with integer spin. The above procedure produces $\mathrm{U}(1)_{2k}$ Chern-Simons theory after gauging one-form $\mathbb{Z}_2$ symmetry. Another way to obtain the result is that gauging the one-form symmetry makes the original U(1) gauge field b no longer well defined, but $b'=2b$ is a well-defined U(1) gauge field. Expressing the original Chern-Simons term $\frac{8k}{4\pi}b\,db$ in terms of the U(1) gauge field b' gives $\mathrm{U}(1)_{2k}$.

APPENDIX E: $\mathrm{O}(2)_{2,L}$ CHERN-SIMONS THEORIES

In this Appendix, we summarize the $(2+1)$D $\mathrm{O}(2)_{2,L}$ gauge theories, which are fermionic spin Chern-Simons theories definable on spin manifolds. For the zero level of $(2+1)$D $\mathbb{Z}_2$ gauge theories [written in terms of $\mathrm{O}(2)_{K,L}$ gauge theories with $L\in\mathbb{Z}_8$ levels in the previous Appendix], the $\mathrm{O}(2)_{2,0}$ gauge theory has the same chiral algebra as the $\mathrm{U}(1)_8$ gauge theory, and thus we have

$$\mathrm{O}(2)_{2,0}\ \mathrm{CS} \leftrightarrow \mathrm{U}(1)_8\ \mathrm{CS}. \tag{E1}$$

In general, we denote the Lth $\mathbb{Z}_2$ gauge theory by T_L (with an action $Lf[B]$ for the $\mathbb{Z}_2$ gauge field B), and have the equivalence

$$\mathrm{O}(2)_{2,L}\ \mathrm{CS} \leftrightarrow \frac{\mathrm{U}(1)_8\times T_L}{\mathbb{Z}_2}\ \mathrm{CS}, \tag{E2}$$

where the quotient denotes gauging a diagonal $\mathbb{Z}_2$ one-form symmetry generated by the composite line of the tensor product of the charge-4 Wilson line in $\mathrm{U}(1)_8$ and the nontransparent fermion line in T_L [if we express $T_L\leftrightarrow \mathrm{Spin}(L)_{-1}\times \mathrm{SO}(L)_1$, it is the Wilson line in the vector representation of $\mathrm{Spin}(L)$]. Here T_L can be written as another $\mathbb{Z}_8$ class of fermionic spin TQFTs [47,49] as the $\mathrm{Spin}(L)_{-1}\times\mathrm{SO}(L)_1$ Chern-Simons gauge theory in $(2+1)$D [37]. Explicitly, we can express the relations with the following CS theories:

$$T_1 \leftrightarrow \overline{\text{Ising}}\times(\text{spin-Ising}), \tag{E3}$$

$$T_2 \leftrightarrow \mathrm{U}(1)_{-4}\times\mathrm{U}(1)_1 \simeq K \text{ matrix } \begin{pmatrix}0&2\\2&1\end{pmatrix}\ \mathrm{CS}, \tag{E4}$$

$$T_3 \leftrightarrow \mathrm{SU}(2)_{-2}\times\mathrm{SO}(3)_1, \tag{E5}$$

$$\begin{aligned} T_4 &\leftrightarrow \mathrm{SU}(2)_{-1}\times\mathrm{SU}(2)_{-1}\times\mathrm{SO}(4)_1\\ &\simeq K \text{ matrix } \begin{pmatrix}0&2\\2&2\end{pmatrix}\ \mathrm{CS}\times\{1,f\}, \end{aligned} \tag{E6}$$

$$T_5 \leftrightarrow \mathrm{SU}(2)_2\times\mathrm{SO}(3)_{-1}, \tag{E7}$$

$$T_6 \leftrightarrow \mathrm{U}(1)_4\times\mathrm{U}(1)_{-1} \simeq K \text{ matrix } \begin{pmatrix}0&2\\2&-1\end{pmatrix}\ \mathrm{CS}, \tag{E8}$$

$$T_7 \leftrightarrow \text{Ising}\times\overline{(\text{spin-Ising})}, \tag{E9}$$

$$\begin{aligned} T_8 = T_0 &\leftrightarrow \text{untwisted } \mathbb{Z}_2 \text{ gauge theory}\times\{1,f\}\\ &\simeq K \text{ matrix } \begin{pmatrix}0&2\\2&0\end{pmatrix}\ \mathrm{CS}\times\{1,f\}. \end{aligned} \tag{E10}$$

and $T_{-L}=\overline{T_L}$ where the overbar denotes its time reversal CT (i.e., particle-hole conjugate) image. The $\mathrm{Spin}(L)_{-1}\times\mathrm{SO}(L)_1$ theories have a net zero chiral central charge $c_-=c_L-c_R=0$, and they are equivalent to $(2+1)$D Kitaev spin liquids [70] tensored with suitable invertible spin TQFTs (with only $\{1,f\}$, a trivial operator and a transparent spin-1/2 fermionic line operator) to cancel the chiral central charge. Here, the K-matrix CS theories have a gauge group given by products of $\mathrm{U}(1)\times\mathrm{U}(1)\times\cdots$ groups, with a symmetric-bilinear integer matrix K. In our case, only for an even integer L, we have the K matrix $=\left(\begin{smallmatrix}0&2\\2&L/2 \bmod 4\end{smallmatrix}\right)$ which corresponds to an Abelian CS theory. The $\mathbb{Z}_8$ class of fermionic spin TQFTs can be obtained by gauging the $\mathbb{Z}_2$ internal symmetry of fermionic symmetry-protected topological states generated by the spin bordism group $\Omega_3^{\mathrm{Spin}}(B\mathbb{Z}_2)=\mathbb{Z}_8$. Their $\mathbb{Z}_8$ class bordism invariant as an invertible TQFT can be also written

schematically as

$$e^{iS[a,s]} = e^{\frac{2\pi i\nu}{8}\mathrm{ABK}[\mathrm{PD}(a),\ s|_{\mathrm{PD}(a)}]}$$

with $\nu \in \mathbb{Z}_8$, a spin structure $s \in \mathrm{Spin}(M^3)$, and the background $\mathbb{Z}_2$ gauge connection $a \in H^1(M^3, \mathbb{Z}_2)$. Here ABK[...] denotes the $\mathbb{Z}_8$-valued Arf-Brown-Kervaire invariant of Pin^- 2-manifold from the Poincaré dual (PD) of a [49]. The $s|_{\mathrm{PD}(a)}$ is the Pin^- structure on PD(a). For more details, see Table 2 of [49]. Moreover, if we disregard the thermal Hall conductance (the chiral central charge c_-) difference, the T_L can also be related to the $\mathrm{Spin}(L)_{-1}$ Chern-Simons gauge theory in $(2+1)$D, which is a bosonic nonspin TQFT with a $\mathrm{Spin}(L)$ gauge group at the level -1 [37] with a chiral central charge $c_- = -L/2 \mod 4$. The relation of the $\mathbb{Z}_8$ class here and the Kitaev's $\mathbb{Z}_{16}$ class [70] is also examined in other recent work on non-Abelian fractional quantum Hall states (see [71,72]). We also thank G. Moore for pointing out another discussion on the $\mathbb{Z}_8$ classes of 3D spin CS theory from the symmetric bilinear K-matrix Abelian CS theory perspective [73].

To compare this work to Ref. [15], we note that Ref. [15] writes the TQFTs for Pfaffian, PH-Pfaffian, and anti-Pfaffian states as

$$\text{Pfaffian}: \frac{\mathrm{U}(1)_8 \times \mathrm{Ising}}{\mathbb{Z}_2} - 4\mathrm{CS}_{\mathrm{grav}}, \quad c_- = 1 + 1/2 + 4/2 = 7/2, \tag{E11}$$

$$\text{PH-Pfaffian}: \frac{\mathrm{U}(1)_8 \times \overline{\mathrm{Ising}}}{\mathbb{Z}_2} - 4\mathrm{CS}_{\mathrm{grav}}, \quad c_- = 1 - 1/2 + 4/2 = 5/2, \tag{E12}$$

$$\text{Anti-Pfaffian}: \frac{\mathrm{U}(1)_8 \times \mathrm{SU}(2)_{-2}}{\mathbb{Z}_2} - 4\mathrm{CS}_{\mathrm{grav}}, \quad c_- = 1 - 3/2 + 4/2 = 3/2, \tag{E13}$$

whereas here we write

$$\text{Pfaffian}: \mathrm{O}(2)_{2,-1}\ \mathrm{CS} - 5\mathrm{CS}_{\mathrm{grav}}, \quad c_- = 1 + 5/2 = 7/2, \tag{E14}$$

$$\text{PH-Pfaffian}: \mathrm{O}(2)_{2,1}\ \mathrm{CS} - 3\mathrm{CS}_{\mathrm{grav}}, \quad c_- = 1 + 3/2 = 5/2, \tag{E15}$$

$$\text{Anti-Pfaffian}: \mathrm{O}(2)_{2,3}\ \mathrm{CS} - \mathrm{CS}_{\mathrm{grav}}, \quad c_- = 1 + 1/2 = 3/2. \tag{E16}$$

In T_L, the $\mathbb{Z}_{2,[1]}$ symmetry acts on the magnetically charged line, which is the line operator associated to the so-called σ anyon. In the condensed-matter terminology, this is called the *magnetic vortex line* or *vison loop*. $\mathbb{Z}_{2,[1]}$ takes this line to minus itself ($-\sigma$). In the $\mathrm{U}(1)_8$ Chern-Simons theory, the $\mathbb{Z}_{2,[1]}$ symmetry also transforms the lines with *odd* U(1) charges to minus themselves. In other words, the line operators of the σ anyon in T_L and of odd U(1) charge in $\mathrm{U}(1)_8$ are both charged objects under the diagonal $\mathbb{Z}_{2,[1]}$ one-form symmetry. As already mentioned in the main text, the $\mathbb{Z}_{2,[1]}$ symmetry generators are line operators in the $\mathrm{U}(1)_8$ theory with U(1) charge 4 and the fermionic line f in T_L.

Another way to think of the $\mathbb{Z}_{2,[1]}$ symmetry transformation is that it arises when the charged lines are linked with the symmetry generator lines. Then, the path integral picks up an extra (-1) sign. The link configurations resulting in this sign are as follows.

(i) In the $\mathrm{U}(1)_8$ Chern-Simons theory, when the odd U(1) charge line links with the U(1) charge-4 line, we get a statistical Berry phase $\exp(\frac{2\pi i}{8}\mathbb{Z}_{\mathrm{odd}} \times 4) = (-1)$.

(ii) In the T_L theory, when the σ line links with the the fermionic f line, we get a statistical Berry phase (-1).

We reviewed in Appendix D what it means to gauge a $\mathbb{Z}_{2,[1]}$ symmetry. By gauging the diagonal $\mathbb{Z}_{2,[1]}$ symmetry described above, we reduce the 24 line operators in the $\mathrm{U}(1)_8 \times T_L$ theory to the 12 line operators in the $\frac{\mathrm{U}(1)_8 \times T_L}{\mathbb{Z}_2}$ theory. See Tables I, II, and III.

1. Hall conductivity

The theory also has a $\mathbb{Z}_4$ one-form global symmetry generated by the line with U(1) charge 2 in the $\mathrm{U}(1)_8$ Chern-Simons theory. One can use this one-form symmetry to couple to a background electromagnetic U(1) gauge field A at level 1 as $\frac{1}{2\pi}(2b)dA = \frac{2b}{2\pi}dA$. The $\mathrm{U}(1)_8$ action, including the coupling to the probe electromagnetic background, is

$$\frac{8}{4\pi} b db + \frac{2b}{2\pi} dA, \tag{E17}$$

where b is the gauge field of $\mathrm{U}(1)_8$ Chern-Simons theory, and A couples to the properly quantized U(1) gauge field $2b$. This system gives the Hall conductance

$$\sigma_{xy} = 2^2/8 = 1/2.$$

In addition, we can add a Chern-Simons action for the background gauge field A:

$$\int_{3d} \left(\frac{8}{4\pi} b\, db + \frac{2b}{2\pi} dA \right) + \frac{r}{4\pi} A\, dA, \tag{E18}$$

where the coefficient $r \in \mathbb{Z}$ is quantized to be an integer in fermionic systems. Then the system has a quantum Hall conductance

$$\sigma_{xy} = \tfrac{1}{2} + r \tag{E19}$$

measured in units of e^2/h. In the application to the experiment with quantum Hall conductivity $\sigma_{xy} = \frac{5}{2}$ (see [15] and the references therein), we take

$$r = 2.$$

Here the $r = 2$ corresponds to the lowest (zeroth) Landau levels with both spin-up and -down complex fermions, which contribute $\sigma_{xy} = 2$ quantum Hall conductance. The first Landau level contributes another $\sigma_{xy} = \frac{1}{2}$ from the half-filled first Landau level with spin-polarized fermions.

The discussion does not change when there are fermions in the nontrivial one-dimensional representation of $\mathbb{Z}_2$ [i.e., they are coupled to T_L but not $\mathrm{U}(1)_8$] that do not couple to the background A. There is another way to see the quantum Hall conductance using the $\mathbb{Z}_4$ one-form symmetry. The line generating that symmetry has spin $1/4$, and thus the one-form symmetry has the anomaly

$$\frac{8}{4\pi} \int_{4d} B_2 B_2, \tag{E20}$$

where B_2 is the two-form background field of the $\mathbb{Z}_4$ one-form symmetry. The anomaly then implies that the coupling to A by fixing the value $B_2 = \frac{1}{4}\,dA$ has a half-integer Hall conductance (see Appendix E of [74]). The one-form symmetry is present in massive or massless theories with the same 't Hooft anomaly since the one-form symmetry is preserved by mass deformations, and thus the quantum Hall conductance is the same across the phase diagram.

2. Quantum numbers of quasiexcitations

Using (E2) and (E18), we see that a line with odd charge in the $U(1)_8$ theory is identified with the σ line in T_L theory. It is therefore the line operator of a non-Abelian anyon (when L is odd) with quantum dimension 2. Let us label this line operator as

$$(\text{odd}, \sigma).$$

Moreover, we can determine the U(1) electromagnetic charge of this anyonic quasiexcitation from the level $K = 8$ and the charge vector $q = 2$ in (E18) via

$$Q_{(\text{odd},\sigma)} = \frac{1}{K} q = \frac{1}{8} 2 = \frac{1}{4}.$$

This means our theory has fractional U(1) electromagnetic charges $\pm\frac{1}{4}$ from quasiparticle (odd, σ) and quasihole excitations.

Two such non-Abelian anyons (odd, σ) fuse to Abelian anyons, also called semions, with quantum dimension 1:

$$(\text{even}, s).$$

The semions have fractional spin statistics with spin $\frac{1}{4}$, and also have fractional electromagnetic charges:

$$Q_{(\text{even},s)} = \frac{1}{K} q = \frac{1}{8} 2 \times 2 = \frac{1}{2}.$$

Therefore, there are fractional U(1) electromagnetic charges in the theory $\pm\frac{1}{2}$ from the quasiparticle semion (even, s) and the corresponding quasihole.

APPENDIX F: MANY-BODY WAVE FUNCTIONS

In this Appendix, we recall and examine the electron wave functions for the non-Abelian Pf/PHPf/APf states and also Abelian states. In contrast to the EFT language used in the bulk of our work (which uses the second-quantization language), this Appendix is formulated in a many-body quantum mechanics picture (the first-quantization language). This Appendix can be a companion to Sec. III.

1. Pfaffian state for $\kappa_{xy} = 7/2$

The Pfaffian state wave function Ψ_{Pf} was introduced by Moore-Read [2,75] for a $\nu = 1/2$ fractional quantum Hall state in the zeroth Landau level. It is a rotationally invariant state. The wave function is

$$\Psi_{\text{Pf}}(\{z_i\}) = \text{Pf}\left(\frac{1}{z_i - z_j}\right)\left(\prod_{1=i<j}^{N} (z_i - z_j)^k\right) e^{-\sum_{i=1}^{N} |z_i|^2/4\ell_B^2}. \tag{F1}$$

In particular, we look at $k = 2$, for N electrons, and for a magnetic length $\ell_B = \sqrt{\hbar c/(|e|B)}$ for magnetic field B. Here $z_i^* \equiv \overline{z_i}$ is the complex conjugate of the coordinate $z_i = x_i + i y_i \in \mathbb{C}$. The Pf is the Pfaffian of the rank-N antisymmetric matrix $M_{ij} = 1/(z_i - z_j)$, so $(\text{Pf}(M_{ij}))^2 = \det(M_{ij})$. Namely, for an even positive N, we have a degree-$N/2$ polynomial

$$\text{Pf}(M_{ij}) = \frac{1}{2^{N/2}(N/2)!} \sum_{\sigma \in S_N} \text{sgn}\sigma \prod_{l=1}^{N/2} M_{\sigma(2l-1)\sigma(2l)},$$

with the symmetry group S_N and $\text{sgn}\sigma = \pm 1$ the signature of the element $\sigma \in S_N$, so

$$\text{Pf}\left(\frac{1}{z_i - z_j}\right) = \frac{1}{2^{N/2}(N/2)!} \sum_{\sigma \in S_N} \text{sgn}\sigma \prod_{l=1}^{N/2} \frac{1}{z_{\sigma(2l-1)} - z_{\sigma(2l)}}.$$

The $\text{Pf}(\frac{1}{z_i - z_j})$ factor is crucial to obtain an antisymmetric wave function, as appropriate for a fermionic electron system. The Laughlin-type factor $(\prod_{1=i<j}^{N}(z_i - z_j)^2)$ with second-order zeros dictates that there are repulsive interactions between electrons. The $\text{Pf}(\frac{1}{z_i - z_j})$ factor cancels some of the zeros present in the Laughlin-type factor $(\prod_{1=i<j}^{N}(z_i - z_j)^2) e^{-\sum_{i=1}^{N} |z_i|^2/4\ell_B^2}$, making the electrons less repulsive on net. This implies that electrons in Ψ_{Pf} are closer together than those in a purely Laughlin-type state. All the electrons are spin polarized in the Ψ_{Pf} state.

Filling fraction. To determine the filling fraction ν of Ψ_{Pf}, we compute the angular momentum operator $L_{z_i} = \hbar(z_i \partial_{z_i} - z_i^* \partial_{z_i^*})$ acting on the ith electron. The highest power of z_i in Ψ_{Pf} is $z_i^{k(N-1)-1}$ where $k(N-1)-1$ is from the Laughlin factor and -1 is from the Pf factor. This gives rise to the angular momentum $k\hbar$ for the ith electron, which encircles the larger area of the droplet with a radius $r_k = \sqrt{2[k(N-1)-1]}\ell_B$ (at the location where the wave-function density is maximal). Recall $\Phi_0 = 2\pi(\ell_B)^2 B = hc/|e|$, so we verify that Ψ_{Pf} has the

$$\nu = \frac{\text{number of particles}}{\text{number of flux quanta}} = \frac{N}{\Phi_B/\Phi_0} = \frac{N}{(\pi(r_k)^2)/(2\pi(\ell_B)^2)} \simeq 1/k, \quad \text{as } N \to \infty$$

(i.e., $\nu = 1/2$ and $\sigma_{xy} = 1/2$ for $k = 2$ for the Moore-Read Pfaffian). To employ this wave function to the study of $\nu = 5/2$, we employ the Pf state for the first half-filled, spin-polarized Landau level, while we also include spin-up and -down electrons fully occupying the zeroth Landau levels. This gives a total filling fraction of $\nu = 5/2$; also, $\sigma_{xy} = 5/2$. The interaction produces an energy gap the order of the Coulomb interaction energy e^2/ℓ_B, so this state is *incompressible*.

Quasiexcitations. We can obtain a quasihole by adding a hole excitation in a complex coordinate ζ:

$$\begin{aligned}\Psi_{\text{Pf}}^{\text{hole}}(\zeta; \{z_i\}) &\propto \left(\prod_{i'=1}^{N} (\zeta - z_{i'})\right)\Psi_{\text{Pf}}(\{z_i\}) \\ &= \text{Pf}\left(\frac{(\zeta - z_i)(\zeta - z_j) + (\zeta - z_j)(\zeta - z_i)}{z_i - z_j}\right) \\ &\quad \times \left(\prod_{1=i<j}^{N} (z_i - z_j)^k\right) e^{-\sum_{i=1}^{N} |z_i|^2/4\ell_B^2}. \end{aligned} \tag{F2}$$

We could view the z_i as dynamical variables (that should be integrated over to obtain the density), while viewing ζ as a background, or probe, parameter. Because the additional factor ($\prod_{i'=1}^{N}(\zeta - z_{i'})$) introduces more zeros into the wave function, the system becomes less repulsive, so also less dense: this is a hallmark of a hole excitation. If ζ is instead a dynamical variable, then the $(\zeta - z_{i'})^k$ factor introduces an electron at position ζ. For ζ a background parameter, this has the interpretation of removing an electron at ζ. Putting this together, a k-fold factor $(\zeta - z_{i'})^k$ removes an electron at ζ and so, given the electron charge $-|e|$, we have produced a quasihole of charge $|e|/k$. The second line in Eq. (F2) is a rewriting of the first line, by absorbing the quasihole into the Pf factor: $\mathrm{Pf}(\frac{(\zeta_1-z_i)(\zeta_2-z_j)+(\zeta_2-z_j)(\zeta_1-z_i)}{z_i-z_j})|_{\zeta_1=\zeta_2=\zeta}$ which can be regarded as the quasihole splitting into two further fractional quasiholes at ζ_1 and ζ_2, each with charge $|e|/(2k)$. For the Moore-Read Pfaffian at $k = 2$, we have a quasihole of charge $|e|/2$ which further fractionates to a quasihole of charge $|e|/4$.

For each quasihole, there is a corresponding quasiparticle excitation with opposite global symmetry quantum numbers, but with the same spin statistics. The quasiparticles (quasiholes) may be regarded as vortices (antivortices) because the phase of the wave function winds when a particle winds around the quasiexcitation at ζ. For example, the fractionalized charge $|e|/4$ or $-|e|/4$ excitations are in fact the $\pm\pi$ vortices, which we shall identify as the non-Abelian σ anyons in our EFT and TQFTs.

Chiral central charge $c_- = c_L - c_R$ [the degrees of freedom of $(1+1)$D left-moving minus right-moving edge modes) can be determined from two parts of the wave functions. First, the Laughlin sector $(z_i - z_j)^k$ corresponds to $\mathrm{U}(1)_k$ CS theory. It has an edge theory which can be described as a complex chiral boson or fermion, which yields $c_- = 1$. [The readers can find a systematic description of the $(1+1)$D edge theory in Ref. [15].] Second, the Pf factor corresponds to the angular momentum $L_z = 1$ between the composite fermion with a chiral p-wave $(p_x + ip_y)$ pairing [75]. This gives rise to $c_- = 1/2$ corresponding to an edge theory given by a real-valued chiral Majorana mode. The total c_- for the Pfaffian state equation (F1) is $c_- = 3/2$.

Composite fermion pairing. The above discussion is consistent with the fact that the Ising TQFT contributes $c_- = 1/2$ in Eq. (24), which can be induced from the $(p_x + ip_y)$-wave pairing of composite fermions (CF), with angular momentum $\propto(k_x + ik_y)$ for $L_z = 1$. In the Dirac composite Fermi liquid (CFL) picture, the Dirac CF gains a π-Berry phase around the Fermi surface. For Dirac CF, the pairing becomes the $(d_x + id_y)$-wave pairing $\propto(k_x + ik_y)^2$ with $L_z = 2$.

2. Anti-Pfaffian state for $\kappa_{xy} = 3/2$

Anti-Pfaffian (APf) state wave function. The bulk system for the Pfaffian state does not have a time-reversal (CT)/particle-hole symmetry [28], but Ref. [5] considered the particle-hole conjugate wave function in Eq. (F1), dictated by the particle-hole transformation [76], and named it the anti-Pfaffian state:

$$\begin{aligned}\Psi_{\mathrm{APf}}(\{z_i\}) = \int \left(\prod_{i'=1}^{N} d\xi_{i'}\, d\xi_{i'}^*\right) \prod_{i,j'=1}^{N} (z_i - \xi_{j'}) \\ \times \prod_{1=i'<j'}^{N} (\xi_{i'} - \xi_{j'})\, e^{-\sum_{j'=1}^{N} |\xi_{j'}|^2/4\ell_B^2} \Psi_{\mathrm{Pf}}(\{\xi_{i'}^*\}) \\ \times \prod_{1=i<j}^{N} (z_i - z_j)\, e^{-\sum_{i=1}^{N} |z_i|^2/4\ell_B^2}. \end{aligned} \tag{F3}$$

We can break down the Ψ_{APf} state we are interested in [4,5] as a combination of two component pieces. The first piece is the $\nu = 1/2$ Ψ_{APf} with respect to the $\nu = 1$ IQH state. The second piece can be viewed as a $\nu = 1$ integer quantum Hall state (the IQH state with respect to the $\nu = 0$ vacuum). The first part is nothing but the particle-hole conjugate of the $\nu = 1/2$ Ψ_{Pf} with respect to the $\nu = 0$ vacuum. Indeed, the first line in Eq. (F3) corresponds to the first line, while the second line in Eq. (F3) corresponds to the second part. From this description, we see that the filling fraction is $\nu = 1/2$ by construction and the contribution to the chiral central charge of APf from the first part is $c_- = -3/2$ and from the second part is $c_- = 1$ for a total of $c_- = -3/2 + 1 = -1/2$.

The $\mathrm{SU}(2)_{-2}$ TQFT contributes $c_- = -3/2$ in Eq. (26), which can be induced from the $(f_x - if_y)$-wave pairing of CF, with its angular momentum $\propto(k_x - ik_y)^3$ for $L_z = -3$. For Dirac CF, the pairing becomes the $(d_x - id_y)$-wave pairing with $L_z = -2$.

3. Particle-hole Pfaffian state for $\kappa_{xy} = 5/2$

The particle-hole Pfaffian (PH-Pfaffian, or PHPf) wave function [9] (see also [77,78] and other attempts [79,80]) can be written as

$$\begin{aligned}\Psi_{\mathrm{PHPf}}(\{z_i\}) &= \mathcal{P}_{\mathrm{LLL}}\left[\mathrm{Pf}\left(\frac{1}{z_i^* - z_j^*}\right)\left(\prod_{1=i<j}^{N}(z_i - z_j)^2\right) e^{-\sum_{i=1}^{N}|z_i|^2/4\ell_B^2}\right] \\ &\simeq \int \left(\prod_{i'=1}^{N} d\xi_{i'}\, d\xi_{i'}^*\right) \langle\{z_i\}|\{\xi_{i'}\}\rangle \left[\mathrm{Pf}\left(\frac{1}{\xi_{i'}^* - \xi_{j'}^*}\right)\left(\prod_{1=i<j}^{N}(\xi_{i'} - \xi_{j'})^2\right) e^{-\sum_{i'=1}^{N}|\xi_{i'}|^2/4\ell_B^2}\right] \\ &= \int \left(\prod_{i'=1}^{N} d\xi_{i'}\, d\xi_{i'}^*\right) \exp\left(-(|\xi_{i'}|^2 - 2\xi_{i'}^* z_i + |z_i|^2)/(4l_B^2)\right) \left[\mathrm{Pf}\left(\frac{1}{\xi_{i'}^* - \xi_{j'}^*}\right)\left(\prod_{1=i<j}^{N}(\xi_{i'} - \xi_{j'})^2\right) e^{-\sum_{i'=1}^{N}|\xi_{i'}|^2/4\ell_B^2}\right]. \end{aligned} \tag{F4}$$

The $\mathcal{P}_{\rm LLL}$ is the projection onto the lowest Landau level (LLL). From the first line in Eq. (F4), we can see that the filling fraction is still $\nu = 1/2$, as one can read off from the Laughlin factor using the same reasoning from the Pfaffian case. Moreover, the $\mathrm{Pf}(\frac{1}{z_i^* - z_j^*})$ tells us the pairing of composite fermions possesses angular momentum $L_z = -1$ between the composite fermion with an antichiral p-wave $(p_x - ip_y)$ pairing [75], which gives rise to $c_- = 1/2$. The total chiral central charge of the PH-Pfaffian (F3) therefore has $c_- = 1 - 1/2 = 1/2$. The second line in (F4) rewrites the projection in terms of the coherent state projection so the wave function is projected into the LLL.

The above discussion is consistent with the fact that the $\overline{\text{Ising}}$ TQFT contributes $c_- = -1/2$ in (25), which can be induced from the $(p_x - ip_y)$-wave pairing of CF, with angular momentum $\propto (k_x - ik_y)$ at $L_z = -1$. For a Dirac CF picture, the pairing becomes the s-wave pairing with $L_z = 0$.

4. $K = 8$ state for $\kappa_{xy} = 3$

The $K = 8$ state wave function is a bosonic wave function but can be written as a fermionic wave function by dressing it with a fermionic tensor product state:

$$\Psi_{K=8}(\{z_i\}) = \left(\prod_{1=i<j}^{N} (z_i - z_j)^8\right) e^{-\sum_{i=1}^{N} |z_i|^2/4\ell_B^2} \times (\text{fermionic tensor product state}). \quad \text{(F5)}$$

The filling fraction is $\nu = 1/2$ with an appropriate charge coupling, when the charge-$2e$ quasiexcitations are coupled to the U(1) electromagnetic gauge field at level 1. The chiral central charge is $c_- = 1$, as always for a Laughlin wave function. The is consistent with $\mathrm{U}(1)_8$ TQFT with $c_- = 1$.

5. 113 state for $\kappa_{xy} = 2$

The 113-state wave function is a special case of the lmn wave function, known as the Halperin wave function (the multicomponent generalization of Laughlin wave function) with $\mathrm{l} = 1$, $\mathrm{m} = 1$, $\mathrm{n} = 3$ for some $N + N'$ electron system:

$$\begin{aligned}\Psi_{113}(\{z_i\},\{w_{i'}\}) &= \left(\prod_{1=i<j}^{N} (z_i - z_j)^{\mathrm{l}}\right)\left(\prod_{1=i'<j'}^{N'} (w_{i'} - w_{j'})^{\mathrm{m}}\right) \\ &\times \left(\prod_{i}^{N}\prod_{j'}^{N'} (z_i - w_{j'})^{\mathrm{n}}\right) \\ &\times e^{-\sum_{i=1}^{N} |z_i|^2/4\ell_B^2} e^{-\sum_{i'=1}^{N} |w_{i'}|^2/4\ell_B^2}\Big|_{\mathrm{l}=1,\,\mathrm{m}=1,\,\mathrm{n}=3}. \quad \text{(F6)}\end{aligned}$$

The filling fraction is $\nu = 1/2$ with an appropriate charge coupling. The chiral central charge is $c_- = 1 - 1 = 0$ coming from two modes with opposite chiralities.

In general, we expect that quasiparticles and quasiholes of the above many-body wave functions in this Appendix agree with the anyons (and their quantum numbers) of TQFTs shown in Tables I, II, III, IV, and V in Sec. III.

APPENDIX G: ONE-LOOP COMPUTATIONS

1. Fermionic functional determinant

We explicitly carry out the computation of some terms in the fermionic functional determinant given by integrating out a Dirac fermion Ψ in the following Lagrangian in d space-time dimensions:

$$\mathcal{L} = \overline{\Psi}(i\not{D} + m - \not{A} - \chi)\Psi\,. \quad \text{(G1)}$$

The quadratic term in the functional determinant effective action is formally written as

$$\frac{1}{2}\,\mathrm{Tr}\,\frac{\not{p} - m}{p^2 + m^2}(\chi + \not{A})\frac{\not{p} - m}{p^2 + m^2}(\chi + \not{A})\,. \quad \text{(G2)}$$

For the χ^2 piece, we simplify by

$$\begin{aligned}&\frac{1}{2}\,\mathrm{Tr}\,\frac{\not{p} - m}{p^2 + m^2}\,\chi\,\frac{\not{p} - m}{p^2 + m^2}\,\chi \\ &= \frac{1}{2}\,\mathrm{Tr}\,\frac{\not{p} - m}{p^2 + m^2}\,\frac{\not{p} - i\not{\partial} - m}{(p - i\partial)^2 + m^2}\,\chi\,\chi \\ &= \frac{1}{2}\,\mathrm{Tr}\,\frac{-p^2 + m^2 - 2m\not{p} + i(p\partial + m\not{\partial})}{(p^2 + m^2)^2} \\ &\times \sum_{n=0}^{\infty}\left(\frac{2ip\partial + \partial^2}{p^2 + m^2}\right)^n \chi\,\chi\,, \quad \text{(G3)}\end{aligned}$$

where the derivatives only act on the first χ and not the second. The formal expression can be explicitly evaluated by the momentum-space integral

$$\int \frac{d^d p}{(2\pi)^d}\,. \quad \text{(G4)}$$

The trace simply kills all slashed objects. We will compute up to ∂^4 order, so we keep up to $n = 4$ in the sum. By Lorentz invariance, we can perform the following replacements in the integrand:

$$(p\partial)^2 \to \frac{1}{d}p^2\partial^2, \quad (p\partial)^4 \to \frac{3}{d(d+2)}p^4\partial^4. \quad \text{(G5)}$$

The result is[51]

$$\frac{1}{2}\,\chi\left(\frac{|m|}{\pi} - \frac{1}{12\pi|m|}\partial^2 - \frac{1}{240\pi|m|^3}\partial^4 + \mathcal{O}(\partial^6)\right)\chi\,. \quad \text{(G6)}$$

Next, let us consider the χA piece:

$$\begin{aligned}&\frac{1}{2}\,\mathrm{Tr}\,\frac{\not{p} - m}{p^2 + m^2}\,\chi\,\frac{\not{p} - m}{p^2 + m^2}\,\not{A} \\ &= \frac{1}{2}\,\mathrm{Tr}\,\frac{\not{p} - m}{p^2 + m^2}\,\frac{\not{p} - i\not{\partial} - m}{(p - i\partial)^2 + m^2}\,\chi\not{A} \\ &= \frac{1}{2}\,\mathrm{Tr}\,\frac{-p^2 + m^2 - 2m\not{p} + i(p\partial + m\not{\partial})}{(p^2 + m^2)^2} \\ &\times \sum_{n=0}^{\infty}\left(\frac{2ip\partial + \partial^2}{p^2 + m^2}\right)^n \chi\not{A}, \quad \text{(G7)}\end{aligned}$$

[51] The first term is divergent and regularized by analytic continuation in space-time dimension.

where the derivatives only act on χ but not A. Evaluating the trace gives

$$\frac{2^{\lfloor d/2\rfloor}}{2}\,\frac{2mp^\mu - im\partial^\mu}{(p^2+m^2)^2}\sum_{n=0}^{\infty}\left(\frac{2ip\partial+\partial^2}{p^2+m^2}\right)^n \chi A_\mu. \tag{G8}$$

The pieces with only one derivative combine to

$$\begin{aligned}&\frac{2^{\lfloor d/2\rfloor}}{2}\,im\int\frac{d^dp}{(2\pi)^d}\,\frac{-(p^2+m^2)\delta^{\mu\nu}+4p^\mu p^\nu}{(p^2+m^2)^3}\,(\partial_\nu\chi)A_\mu\\ &=\frac{2^{\lfloor d/2\rfloor}}{2}\,im\int\frac{d^dp}{(2\pi)^d}\,\frac{(4/d-1)p^2-m^2}{(p^2+m^2)^3}(\partial^\mu\chi)A_\mu,\end{aligned} \tag{G9}$$

whose coefficient in $d=3$ evaluates to

$$\frac{im}{2\pi^2}\int_0^\infty dp\,p^2\,\frac{(p^2/3-m^2)}{(p^2+m^2)^3}=0\,. \tag{G10}$$

As for the $A\chi$ piece,

$$\begin{aligned}&\frac{1}{2}\,\mathrm{Tr}\,\frac{\not p-m}{p^2+m^2}\not A\,\frac{\not p-m}{p^2+m^2}\,\chi\\ &=\frac{1}{2}\,\mathrm{Tr}\,\frac{\not p-m}{p^2+m^2}\,\gamma^\mu\,\frac{\not p-i\not\partial-m}{(p-i\partial)^2+m^2}\,A_\mu\chi\\ &=\frac{1}{2}\,\mathrm{Tr}\,\frac{(\not p-m)\gamma^\mu(\not p-i\not\partial-m)}{(p^2+m^2)^2}\sum_{n=0}^{\infty}\left(\frac{2ip\partial+\partial^2}{p^2+m^2}\right)^n A_\mu\chi\\ &=\frac{1}{2}\,\mathrm{Tr}\,\frac{-i\not p\gamma^\mu\not\partial-m\gamma^\mu(\not p-i\not\partial)-m\not p\gamma^\mu}{(p^2+m^2)^2}\\ &\quad\times\sum_{n=0}^{\infty}\left(\frac{2ip\partial+\partial^2}{p^2+m^2}\right)^n A_\mu\chi\\ &=\frac{2^{\lfloor d/2\rfloor}}{2}\,\frac{i\varepsilon^{\nu\mu\sigma}p_\nu\partial_\sigma+m(2p^\mu-i\partial^\mu)}{(p^2+m^2)^2}\\ &\quad\times\sum_{n=0}^{\infty}\left(\frac{2ip\partial+\partial^2}{p^2+m^2}\right)^n A_\mu\chi,\end{aligned} \tag{G11}$$

where the derivatives act on A but not χ, and the parity-odd piece with a Levi-Civita symbol is present only if $d=3$. At one derivative order, the parity-odd piece vanishes upon integrating over p, and we are left with the same expression as the χA term (G8) except now the derivative acts on A instead of χ. Thus, upon integration by parts, the $A\chi$ term is an identical contribution to the effective action as the χA term. When $d=3$, the coefficient of $(\partial_\mu\chi)A^\mu$ in the effective Lagrangian vanishes, as we found in (G10).

2. Domain wall tension

Let us discuss how to practically perform the computation of the fermionic one-loop contribution to the domain wall tension, given by the formula (65). The log determinant of the first-order differential operator $\mathbb{D}^{\phi=\phi_0}_{m,g}$ can be related to those of second-order differential operators. Let ε be the Levi-Civita symbol. Formally,

$$\log\det\mathbb{D}^{\phi=\phi_0}_{m,g}=\tfrac{1}{2}\log\det\left(\varepsilon\mathbb{D}^{\phi=\phi_0}_{m,g}\right)^2. \tag{G12}$$

Next, we write everything explicitly in transverse momentum space,

$$\begin{aligned}\log\det\mathbb{D}^{\phi=\phi_0}_{m,g}&=\int\frac{d^2k_\parallel}{(2\pi)^2}\log\det\mathbb{D}^{\phi=\phi_0}_{m,g;k_\parallel}\\ &=\frac{1}{2}\int\frac{d^2k_\parallel}{(2\pi)^2}\log\det\left(\varepsilon\mathbb{D}^{\phi=\phi_0}_{m,g;k_\parallel}\right)^2,\end{aligned} \tag{G13}$$

where

$$\mathbb{D}^{\phi=\phi_0}_{m,g;k_\parallel}\equiv\begin{pmatrix}-\partial_z+m+g\phi_0(z) & k_0-ik_2\\ -k_0-ik_2 & \partial_z+m+g\phi_0(z)\end{pmatrix} \tag{G14}$$

and

$$\left(\varepsilon\mathbb{D}^{\phi=\phi_0}_{m,g;k_\parallel}\right)^2=\begin{pmatrix}-\partial_z^2+[g\phi_0(z)-m]^2-g\phi_0'(z)+k_\parallel^2 & 0\\ 0 & -\partial_z^2+[g\phi_0(z)-m]^2+g\phi_0'(z)+k_\parallel^2\end{pmatrix} \tag{G15}$$

is a diagonal matrix of second-order differential operators. If we define

$$\mathbb{M}^{\phi=\phi_0}_{m,g;k_\parallel}\equiv-\partial_z^2+[g\phi_0(z)-m]^2-g\phi_0'(z)+k_\parallel^2\,, \tag{G16}$$

then

$$\log\det\mathbb{D}^{\phi=\phi_0}_{m,g;k_\parallel}=\tfrac{1}{2}\left(\log\det\mathbb{M}^{\phi=\phi_0}_{m,g;k_\parallel}+\log\det\mathbb{M}^{\phi=\phi_0}_{-m,-g;k_\parallel}\right). \tag{G17}$$

Hence, the integral (65) can written as

$$\delta_f\sigma=-\frac{1}{2}\int\frac{d^2k_\parallel}{(2\pi)^2}\left[\log\frac{\det\mathbb{M}^{\phi=\phi_0}_{m,g;k_\parallel}}{\det\mathbb{M}^{\phi=v}_{m,g;k_\parallel}}\frac{\det\mathbb{M}^{\phi=\phi_0}_{-m,g;k_\parallel}}{\det\mathbb{M}^{\phi=v}_{-m,g;k_\parallel}}\frac{\det\mathbb{M}^{\phi=\phi_0}_{m,-g;k_\parallel}}{\det\mathbb{M}^{\phi=v}_{m,-g;k_\parallel}}\frac{\det\mathbb{M}^{\phi=\phi_0}_{-m,-g;k_\parallel}}{\det\mathbb{M}^{\phi=v}_{-m,-g;k_\parallel}}-\frac{Fg(g+m/v)}{[k_\parallel^2+(gv+m)^2]^{1/2}}-\frac{Fg(g-m/v)}{[k_\parallel^2+(gv-m)^2]^{1/2}}\right]. \tag{G18}$$

To compute the log determinants in the integrand, we apply the Gel'fand-Yaglom theorem to relate $\log\det\mathbb{M}^{\phi}_{m,g;k_\parallel}$ to a boundary-value problem for the second-order differential operator $\mathbb{M}^{\phi}_{m,g;k_\parallel}$, and solve it numerically, as in Ref. [57].

[1] R. Willett, J. P. Eisenstein, H. L. Störmer, D. C. Tsui, A. C. Gossard, and J. H. English, Observation of An Even-Denominator Quantum Number in the Fractional Quantum Hall Effect, Phys. Rev. Lett. **59**, 1776 (1987).

[2] G. Moore and N. Read, Nonabelions in the fractional quantum hall effect, Nucl. Phys. B **360**, 362 (1991).

[3] X. G. Wen, Non-Abelian Statistics in the Fractional Quantum Hall States, Phys. Rev. Lett. **66**, 802 (1991).

[4] M. Levin, B. I. Halperin, and B. Rosenow, Particle-Hole Symmetry and the Pfaffian State, Phys. Rev. Lett. **99**, 236806 (2007).

[5] S.-S. Lee, S. Ryu, C. Nayak, and M. P. A. Fisher, Particle-Hole Symmetry and the $\nu = \frac{5}{2}$ Quantum Hall State, Phys. Rev. Lett. **99**, 236807 (2007).

[6] D. T. Son, Is the Composite Fermion a Dirac Particle? Phys. Rev. X **5**, 031027 (2015).

[7] B. I. Halperin, P. A. Lee, and N. Read, Theory of the half-filled landau level, Phys. Rev. B **47**, 7312 (1993).

[8] T. Jolicoeur, Non-Abelian States with Negative Flux: A New Series of Quantum Hall States, Phys. Rev. Lett. **99**, 036805 (2007).

[9] P. T. Zucker and D. E. Feldman, Stabilization of the Particle-Hole Pfaffian Order by Landau-Level Mixing and Impurities that Break Particle-Hole Symmetry, Phys. Rev. Lett. **117**, 096802 (2016).

[10] M. Banerjee, M. Heiblum, V. Umansky, D. E. Feldman, Y. Oreg, and A. Stern, Observation of half-integer thermal Hall conductance, Nature (London) **559**, 205 (2018).

[11] C. L. Kane and M. P. A. Fisher, Quantized thermal transport in the fractional quantum hall effect, Phys. Rev. B **55**, 15832 (1997).

[12] X.-G. Wen, Topological Order and Edge Structure of $\nu = 1/2$ Quantum Hall State, Phys. Rev. Lett. **70**, 355 (1993).

[13] D. F. Mross, Y. Oreg, A. Stern, G. Margalit, and M. Heiblum, Theory of Disorder-Induced Half-Integer Thermal Hall Conductance, Phys. Rev. Lett. **121**, 026801 (2018).

[14] C. Wang, A. Vishwanath, and B. I. Halperin, Topological order from disorder and the quantized hall thermal metal: Possible applications to the $\nu = 5/2$ state, Phys. Rev. B **98**, 045112 (2018).

[15] B. Lian and J. Wang, Theory of the disordered $\nu = \frac{5}{2}$ quantum thermal Hall state: Emergent symmetry and phase diagram, Phys. Rev. B **97**, 165124 (2018).

[16] X. Chen, L. Fidkowski, and A. Vishwanath, Symmetry enforced non-abelian topological order at the surface of a topological insulator, Phys. Rev. B **89**, 165132 (2014).

[17] M. A. Metlitski, L. Fidkowski, X. Chen, and A. Vishwanath, Interaction effects on 3D topological superconductors: surface topological order from vortex condensation, the 16 fold way and fermionic Kramers doublets, arXiv:1406.3032.

[18] R. H. Morf, Transition from Quantum hall to Compressible States in the Second Landau Level: New Light on the $\nu = 5/2$ Enigma, Phys. Rev. Lett. **80**, 1505 (1998).

[19] E. H. Rezayi and F. D. M. Haldane, Incompressible Paired Hall State, Stripe Order, and the Composite Fermion Liquid Phase in Half-Filled Landau Levels, Phys. Rev. Lett. **84**, 4685 (2000).

[20] M. R. Peterson, T. Jolicoeur, and S. Das Sarma, Finite-Layer Thickness Stabilizes the Pfaffian State for the 5/2 Fractional Quantum Hall Effect: Wave Function Overlap and Topological Degeneracy, Phys. Rev. Lett. **101**, 016807 (2008).

[21] A. E. Feiguin, E. Rezayi, K. Yang, C. Nayak, and S. Das Sarma, Spin polarization of the $\nu = 5/2$ quantum hall state, Phys. Rev. B **79**, 115322 (2009).

[22] H. Wang, D. N. Sheng, and F. D. M. Haldane, Particle-hole symmetry breaking and the $\nu = \frac{5}{2}$ fractional quantum Hall effect, Phys. Rev. B **80**, 241311(R) (2009).

[23] M. Storni, R. H. Morf, and S. Das Sarma, Fractional Quantum Hall State at $\nu = \frac{5}{2}$ and the Moore-Read Pfaffian, Phys. Rev. Lett. **104**, 076803 (2010).

[24] E. H. Rezayi and S. H. Simon, Breaking of Particle-Hole Symmetry by Landau Level Mixing in the $\nu = 5/2$ Quantized Hall State, Phys. Rev. Lett. **106**, 116801 (2011).

[25] Z. Papić, F. D. M. Haldane, and E. H. Rezayi, Quantum Phase Transitions and the ν=5/2 Fractional Hall State in Wide Quantum Wells, Phys. Rev. Lett. **109**, 266806 (2012).

[26] M. P. Zaletel, R. S. K. Mong, F. Pollmann, and E. H. Rezayi, Infinite density matrix renormalization group for multicomponent quantum hall systems, Phys. Rev. B **91**, 045115 (2015).

[27] K. Pakrouski, M. R. Peterson, T. Jolicoeur, V. W. Scarola, C. Nayak, and M. Troyer, Phase Diagram of the $\nu = 5/2$ Fractional Quantum Hall Effect: Effects of Landau-Level Mixing and Nonzero Width, Phys. Rev. X **5**, 021004 (2015).

[28] M. Greiter, X.-G. Wen, and F. Wilczek, Paired Hall State at Half Filling, Phys. Rev. Lett. **66**, 3205 (1991).

[29] Y. Imry and S.-k. Ma, Random-Field Instability of the Ordered State of Continuous Symmetry, Phys. Rev. Lett. **35**, 1399 (1975).

[30] J. T. Chalker and P. D. Coddington, Percolation, quantum tunneling and the integer hall effect, J. Phys. C: Solid State Phys. **21**, 2665 (1988).

[31] S. H. Simon, Interpretation of thermal conductance of the ?=5/2 edge, Phys. Rev. B **97**, 121406(R) (2018).

[32] K. K. W. Ma and D. E. Feldman, Partial equilibration of integer and fractional edge channels in the thermal quantum Hall effect, Phys. Rev. B **99**, 085309 (2019).

[33] S. H. Simon and B. Rosenow, Partial Equilibration of the Anti-Pfaffian Edge Due to Majorana Disorder, Phys. Rev. Lett **124**, 126801 (2020).

[34] S. H. Simon, M. Ippoliti, M. P. Zaletel, and E. H. Rezayi, Energetics of Pfaffian–anti-Pfaffian Domains, Phys. Rev. B **101**, 041302(R) (2020).

[35] H. Asasi and M. Mulligan, Partial equilibration of anti-pfaffian edge modes at $\nu = 5/2$, arXiv:2004.04161.

[36] D. E. Feldman, "Comment on Interpretation of thermal conductance of the $\nu = 5/2$ edge," Phys. Rev. B **98**, 167401 (2018).

[37] C. Córdova, P.-S. Hsin, and N. Seiberg, Global symmetries, counterterms, and duality in Chern-Simons matter theories with orthogonal gauge groups, SciPost Phys. **4**, 021 (2018).

[38] P.-S. Hsin and N. Seiberg, Level/rank duality and chern-simons-matter theories, J. High Energy Phys. 09 (2016) 095.

[39] M. A. Metlitski, L. Fidkowski, X. Chen, and A. Vishwanath, Interaction effects on 3D topological superconductors: surface topological order from vortex condensation, the 16 fold way and fermionic Kramers doublets, arXiv:1406.3032.

[40] C. Wang and T. Senthil, Half-filled Landau level, topological insulator surfaces, and three-dimensional quantum spin liquids, Phys. Rev. B **93**, 085110 (2016).

[41] M. A. Metlitski, S-duality of $u(1)$ gauge theory with $\theta = \pi$ on non-orientable manifolds: Applications to topological insulators and superconductors, arXiv:1510.05663.

[42] C. Wang and M. Levin, Anomaly Indicators for Time-Reversal Symmetric Topological Orders, Phys. Rev. Lett. **119**, 136801 (2017).

[43] Y. Tachikawa and K. Yonekura, On time-reversal anomaly of 2+1d topological phases, Prog. Theor. Exp. Phys. **2017**, 033B04 (2017).

[44] C. Córdova, P.-S. Hsin, and N. Seiberg, Time-Reversal Symmetry, Anomalies, and Dualities in (2+1)*d*, SciPost Phys. **5**, 006 (2018).

[45] D. Gaiotto, A. Kapustin, N. Seiberg, and B. Willett, Generalized global symmetries, J. High Energy Phys. 02 (2015) 172.

[46] P.-S. Hsin, H. T. Lam, and N. Seiberg, Comments on one-form global symmetries and their gauging in 3d and 4d, SciPost Phys. **6**, 039 (2019).

[47] N. Seiberg and E. Witten, Gapped boundary phases of topological insulators via weak coupling, Prog. Theor. Exp. Phys. **2016**, 12C101 (2016).

[48] M. V. Medvedyeva, J. Tworzydło, and C. W. J. Beenakker, Effective mass and tricritical point for lattice fermions localized by a random mass, Phys. Rev. B **81**, 214203 (2010).

[49] P. Putrov, J. Wang, and S.-T. Yau, Braiding statistics and link invariants of bosonic/fermionic topological quantum matter in 2+1 and 3+1 dimensions, Ann. Phys. (NY) **384**, 254 (2017).

[50] J. Wang, K. Ohmori, P. Putrov, Y. Zheng, Z. Wan, M. Guo, H. Lin, P. Gao, and S.-T. Yau, Tunneling Topological vacua via extended operators: (spin-)TQFT spectra and boundary deconfinement in various dimensions, Prog. Theor. Exp. Phys. **(2018)**, 053A01 (2018).

[51] M. Guo, K. Ohmori, P. Putrov, Z. Wan, and J. Wang, Fermionic finite-group gauge theories and interacting symmetric/crystalline orders via cobordisms, Commun. Math. Phys. **376**, 1073 (2020).

[52] R. F. Dashen, B. Hasslacher, and A. Neveu, Nonperturbative methods and extended hadron models in field theory 1. semiclassical functional methods, Phys. Rev. D **10**, 4114 (1974).

[53] R. F. Dashen, B. Hasslacher, and A. Neveu, Nonperturbative methods and extended hadron models in field theory 2. two-dimensional models and extended hadrons, Phys. Rev. D **10**, 4130 (1974).

[54] T. Dimofte, D. Gaiotto, and N. M. Paquette, Dual boundary conditions in 3d SCFT's, J. High Energy Phys. 05 (2018) 060.

[55] D. Gaiotto, Z. Komargodski, and N. Seiberg, Time-reversal breaking in QCD_4, walls, and dualities in 2 + 1 dimensions, J. High Energy Phys. 01 (2018) 110.

[56] J. Wang, Y.-Z. You, and Y. Zheng, Gauge enhanced quantum criticality and time reversal domain wall: SU(2) Yang-Mills dynamics with topological terms, Phys. Rev. Res. **2**, 013189 (2020).

[57] A. Parnachev and L. G. Yaffe, One loop quantum energy densities of domain wall field configurations, Phys. Rev. D **62**, 105034 (2000).

[58] A. Rebhan, P. van Nieuwenhuizen, and R. Wimmer, One loop surface tensions of (supersymmetric) kink domain walls from dimensional regularization, New J. Phys. **4**, 31 (2002).

[59] M. Shifman, *Advanced Topics in Quantum Field Theory.* (Cambridge University Press, Cambridge, UK, 2012), http://www.cambridge.org/mw/academic/subjects/physics/theoretical-physics-and-mathematical-physics/advanced-topics-quantum-field-theory-lecture-course?format=AR.

[60] D. K. Campbell and Y.-T. Liao, A semiclassical analysis of bound states in the two-dimensional sigma model, Phys. Rev. D **14**, 2093 (1976).

[61] H. Nastase, M. A. Stephanov, P. van Nieuwenhuizen, and A. Rebhan, Topological boundary conditions, the BPS bound, and elimination of ambiguities in the quantum mass of solitons, Nucl. Phys. B **542**, 471 (1999).

[62] E. Farhi, N. Graham, P. Haagensen, and R. L. Jaffe, Finite quantum fluctuations about static field configurations, Phys. Lett. B **427**, 334 (1998).

[63] N. Graham and R. L. Jaffe, Unambiguous one loop quantum energies of (1+1)-dimensional bosonic field configurations, Phys. Lett. B **435**, 145 (1998).

[64] N. Graham and R. L. Jaffe, Fermionic one loop corrections to soliton energies in (1+1)-dimensions, Nucl. Phys. B **549**, 516 (1999).

[65] R. Rajaraman, *Solitons and Instantons. An Introduction to Solitons and Instantons in Quantum Field Theory* (Elsevier, Amsterdam, 1982).

[66] J. Wang, *Mother Effective Field Theory for Fractional Quantum Hall Systems near* $\nu = 5/2$, https://www.youtube.com/watch?v=nkEf65XK07I (Seminar Talk at Ultra Quantum Matter Simons Collaboration May 26th, 2020 and at Harvard CMSA-Weizmann Institute of Science July 8, 2020).

[67] G. W. Moore and N. Seiberg, Naturality in conformal field theory, Nucl. Phys. B **313**, 16 (1989).

[68] G. W. Moore and N. Seiberg, Taming the Conformal Zoo, Phys. Lett. B **220**, 422 (1989).

[69] F. A. Bais and J. K. Slingerland, Condensate induced transitions between topologically ordered phases, Phys. Rev. B **79**, 045316 (2009).

[70] A. Kitaev, Anyons in an exactly solved model and beyond, Ann. Phys. (NY) **321**, 2 (2006).

[71] K. K. W. Ma and D. E. Feldman, The sixteenfold way and the quantum Hall effect at half-integer filling factors, Phys. Rev. B **100**, 035302 (2019).

[72] R. Ma and Y.-C. He, Emergent QCD_3 Quantum Phase Transitions of Fractional Chern Insulators, Phys. Rev. Res. **2**, 033348 (2020).

[73] D. Belov and G. W. Moore, Classification of Abelian spin Chern-Simons theories, arXiv:hep-th/0505235.

[74] F. Benini, C. Córdova, and P.-S. Hsin, On 2-Group Global Symmetries and their Anomalies, J. High Energy Phys. 03 (2019) 118.

[75] N. Read and D. Green, Paired states of fermions in two dimensions with breaking of parity and time-reversal symmetries and the fractional quantum hall effect, Phys. Rev. B **61**, 10267 (2000).

[76] S. M. Girvin, Particle-hole symmetry in the anomalous quantum hall effect, Phys. Rev. B **29**, 6012 (1984).

[77] A. C. Balram, M. Barkeshli, and M. S. Rudner, Parton construction of a wave function in the anti-pfaffian phase, Phys. Rev. B **98**, 035127 (2018).

[78] R. V. Mishmash, D. F. Mross, J. Alicea, and O. I. Motrunich, Numerical exploration of trial wave functions for the particle-hole-symmetric Pfaffian, Phys. Rev. B **98**, 081107(R) (2018).

[79] J. Yang, Dirac composite fermion - A particle-hole spinor, arXiv:1711.08520.

[80] J. Yang, A compressed particle-hole symmetric Pfaffian state for $\nu = 5/2$ quantum Hall effect, arXiv:2001.01915.